

Binary Classification of Gaussian Mixtures: Abundance of Support Vectors, Benign Overfitting and Regularization *

Ke Wang[†] Christos Thrampoulidis[‡]

Abstract

Deep neural networks generalize well despite being exceedingly overparameterized and being trained without explicit regularization. This curious phenomenon has inspired extensive research activity in establishing its statistical principles: Under what conditions is it observed? How do these depend on the data and on the training algorithm? When does regularization benefit generalization? While such questions remain wide open for deep neural nets, recent works have attempted gaining insights by studying simpler, often linear, models. Our paper contributes to this growing line of work by examining binary linear classification under a generative Gaussian mixture model in which the feature vectors take the form $\mathbf{x} = \pm\boldsymbol{\eta} + \mathbf{q}$, where for a mean vector $\boldsymbol{\eta}$ and feature noise $\mathbf{q} \sim \mathcal{N}(0, \boldsymbol{\Sigma})$. Motivated by recent results on the implicit bias of gradient descent, we study both max-margin SVM classifiers (corresponding to logistic loss) and min-norm interpolating classifiers (corresponding to least-squares loss). First, we leverage an idea introduced in [V. Muthukumar et al., [arXiv:2005.08054](#), (2020)] to relate the SVM solution to the min-norm interpolating solution. Second, we derive novel non-asymptotic bounds on the classification error of the latter. Combining the two, we present novel sufficient conditions on the covariance spectrum and on the signal-to-noise ratio (SNR) $SNR = \|\boldsymbol{\eta}\|_2^2 / \boldsymbol{\eta}^T \boldsymbol{\Sigma} \boldsymbol{\eta}$ under which interpolating estimators achieve asymptotically optimal performance as overparameterization increases. Interestingly, our results extend to a noisy model with constant probability noise flips. Contrary to previously studied discriminative data models, our results emphasize the crucial role of the SNR and its interplay with the data covariance. Finally, via a combination of analytical arguments and numerical demonstrations we identify conditions under which the interpolating estimator performs better than corresponding regularized estimates.

1 Introduction

1.1 Motivation

Deep-learning models are increasingly more complex. They are designed with a huge number of parameters that far exceed the size of typical training data sets and training is often completed without any explicit regularization [Krizhevsky et al., 2012, Montufar et al., 2014, Poggio et al., 2017, Goodfellow et al., 2016]. As a consequence, after training, the models perfectly fit (or, so called interpolate) the data. Classical statistical wisdom suggests that such interpolating models overfit and as such they generalize poorly, e.g. Hastie et al. [2009]. But, the reality of modern deep-learning practice is very different: such overparameterized learning architectures achieve state-of-the-art generalization performance despite interpolating the data [Zhang et al., 2016, Belkin et al., 2018a, Nakkiran et al., 2019]. Interestingly, similar empirical findings, albeit in much simpler learning settings have been recorded in the literature even before the era of deep learning [Vallet et al., 1989, Oppen et al., 1990, Duin, 2000]; see discussion in Loog et al. [2020]. Empirical observations like these raise a series of important questions [Duin, 2000, Zhang et al., 2016, Belkin et al., 2018a,c]: *Why*

*A preliminary version of this work Wang and Thrampoulidis [2021] is presented as ICASSP 2021.

[†]Department of Statistics and Applied Probability, University of California, Santa Barbara, CA 93106 USA (ke-wang01@ucsb.edu).

[‡]Department of Electrical and Computer Engineering, University of British Columbia, Vancouver, BC V6T 1Z4 Canada (cthrampo@ece.ubc.ca). Department of Electrical and Computer Engineering, University of California, Santa Barbara, CA 93106 USA (cthrampo@ucsb.edu).

and when are larger models better? What is the role of the training algorithm in this process? Can infinite overparameterization result in better generalization than any finite number of parameters or even training with explicit regularization? Answering these questions is considered one of the main challenges in modern learning theory and has attracted significant research attention over the past couple of years or so, e.g., Belkin et al. [2018a,b], Mei and Montanari [2019], Hastie et al. [2019], Liang et al. [2019], Liao et al. [2020], Deng et al. [2019], Ba et al. [2019], Muthukumar et al. [2020a], Yang et al. [2020], Chatterji et al. [2020].

Among the earliest attempts towards analytically investigating the question “why do overparameterized models generalize well?” focused on linear-regression including both asymptotic and non-asymptotic analyses [Hastie et al., 2019, Belkin et al., 2019, Muthukumar et al., 2020b, Tsigler and Bartlett, 2020]. While certainly a simplified model, this is a natural first step towards gaining insights about more complex models. Closest to our work, Bartlett et al. [2020] derived non-asymptotic bounds on the squared prediction risk of the min-norm linear interpolator for a linear regression model with additive Gaussian noise and (sub)-Gaussian covariates. They subsequently used these bounds and identified conditions on the spectrum of the data covariance such that the risk asymptotically approaches the optimal Bayes error despite perfectly fitting to noisy data. This behavior was termed “benign overfitting” in their paper and the terminology has already been widely adapted in the literature.

A step further in the direction of understanding generalization in overparameterized regimes is the study of linear classification models, since arguably most deep learning success stories apply to classification settings. Classification is not only more relevant, but also typically harder to analyze. The challenge is that even in linear settings, the solution to logistic loss minimization is *not* given in closed form. This is to be contrasted to the solution to least-squares minimization typically used in regression (e.g. [Bartlett et al., 2020, Hastie et al., 2019]). As such, central questions have remained largely unexplored until very recently.

Sur and Candès [2019], Salehi et al. [2019], Montanari et al. [2019], Deng et al. [2019], Kini and Thrampoulidis [2020], Mignacco et al. [2020], Kammoun and Alouini [2020], Salehi et al. [2020] study overparameterized binary linear classification in the proportional asymptotic regime, where the size n of the training set and the size p of the parameter vector grow large at a fixed rate. These works overcome the aforementioned challenge by relying on powerful tools from modern high-dimensional statistics [Stojnic, 2013, Thrampoulidis et al., 2015, 2018] and yield asymptotic error predictions that are sharp, but remain limited to the proportional regime and are expressed in terms of complicated—and often hard to interpret and evaluate—systems of nonlinear equations.

A different approach, resulting in more general non-asymptotic, albeit non-sharp, bounds was initiated by Muthukumar et al. [2020a] who studied a ‘Signed’ classification model with Gaussian features. Their key observation, that drives their analysis, is that the max-margin classifier linearly interpolates the data given sufficient overparameterization. This allowed the authors to establish a tight link between the (hard to directly analyze) SVM and the (amenable to analysis) LS solutions. In turn, this resulted in identifying sufficient conditions on the covariance spectrum needed for benign overfitting. While this paper was being prepared, a follow-up work Hsu et al. [2020] has extended their analysis to binary classification under generalized linear models (including the ‘Signed’ model as a special case) and to subGaussian/Haar-distributed features. Motivated by these works, we investigate the following related open questions: *Does the max-margin classifier interpolate data that are generated from generative (rather than discriminative) models? If so, under what conditions? How do optimally tuned regularized estimators compare to interpolating classifiers? Are there settings in which the latter perform better? How does label noise affect any interpolating properties of the max-margin classifier? What does this imply for benign overfitting?*

1.2 Contributions and novelty

We answer the questions above by focusing on the popular Gaussian mixture model (GMM). Unlike discriminative classification models, the GMM specifies the feature conditional distribution $\mathbf{x}|y$, setting it to be a multivariate Gaussian that is centered around a mean vector $y\boldsymbol{\eta}$ (of their respective class $y = \pm 1$) and has covariance matrix $\boldsymbol{\Sigma}$ (Section 2 for details). We outline our contributions below and

then highlight the novelties compared to prior work.

(i) *Abundance of support vectors (Section 3)*: We show for the first time that the max-margin classifier *linearly interpolates* GMM data given sufficient overparameterization. Notably, our analytic sufficient conditions for this to happen involve not only the covariance spectrum, but also the problem’s signal-to-noise-ratio (SNR), which we define as $SNR = \|\boldsymbol{\eta}\|_2^4 / \boldsymbol{\eta}^T \boldsymbol{\Sigma} \boldsymbol{\eta}$. Thus, we uncover a key difference compared to discriminative data (e.g. Signed model [Muthukumar et al., 2020a, Hsu et al., 2020]). We complement our sufficient conditions with numerical results that suggest their tightness.

(ii) *Non-asymptotic bounds for min-norm estimators (Section 4)*: We derive novel *non-asymptotic* error bounds for the min-norm linear interpolator. Our bounds explicitly capture the effect of the overparameterization ratio, of the covariance spectrum and of the SNR.

(iii) *Interpolators’ risk under high overparameterization (Section 5)*: Combining our findings above, we derive sufficient conditions on the spectrum of $\boldsymbol{\Sigma}$ and on the SNR that guarantee both the SVM and the LS solutions (a) perfectly interpolate the data, and, (b) achieve asymptotically optimal risk as overparameterization increases. Our conditions improve upon the state of the art [Chatterji and Long, 2020] in the noiseless case (see discussion below).

(iv) *The effect of regularization (Section 6)*: We study the effect of ridge-regularization on the risk. Interestingly, we identify regimes that the interpolating estimator (corresponding to zero regularization) outperforms regularized estimates in the overparameterized regime.

(v) *Interpolation and benign overfitting in noisy models (Section 7)*: We extend our findings to a *noisy* isotropic Gaussian mixture model, where labels are corrupted with constant probability. First, we find that the favorable interpolating property of SVM continues to hold, but under stronger conditions due to the label corruptions. Second, in the regime of interpolation, we upper bound the risk of the minimum-norm interpolator and use this result to identify regimes of benign overfitting, i.e. regimes where the SVM risk asymptotically approaches the Bayes risk despite perfectly fitting the data.

On the technical front, while our analysis uses tools similar to those in Bartlett et al. [2020], Muthukumar et al. [2020a], there are key differences in the GMM, which further complicate the analysis and impose new challenges. This can be illustrated at a high-level as described below (see also Section 8). We will show that at the heart of our analysis lies the challenge of upper/lower-bounding quadratic forms such as $\mathbf{y}^T (\mathbf{X} \mathbf{X})^{-1} \mathbf{y}$, where \mathbf{y} is the label vector and \mathbf{X} is the feature matrix of the training set. Under the GMM, and unlike in linear regression and discriminative classification models, the matrix \mathbf{X} “includes” both the label vector \mathbf{y} and the mean vector $\boldsymbol{\eta}$. Hence, considering \mathbf{y} and \mathbf{X} separately as in Bartlett et al. [2020], Muthukumar et al. [2020a] leads to sub-optimal bounds. Instead, we first show that it is possible to decompose the original quadratic form of interest into several more primitive quadratic forms on inverse-Wishart matrices (rather than on the original Gram matrix). This decomposition is central to our proof technique, but the technical challenge remains because: (a) the decomposition involves the new quadratic forms in a convoluted way requiring us to establish both lower and upper bounds for each one of them and then combine them carefully, and, (b) while more primitive, the desired bounds for the new quadratic forms do *not* follow from previous works. Besides, as mentioned above, a particular distinguishing feature of GMM compared to previous works is that in the process of doing the above we need to carefully capture the impact of not only the covariance spectrum, but also of the model’s SNR. Compared to previous works, we also complement our analysis with numerical results validating the tightness of our findings. Also, we study the effect of regularization and identify regimes in which interpolating estimators have optimal performance. Compared to Muthukumar et al. [2020a], Hsu et al. [2020] we also extend our results to a noisy model with constant probability label corruptions.

The most closely related work in terms of problem setting and results is the recent paper by Chatterji and Long [2020], which thus deserves its own discussion. Chatterji and Long [2020] are the first to derive non-asymptotic risk bounds for overparameterized binary mixture models and use them to characterize benign-overfitting conditions. Notably, their bounds hold for sub-Gaussian features and for an adversarial noisy model that is more general than ours. On the other hand, in the special case of GMM, our results improve upon theirs as follows. In the noiseless case, we significantly relax the conditions under which interpolating estimators asymptotically attain Bayes optimal performance with increasing overparameterization. Also, our risk bounds capture the key role of the covariance

structure unlike theirs. In the noisy case, our benign overfitting conditions are the same, but our risk bounds on the min-norm interpolator hold under relaxed scaling assumptions. It is worth mentioning that our proof strategy towards upper bounding the risk of SVM is also entirely different compared to Chatterji and Long [2020]. In comparison to Chatterji and Long [2020], we are also the first to establish interpolating conditions for the SVM solution under GMM data. Finally, our risk bounds also hold for regularized least-squares.

A more elaborate discussion on the above closely related works, as well as, a comparison to classical margin-based bounds is deferred to Section 9 due to space limitations. The Appendix includes detailed proofs of all our results.

Notation. For a vector $\mathbf{v} \in \mathbb{R}^p$, let $\|\mathbf{v}\|_2 = \sqrt{\sum_{i=1}^p v_i^2}$, $\|\mathbf{v}\|_1 = \sum_{i=1}^p |v_i|$, $\|\mathbf{v}\|_{-1} = \sum_{i=2}^p |v_i|$, $\|\mathbf{v}\|_\infty = \max_i \{|v_i|\}$ and \mathbf{e}_i denotes the i -th standard basis vector. For a matrix \mathbf{M} , $\|\mathbf{M}\|_2$ denotes its operator norm. $[n]$ denotes the set $\{1, 2, \dots, n\}$. We also use standard ‘‘Big O’’ notations $\Theta(\cdot)$, $\omega(\cdot)$, e.g., see Corman et al. [2009, Chapter 3]. Finally, we write $\mathcal{N}(\boldsymbol{\mu}, \boldsymbol{\Sigma})$ for the (multivariate) Gaussian distribution of mean $\boldsymbol{\mu}$ and covariance matrix $\boldsymbol{\Sigma}$, and, $Q(x) = \mathbb{P}(Z > x)$, $Z \sim \mathcal{N}(0, 1)$ for the Q-function of a standard normal. Throughout, ‘constants’ refer to numbers that do *not* depend on the problem dimensions n or p .

2 Learning Model

2.1 Data model

Consider the following supervised binary classification problem under a *Gaussian mixtures model* (GMM). Let $\mathbf{x} \in \mathbb{R}^p$ denote the feature vector and $y \in \{-1, +1\}$ its class label. The class label y takes one of the values $\{\pm 1\}$ with probabilities $\pi_{\pm 1}$ such that $\pi_{+1} + \pi_{-1} = 1$. The class-conditional probability $p(\mathbf{x}|y)$ follows Gaussian distribution. Specifically, conditional on $y = \pm 1$, the feature vector \mathbf{x} is a Gaussian vector with mean vector $\pm \boldsymbol{\eta} \in \mathbb{R}^p$ and an invertible covariance matrix $\boldsymbol{\Sigma}$. Summarizing, the data pair (\mathbf{x}, y) is generated such that

$$y = \begin{cases} 1, & \text{w.p. } \pi_{+1} \\ -1, & \text{w.p. } 1 - \pi_{+1} \end{cases} \quad \text{and} \quad \mathbf{x}|y \sim \mathcal{N}(y\boldsymbol{\eta}, \boldsymbol{\Sigma}). \quad (1)$$

We denote the eigenvalues of $\boldsymbol{\Sigma}$ by $\boldsymbol{\lambda} := [\lambda_1, \dots, \lambda_p]$, with $\lambda_1 \geq \lambda_2 \geq \dots \geq \lambda_p$, and write the eigen-decomposition of $\boldsymbol{\Sigma}$ as $\boldsymbol{\Sigma} = \sum_{i=1}^p \lambda_i \mathbf{v}_i \mathbf{v}_i^T = \mathbf{V} \boldsymbol{\Lambda} \mathbf{V}^T$, where $\boldsymbol{\Lambda}$ is a diagonal matrix whose diagonal elements are eigenvalues of $\boldsymbol{\Sigma}$ and the columns of matrix \mathbf{V} are eigenvectors of $\boldsymbol{\Sigma}$. Using the eigenvectors of $\boldsymbol{\Sigma}$ as a basis, the mean vector $\boldsymbol{\eta}$ can be expressed as $\boldsymbol{\eta} = \mathbf{V} \boldsymbol{\beta}$, where $\boldsymbol{\beta} \in \mathbb{R}^p$. Note that $\|\boldsymbol{\eta}\|_2 = \|\boldsymbol{\beta}\|_2$.

Consider training set $\{(\mathbf{x}_i, y_i)\}_{i=1}^n$ composed of n IID data pairs generated according to the GMM in (1). Let $\mathbf{X} = [\mathbf{x}_1, \mathbf{x}_2, \dots, \mathbf{x}_n]^T \in \mathbb{R}^{n \times p}$ denote the feature matrix and $\mathbf{y} = [y_1, \dots, y_n]^T$ denote the class-label vector. Following (1), the data matrix \mathbf{X} can be expressed as follows for a ‘‘noise matrix’’ $\mathbf{Q} \in \mathbb{R}^{n \times p}$ with independent $\mathcal{N}(\mathbf{0}, \boldsymbol{\Sigma})$ rows,

$$\mathbf{X} = \mathbf{y} \boldsymbol{\eta}^T + \mathbf{Q}.$$

2.1.1 Data covariance structure

One of our contributions is demonstrating how the classification performance on data from the GMM depends crucially on the structure of the data covariance. To explicitly capture this dependency, we consider two ensembles for the spectrum of the data covariance $\boldsymbol{\Sigma}$.

Definition 2.1 (Balanced ensemble). No eigenvalues of $\boldsymbol{\Sigma}$ are significantly larger than others. Specifically, there exists a constant $b > 1$ such that

$$bn\lambda_1 \leq \|\boldsymbol{\lambda}\|_{-1}, \quad (2)$$

where $\|\boldsymbol{\lambda}\|_{-1} = \sum_{i=2}^p \lambda_i$. An example of special interest is the isotropic case $\boldsymbol{\Sigma} = \mathbf{I}$ with sufficient overparameterization, i.e., $p > Cn$, for some constant $C > 1$.

Definition 2.2 (Bi-level ensemble). One eigenvalue of Σ is much larger than others. Specifically, there exist constants $b_1, b_2 > 1$ such that

$$b_1 n \lambda_1 \geq \|\boldsymbol{\lambda}\|_{-1} \quad \text{and} \quad b_2 n \lambda_2 \leq \sum_{i=3}^p \lambda_i. \quad (3)$$

The different nature of the two models leads to different conclusions on how the covariance structure affects our key results on abundance of support vectors and benign overfitting. Similar data covariance structures were considered in Muthukumar et al. [2020a], but for the discriminative model $y_i = \text{Sign}(\mathbf{x}_i^T \boldsymbol{\eta})$, $i \in [n]$ with features $\mathbf{x}_i \sim \mathcal{N}(0, \Sigma)$. The two ensembles above are also related to the notions of effective ranks introduced by Bartlett et al. [2020] in the study of benign overfitting for linear regression (see Section 9.2.1 for details).

2.1.2 Key summary quantities

As mentioned, our results naturally depend on the spectrum of Σ . Specifically, we will identify $\|\boldsymbol{\lambda}\|_1$ and $\|\boldsymbol{\lambda}\|_2$ as two key relevant summary quantities. But as hinted by (1) the data covariance Σ is expected to interplay with the mean vector $\boldsymbol{\eta}$ in the results. We will show that this interplay is captured by the *the signal strength in the direction of Σ* , which we denote

$$\sigma^2 := \|\boldsymbol{\eta}\|_{\Sigma}^2 := \boldsymbol{\eta}^T \Sigma \boldsymbol{\eta} = \boldsymbol{\beta}^T \Lambda \boldsymbol{\beta}.$$

Finally, the signal strength $\|\boldsymbol{\eta}\|_2$ will also be important. Note that the two quantities σ^2 and $\|\boldsymbol{\eta}\|_2$ define a natural notion of signal-to-noise ratio (SNR) for the GMM. To better see this, take inner products of both sides of (1) with $\boldsymbol{\eta}$ to express the label-feature relation as $\mathbf{x} = \boldsymbol{\eta} \mathbf{y} + \mathbf{q} \implies \mathbf{y} = \frac{\boldsymbol{\eta}^T \mathbf{x}}{\|\boldsymbol{\eta}\|_2^2} - \frac{\boldsymbol{\eta}^T \mathbf{q}}{\|\boldsymbol{\eta}\|_2^2}$, where $\mathbf{q} \sim N(\mathbf{0}, \Sigma)$. Then, following the standard definition in random-design regression and noting that $\frac{\text{Var}(\boldsymbol{\eta}^T \mathbf{x})}{\text{Var}(\boldsymbol{\eta}^T \mathbf{q})} = \frac{c \|\boldsymbol{\eta}\|_2^4 + \boldsymbol{\eta}^T \Sigma \boldsymbol{\eta}}{\boldsymbol{\eta}^T \Sigma \boldsymbol{\eta}} = \frac{c \|\boldsymbol{\eta}\|_2^4}{\boldsymbol{\eta}^T \Sigma \boldsymbol{\eta}} + 1$, for $0 \leq c \leq 1$ depending on π_{+1} , we let $\text{SNR} := \frac{\|\boldsymbol{\eta}\|_2^4}{\boldsymbol{\eta}^T \Sigma \boldsymbol{\eta}} = \frac{\|\boldsymbol{\beta}\|_2^4}{\boldsymbol{\beta}^T \Lambda \boldsymbol{\beta}}$; Lemma 1 bounds the classification error in terms of the same quantity, which further validates its role as the SNR.

2.2 Training algorithm

Given access to the training set, we train a linear classifier $\hat{\boldsymbol{\eta}}$ by minimizing the empirical risk $\hat{\mathcal{R}}_{\text{emp}}(\mathbf{w}) := \frac{1}{n} \sum_{i=1}^n \ell(y_i \cdot \mathbf{w}^T \mathbf{x}_i)$, where the loss function ℓ is chosen as: (i) Least-squares (LS): $\ell(t) = (1 - t)^2$, or, (ii) Logistic: $\ell(t) = \log(1 + e^{-t})$. Throughout, we focus on the *overparameterized* regime $p > n$. As is common, we run gradient descent (GD) on the empirical risk. The following results characterizing the *implicit bias* of GD for the square and logistic losses in the overparameterized regime are well-known. For one, when data can be linearly interpolated (i.e., $\exists \boldsymbol{\beta} \in \mathbb{R}^p$ such that $y_i = \mathbf{x}_i^T \boldsymbol{\beta}$, $\forall i \in [n]$), then GD on square loss with sufficiently small step size converges (as the number of iterations grow to infinity) to the solution of *min-norm interpolation*, e.g. Hastie et al. [2019]:

$$\hat{\boldsymbol{\eta}}_{\text{LS}} = \arg \min_{\mathbf{w}} \|\mathbf{w}\|_2 \quad \text{subject to} \quad y_i = \mathbf{w}^T \mathbf{x}_i, \forall i \in [n]. \quad (4)$$

Second, when data are linearly separable (i.e., $\exists \boldsymbol{\beta} \in \mathbb{R}^p$ such that $y_i(\mathbf{x}_i^T \boldsymbol{\beta}) \geq 1$, $\forall i \in [n]$), then the normalized iterates of GD on logistic loss converge in direction ¹ to the solution of *hard-margin SVM* [Soudry et al., 2018, Ji and Telgarsky, 2019] (see also Rosset et al. [2003] for earlier similar results):

$$\hat{\boldsymbol{\eta}}_{\text{SVM}} = \arg \min_{\mathbf{w}} \|\mathbf{w}\|_2 \quad \text{subject to} \quad y_i \mathbf{w}^T \mathbf{x}_i \geq 1, \forall i \in [n]. \quad (5)$$

Now, specializing to data from the GMM, it can be shown that when $p > n + 2$, then the data can be linearly interpolated with high probability (whp.). In turn, this easily implies that data are also linearly separable. See Appendix I for a formal statement and proof of these claims. Combining

¹Precisely, convergence is in the sense of the normalized GD iterations $\boldsymbol{\eta}^t$, i.e. $\|\frac{\boldsymbol{\eta}^t}{\|\boldsymbol{\eta}^t\|_2} - \frac{\hat{\boldsymbol{\eta}}_{\text{SVM}}}{\|\hat{\boldsymbol{\eta}}_{\text{SVM}}\|_2}\|_2 \xrightarrow{t \rightarrow \infty} 0$.

those, in the overparameterized regime, whp., GD on data from the GMM converges to either (4) or (5) for a square and logistic loss, respectively.

The behavior above holds when no explicit regularization is used. To see the role of regularization, we also consider the ridge estimator given by

$$\hat{\boldsymbol{\eta}}_\tau = \arg \min_{\boldsymbol{w}} \{\|\mathbf{y} - \mathbf{X}\boldsymbol{w}\|_2^2 + \tau\|\boldsymbol{w}\|_2^2\} = \mathbf{X}^T(\mathbf{X}\mathbf{X}^T + \tau\mathbf{I})^{-1}\mathbf{y}. \quad (6)$$

Note that $\hat{\boldsymbol{\eta}}_{\text{LS}}$ can be obtained from (6) by setting $\tau = 0$ ($\mathbf{X}\mathbf{X}^T$ is non-singular whp. for $p > n$, e.g., Vershynin [2018]).

Henceforth, we focus on the classifiers in (5), (4), (6). With some abuse of terminology, we often refer to the minimum-norm interpolator in (4) as LS solution for brevity.

2.3 Classification error

For a new sample (\boldsymbol{x}, y) , the classifier $\hat{\boldsymbol{\eta}}$ classifies \boldsymbol{x} as $\hat{y} = \text{sign}(\hat{\boldsymbol{\eta}}^T \boldsymbol{x})$. Then, the classification error is measured by the expected 0-1 loss risk

$$\mathcal{R}(\hat{\boldsymbol{\eta}}) = \mathbb{E}[\mathbb{I}(\hat{y} \neq y)] = \mathbb{P}(\hat{\boldsymbol{\eta}}^T(y\boldsymbol{x}) < 0), \quad (7)$$

where the expectation is over the distribution of (\boldsymbol{x}, y) generated as in (1). The following simple lemma gives an upper bound on $\mathcal{R}(\hat{\boldsymbol{\eta}})$.

Lemma 1. *Under the Gaussian-mixtures model, the classification error of a classifier $\hat{\boldsymbol{\eta}}$ satisfies, $\mathcal{R}(\hat{\boldsymbol{\eta}}) = Q(\frac{\hat{\boldsymbol{\eta}}^T \boldsymbol{\eta}}{\sqrt{\hat{\boldsymbol{\eta}}^T \boldsymbol{\Sigma} \hat{\boldsymbol{\eta}}})$. In particular, if $\hat{\boldsymbol{\eta}}^T \boldsymbol{\eta} > 0$, then $\mathcal{R}(\hat{\boldsymbol{\eta}}) \leq \exp(-\frac{(\hat{\boldsymbol{\eta}}^T \boldsymbol{\eta})^2}{2\hat{\boldsymbol{\eta}}^T \boldsymbol{\Sigma} \hat{\boldsymbol{\eta}}})$.*

Proof. For a new draw \boldsymbol{x}, y , using $\boldsymbol{x} = y\boldsymbol{\eta} + \boldsymbol{\Sigma}^{1/2}\boldsymbol{z}$, $\boldsymbol{z} \sim \mathcal{N}(\mathbf{0}, \mathbf{I})$ and symmetry of the Gaussian distribution, it can be easily checked that $\mathcal{R}(\hat{\boldsymbol{\eta}}) = \mathbb{P}(\hat{\boldsymbol{\eta}}^T(y\boldsymbol{q}) < -\hat{\boldsymbol{\eta}}^T \boldsymbol{\eta}) = \mathbb{P}(\boldsymbol{\Sigma}^{1/2}\hat{\boldsymbol{\eta}}^T \boldsymbol{z} > \hat{\boldsymbol{\eta}}^T \boldsymbol{\eta})$. Now, $\boldsymbol{\Sigma}^{1/2}\hat{\boldsymbol{\eta}}^T \boldsymbol{z}$ is a zero-mean Gaussian random variable with variance $\hat{\boldsymbol{\eta}}^T \boldsymbol{\Sigma} \hat{\boldsymbol{\eta}}$. Thus, the advertised bounds follow directly: the first, by definition of the Q-function, and, the second, by the Chernoff bound for the Q-function, e.g., Wainwright [2019, Ch. 2]. \square

Thanks to the lemma above, our goal of upper bounding the classification error, reduces to that of lower bounding the ratio $\frac{(\hat{\boldsymbol{\eta}}^T \boldsymbol{\eta})^2}{2\hat{\boldsymbol{\eta}}^T \boldsymbol{\Sigma} \hat{\boldsymbol{\eta}}}$. We do this in Section 4 for the classifiers $\hat{\boldsymbol{\eta}}_\tau$ and $\hat{\boldsymbol{\eta}}_{\text{LS}}$. In large, this is possible because these estimators can be conveniently written in closed forms (see (6)). In contrast, the SVM solution *cannot* be expressed in closed form. To get around this challenge, Section 3 establishes sufficient conditions under which the SVM-solution $\hat{\boldsymbol{\eta}}_{\text{SVM}}$ linearly interpolates the data, thus, it coincides with the LS solution.

3 Link between SVM and linear-interpolation

This section establishes a link between the SVM solution in (5) and the LS solution in (4) for general $\boldsymbol{\Sigma}$. Specifically, Theorem 1 below identifies sufficient conditions under which all training data points become support vectors, i.e., $\hat{\boldsymbol{\eta}}_{\text{SVM}}$ linearly interpolates the data: $\boldsymbol{x}_i^T \hat{\boldsymbol{\eta}}_{\text{SVM}} = y_i$, $\forall i \in [n]$.

Theorem 1. *Assume n training samples following the GMM defined in Section 2. There exist constants $C_1, C_2 > 1$ such that, if the following conditions on the eigenvalues of $\boldsymbol{\Sigma}$ and on the signal strength in the direction of $\boldsymbol{\Sigma}$ defined as $\sigma^2 \triangleq \sum_{i=1}^p \lambda_i \beta_i^2$ hold:*

$$\|\boldsymbol{\lambda}\|_1 > 72(\|\boldsymbol{\lambda}\|_2 \cdot n\sqrt{\log n} + \|\boldsymbol{\lambda}\|_\infty \cdot n\sqrt{n} \log n + 1), \quad (8)$$

$$\|\boldsymbol{\lambda}\|_1 > C_1 n \sqrt{\log(2n)} \sigma, \quad (9)$$

then, the SVM-solution $\hat{\boldsymbol{\eta}}_{\text{SVM}}$ satisfies the linear interpolation constraint in (4) with probability at least $(1 - \frac{C_2}{n})$.

For the isotropic case, condition (8) can be sharpened as shown in the following theorem.

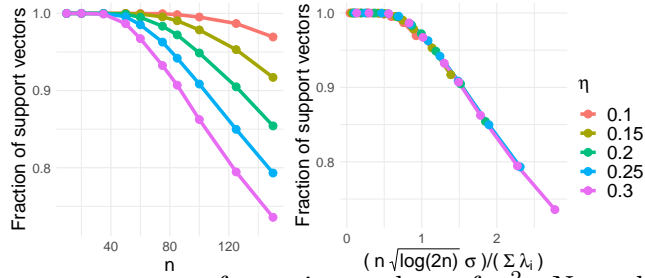


Figure 1: Proportion of support vectors for various values of σ^2 . Note that the five curves nearly overlap when plotted versus $n\sqrt{\log(2n)}\sigma^2/\|\boldsymbol{\lambda}\|_1$ as predicted by (9) in our Theorem 1 confirming its tightness. See text for details on choices of $\boldsymbol{\eta}$, $\boldsymbol{\Sigma}$ and p .

Theorem 2. Assume n training samples following the GMM with $\boldsymbol{\Sigma} = \mathbf{I}$. There exist constants $C_1, C_2 > 1$ such that, if the following conditions on the number of features p and the mean-vector $\boldsymbol{\eta}$ hold:

$$p > 10n \log n + n - 1 \quad \text{and} \quad p > C_1 n \sqrt{\log(2n)} \|\boldsymbol{\eta}\|_2, \quad (10)$$

then, the SVM-solution $\hat{\boldsymbol{\eta}}_{\text{SVM}}$ satisfies the linear interpolation constraint in (4) with probability at least $(1 - \frac{C_2}{n})$.

The theorems establish two sufficient conditions each for all training samples to become support vectors. In the isotropic setting, the first condition requires that the number of features p is significantly larger than the number of observations n . For the anisotropic case, the corresponding condition is related to the effective ranks r_0 and R_0 [Bartlett et al., 2020, Muthukumar et al., 2020a], i.e. $r_k := (\sum_{i>k}^p \lambda_i) / \lambda_{k+1}$ and $R_k = (\sum_{i>k}^p \lambda_i)^2 / (\sum_{i>k}^p \lambda_i^2)$. The condition requires that the covariance spectrum has sufficiently slowly decaying eigenvalues (corresponding to sufficiently large R_0), and that it is not too “spiky” (corresponding to sufficiently large r_0). Muthukumar et al. [2020a, Remark 4] provides a detailed discussion on how the effective ranks relate to different spectrum regimes. Specifically, the bi-level ensemble (Definition 2.2) does *not* satisfy (8). To see that, (8) implies $\|\boldsymbol{\lambda}\|_1 > 72n\sqrt{n}(\log n)\lambda_1$, meaning that $n\lambda_1$ should not be large compared to the sum of other eigenvalues. In contrast, the bi-level ensemble requires $b_1 n \lambda_1 > \|\boldsymbol{\lambda}\|_{-1}$. The second conditions in the two theorems above are the same to each other, since $\sigma = \|\boldsymbol{\eta}\|_2$ in the isotropic setting. These latter conditions relate to the SNR and constrain the signal strength in the direction of $\boldsymbol{\Sigma}$.

To better interpret the result of the two theorems we show corresponding numerical results in Figure 1. As explained, the figure also confirms the tightness of our theoretical prediction. In all our simulations throughout this paper, we fix $\pi_+ = 0.5$ and plot averages over 300 Monte-Carlo realizations. For simplicity, we choose diagonal $\boldsymbol{\Sigma}$; thus, $\boldsymbol{\eta} = \boldsymbol{\beta}$. In Fig. 1, we guarantee (8) by setting $p = 1500$ and varying n up to 150. For the eigenvalues of $\boldsymbol{\Sigma}$, we set $\lambda_1 = 7.5$, $\lambda_2 = \dots = \lambda_{p-1} = 1$ and $\lambda_p = 0.2$. For $\boldsymbol{\eta}$, we chose $\eta_1 = \dots = \eta_p = \eta$, where $\eta = 0.1, 0.15, 0.2, 0.25$ or 0.3 . Fig. 1(Left) shows how the fraction of support vectors changes with n for different η . Smaller η results in higher proportion of support vectors. In order to verify the second condition in (9), Fig. 1(Right) plots the same curves over a re-scaled axis $n\sqrt{\log(2n)}\sigma/\|\boldsymbol{\lambda}\|_1$ (as suggested by (9)). Note that the 5 curves corresponding to different settings overlap in this new scaling, which agrees with the prediction of Theorem 1.

Next, we explain how Theorems 1 and 2 are useful for our purpose of studying the classification error of $\hat{\boldsymbol{\eta}}_{\text{SVM}}$. Suppose (8) and (9) (or (10) in the isotropic case) hold. Then $\hat{\boldsymbol{\eta}}_{\text{SVM}} = \hat{\boldsymbol{\eta}}_{\text{LS}} = \mathbf{X}^T(\mathbf{X}\mathbf{X}^T)^{-1}\mathbf{y}$. Thus, under these conditions we can analyze the classification error of (5), by studying the simpler LS solution in (4). This observation was recently first exploited in Muthukumar et al. [2020a] and sharpened in Hsu et al. [2020], but for a different data model. To see why the above statement is true, note that when (8) and (9) (or (10)) hold, then $\hat{\boldsymbol{\eta}}_{\text{SVM}}$ satisfies the linear interpolation constraints; thus, it is feasible in (4). Consequently, $\hat{\boldsymbol{\eta}}_{\text{SVM}}$ is in fact optimal in (4). To see the latter, assume for the sake of contradiction that $\|\hat{\boldsymbol{\eta}}_{\text{LS}}\|_2 < \|\hat{\boldsymbol{\eta}}_{\text{SVM}}\|_2$. But, for all $i \in [n]$, $y_i(\hat{\boldsymbol{\eta}}_{\text{LS}}^T \mathbf{x}_i) = y_i^2 \geq 1$; thus, $\hat{\boldsymbol{\eta}}_{\text{LS}}$ is feasible in (5), which contradicts our assumption. We will rely on this observation in Section 5 to study benign overfitting of SVM.

Finally, we compare our result to [Muthukumar et al. \[2020a\]](#) that established similar conditions to [Theorem 1](#), but for a ‘Signed’ model: $y_i = \text{sign}(\mathbf{x}_i^T \boldsymbol{\eta})$ with $\mathbf{x}_i \sim \mathcal{N}(\mathbf{0}, \boldsymbol{\Sigma})$. Interestingly, [Muthukumar et al. \[2020a\]](#) obtained sufficient conditions that are identical to the first conditions in [Theorems 1 and 2](#). More recently, [Hsu et al. \[2020\]](#) sharpened the overparameterization condition [\(8\)](#) to $\|\boldsymbol{\lambda}\|_1 \geq C_1 \sqrt{n} \|\boldsymbol{\lambda}\|_2$ and $\|\boldsymbol{\lambda}\|_1 \geq C_2 n \log n \|\boldsymbol{\lambda}\|_\infty$ with large constants C_1 and C_2 for the anisotropic case. While their proof technique does not appear to be easily extended to the analysis of GMM, sharpening [\(8\)](#) can be an interesting future work. *The second conditions related to SNR are tailored to the GMM.* Intuitively, this is explained since in the ‘Signed’ model, the data are insensitive to the value of the signal strength $\|\boldsymbol{\eta}\|_2^2$; what matters is only the direction of $\boldsymbol{\eta}$. In contrast, both the direction and the scaling of the mean vector $\boldsymbol{\eta}$ are important in the GMM as apparent from [\(1\)](#). Our analysis captures this in a concrete way. Note that the first condition in [Theorem 2](#) is sharper than in [Theorem 1](#). This is because, in the isotropic case, we can leverage special properties of Wishart matrices; see [Section 8.2](#) for more details.

4 Classification error

This section includes upper bounds on the classification error of the unregularized min-norm LS solution $\hat{\boldsymbol{\eta}}_{\text{LS}}$ and ℓ_2 -regularized LS solution $\hat{\boldsymbol{\eta}}_\tau$ for the isotropic, balanced and bi-level ensembles. The implications of our bounds on $\hat{\boldsymbol{\eta}}_{\text{LS}}$ and $\hat{\boldsymbol{\eta}}_\tau$ are discussed later in [Sections 5 and 6](#). The bounds that we provide can be achieved with probability $1 - \delta$ over the randomness of the training set. We will assume throughout that $0 \leq \delta \leq 1/C$ for some universal constant C .

4.1 Balanced ensemble

Recall from [Lemma 1](#) that $\hat{\boldsymbol{\eta}}^T \boldsymbol{\eta} > 0$ is needed to ensure that $\mathcal{R}(\hat{\boldsymbol{\eta}}) < 1/2$. The following lemma shows that this favorable event occurs with high probability provided sufficiently large overparameterization and high SNR.

Lemma 2. *Assume the balanced $\boldsymbol{\Sigma}$ ensemble ([Definition 2.1](#)). Fix $\delta \in (0, 1)$ and suppose n is large enough such that $n > c \log(1/\delta)$ for some $c > 1$. Then, there exist constants $C_1, C_2 > 1$ such that with probability at least $1 - \delta$, $\hat{\boldsymbol{\eta}}_\tau^T \boldsymbol{\eta} > 0$ provided that*

$$\|\boldsymbol{\eta}\|_2^2 > \frac{C_1 n \sigma^2}{\tau + \|\boldsymbol{\lambda}\|_1} + C_2 \sigma. \quad (11)$$

We are now ready to state our main result for the balanced ensemble.

Theorem 3. *Assume the balanced $\boldsymbol{\Sigma}$ ensemble ([Definition 2.1](#)). Fix $\delta \in (0, 1)$ and suppose large enough $n > c \log(1/\delta)$ for some $c > 1$. Further assume that [\(11\)](#) holds for constants C_1 and $C_2 > 1$. Then, there exists constants $C_3, C_4 > 1$ such that with probability at least $1 - \delta$,*

$$\mathcal{R}(\hat{\boldsymbol{\eta}}_\tau) \leq \exp \left(\frac{- \left(\|\boldsymbol{\eta}\|_2^2 - \frac{C_1 n \sigma^2}{\tau + \|\boldsymbol{\lambda}\|_1} - C_2 \sigma \right)^2}{C_3 \max \left\{ 1, \frac{n^2 \sigma^2}{(\tau + \|\boldsymbol{\lambda}\|_1)^2} \right\} \|\boldsymbol{\lambda}\|_2^2 + C_4 \sigma^2} \right). \quad (12)$$

The bound for the unregularized LS estimator $\hat{\boldsymbol{\eta}}_{\text{LS}}$ can be obtained from [\(12\)](#) by setting $\tau = 0$. Thus, with probability at least $1 - \delta$, $\mathcal{R}(\hat{\boldsymbol{\eta}}_{\text{LS}})$ is upper bounded by

$$\exp \left(\frac{- \left(\|\boldsymbol{\eta}\|_2^2 - \frac{C_1 n \sigma^2}{\|\boldsymbol{\lambda}\|_1} - C_2 \sigma \right)^2}{C_3 \max \left\{ 1, \frac{n^2 \sigma^2}{\|\boldsymbol{\lambda}\|_1^2} \right\} \|\boldsymbol{\lambda}\|_2^2 + C_4 \sigma^2} \right). \quad (13)$$

By [\(13\)](#) we notice that the classification error depends on $\|\boldsymbol{\eta}\|_2^2$, $\|\boldsymbol{\lambda}\|_2^2$ and σ^2 . Specifically, increasing $\|\boldsymbol{\eta}\|_2^2$ and/or decreasing either $\|\boldsymbol{\lambda}\|_2^2$ or σ^2 can make the bound smaller. Increasing overparameterization can also help the bound decrease. To see that, consider for example the case $\lambda_1 = \lambda_2 = \dots = \lambda_p$. Then, $\frac{n \sigma^2}{\|\boldsymbol{\lambda}\|_1} = \frac{n}{p} \|\boldsymbol{\eta}\|_2^2$ is directly related to the overparameterization ratio p/n and the numerator becomes $(\|\boldsymbol{\eta}\|_2^2 (1 - C_1 \frac{n}{p}) - C_2 \sigma)^2$.

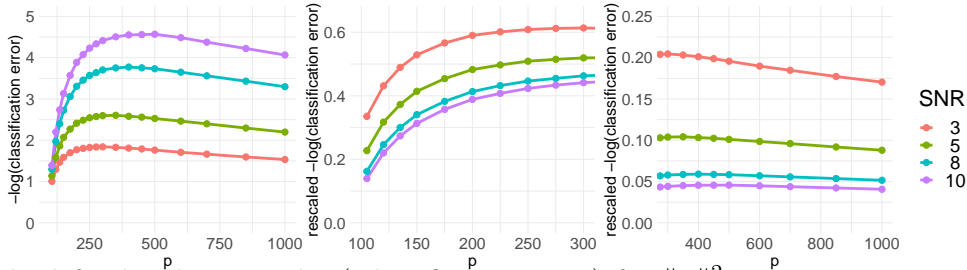


Figure 2: The left plot depicts $-\log(\text{classification error})$ for $\|\boldsymbol{\eta}\|_2^2 = 3, 5, 8, 10$ as a function of p . The middle and right figures depict $-\log(\text{test error})/\|\boldsymbol{\eta}\|_2^2$ for small p (aka High-SNR regime) and $-\log(\text{test error})/\|\boldsymbol{\eta}\|_2^4$ for large p (aka Low-SNR regime), respectively. The rescalings are as suggested by our bounds (15) and (16), respectively. Note that, after rescaling, the error curves indeed become almost parallel as suggested by Corollary 4.1.

4.2 Isotropic ensemble

We have a slightly sharper bound on the classification error of the unregularized estimator in the isotropic regime, which is also easier to interpret. For simplicity, we only state the result for the min-norm interpolating solution (aka $\tau = 0$).

Theorem 4. *Assume $\boldsymbol{\Sigma} = \mathbf{I}$. Fix $\delta \in (0, 1)$ and suppose large enough $n > c \log(1/\delta)$ for some $c > 1$. There exist constants $C, b > 1$ such that with probability at least $1 - \delta$, $\hat{\boldsymbol{\eta}}_{\text{LS}}^T \boldsymbol{\eta} > 0$ provided that $p > b \cdot n$ and $(1 - \frac{n}{p})\|\boldsymbol{\eta}\|_2 > C$. Further assume that these two conditions hold for $C, b > 1$. Then, there exist constants $C_1, C_2 > 1$ such that with probability at least $1 - \delta$:*

$$\mathcal{R}(\hat{\boldsymbol{\eta}}_{\text{LS}}) \leq \exp\left(-\|\boldsymbol{\eta}\|_2^2 \frac{\left((1 - \frac{n}{p})\|\boldsymbol{\eta}\|_2 - C_1\right)^2}{C_2\left(\frac{p}{n} + \|\boldsymbol{\eta}\|_2^2\right)}\right). \quad (14)$$

The bound depends on the overparameterization ratio p/n and the SNR $\|\boldsymbol{\eta}\|_2^2$ when $\boldsymbol{\Sigma} = \mathbf{I}$. To clarify the dependence, it is instructive to consider separately the following two regimes. (a) High-SNR regime: $\|\boldsymbol{\eta}\|_2^2 > \frac{p}{n}$. (b) Low-SNR regime: $\|\boldsymbol{\eta}\|_2^2 \leq \frac{p}{n}$.

The following is an immediate corollary of Theorem 4 specialized to the two regimes

Corollary 4.1. *Let the same assumptions of Theorem 4 hold. Then, there exists constants $C_1 > 1, C_2 > 0$ such that with probability at least $1 - \delta$, in the high-SNR regime:*

$$\mathcal{R}(\hat{\boldsymbol{\eta}}_{\text{LS}}) \leq \exp\left(-C_2 \cdot \|\boldsymbol{\eta}\|_2^2 \cdot \left(\left(1 - \frac{n}{p}\right) - C_1 \frac{1}{\|\boldsymbol{\eta}\|_2}\right)^2\right), \quad (15)$$

and, in the low-SNR regime:

$$\mathcal{R}(\hat{\boldsymbol{\eta}}_{\text{LS}}) \leq \exp\left(-C_2 \cdot \|\boldsymbol{\eta}\|_2^4 \frac{\left(\left(1 - \frac{n}{p}\right) - C_1 \frac{1}{\|\boldsymbol{\eta}\|_2}\right)^2}{p/n}\right). \quad (16)$$

We use simulations to validate the above bounds. In Fig. 2(Left) we fix $n = 100$ and plot the classification error (in log-scale) as a function of p for four different SNR values 3, 5, 8 and 10. Observe that $-\log \mathcal{R}(\hat{\boldsymbol{\eta}}_{\text{LS}})$ initially increases until it reaches its maximum at some value of $p > n$ and then decreases as p gets even larger. This “increasing/decreasing” pattern is explained by the transition from the high-SNR to the low-SNR regime as per Corollary 4.1. On one hand, the negative of the exponent of the high-SNR bound (15) is increasing with p for $\|\boldsymbol{\eta}\|_2^2$. On the other hand, as p increases, and we move in the low-SNR regime, the negative of the exponent in (16) decreases with p when p is large enough. Additionally, in Figs. 2(Middle,Right), we plot re-normalized values $-\log \mathcal{R}(\hat{\boldsymbol{\eta}}_{\text{LS}})/\|\boldsymbol{\eta}\|_2^2$ and $-\log \mathcal{R}(\hat{\boldsymbol{\eta}}_{\text{LS}})/\|\boldsymbol{\eta}\|_2^4$. Notice that after appropriate normalization the curves become almost parallel to each other and almost overlap for large values of $\|\boldsymbol{\eta}\|_2^2$, as suggested by (15) and (16).

4.3 Bi-level ensemble

In this section we study the classification error under the bi-level ensemble in Definition 2.2, i.e. when one eigenvalue of Σ is much larger than the rest. Compared to the balanced ensemble, the analysis here depends on a more intricate way on the interaction between the mean vector and the spectrum of Σ . To better understand this interaction we will assume β is one-sparse, i.e., the signal is concentrated in one direction. We will also assume, this time without loss of generality,² that Σ is diagonal; thus, $\beta = \eta$. Hence, taking β to be one-sparse with (say) the k -th element non-zero, the SNR becomes $\frac{\beta_k^2}{\lambda_k} = \frac{\eta_k^2}{\lambda_k}$. Specifically, $k = 1$ corresponds to the smallest SNR, for which we expect highest classification risk among all other choices of k . For better classification performance, large signal and noise components should *not* be in the same direction. This motivates the following assumption.

Assumption 1. The covariance matrix Σ is diagonal and its diagonal elements follow the bi-level structure in Definition 2.2. η is one-sparse with nonzero k -th element η_k and $k \neq 1$.

Under Assumption 1, the signal strength in the direction of Σ is $\sigma^2 = \lambda_k \eta_k^2$ and the ratio needed to be lower bounded $\frac{(\hat{\eta}^T \eta)^2}{\hat{\eta}^T \Sigma \hat{\eta}}$ becomes $\frac{(\eta_k \eta_k)^2}{\sum_{i=1}^p \lambda_i \eta_k^2}$. The following theorem establishes an upper bound on the classification risk for this setting.

Theorem 5. *Let Assumption 1 hold. Fix $\delta \in (0, 1)$ and large enough $n > c \log(1/\delta)$ for some $c > 1$. Let Assumption 1 hold. Then, there exist constants $c_1, c_2 > 1$ such that with probability at least $1 - \delta$, $\hat{\eta}_\tau^T \eta > 0$ provided that $\eta_k^2 > \frac{c_1 n \sigma^2}{\tau + \|\lambda\|_{-1}} + c_2 \sigma$. Further assuming the above condition holds, there exist constants C_i 's > 1 such that with probability at least $1 - \delta$,*

$$\mathcal{R}(\hat{\eta}_\tau) \leq \exp\left(\frac{-\left(\eta_k^2 \left(1 - \frac{C_1 n \lambda_k}{\tau + \|\lambda\|_{-1}}\right) - C_2 \sigma\right)^2}{A + B + C_6(\lambda_k^2 + \sigma^2)}\right) \quad (17)$$

with $A = C_3 \lambda_1^2 \left(\frac{\tau + \|\lambda\|_{-1} + C_4 n \sigma}{\tau + \|\lambda\|_{-1} + n \lambda_1}\right)^2$ and $B = C_5 \left(\sum_{i \neq 1, k} \lambda_i^2\right) \left(1 + \frac{C_4 n \sigma}{\tau + \|\lambda\|_{-1}}\right)^2$.

A bound for unregularized estimator $\hat{\eta}_{\text{LS}}$ can be obtained by setting $\tau = 0$. Recall the SNR under Assumption 1 is $\frac{\eta_k^4}{\sigma^2} = \frac{\eta_k^2}{\lambda_k}$. We observe that the bound above depends not only on the SNR, but also on λ_i , for $i \neq k$, i.e., the spectrum of Σ in *every* direction. Note that similar to previous sections, in (17), the term $\frac{n \lambda_k}{\tau + \|\lambda\|_{-1}}$ on the numerator is related to the sufficiency of overparameterization. As we will see, the role of regularization in the bi-level ensemble is more subtle compared to the balanced ensemble and will be discussed in Section 6.

5 SVM generalization under high overparameterization

Now that we have captured the classification error of the min-norm LS estimator $\hat{\eta}_{\text{LS}}$ in (13) and (14), and we have established conditions ensuring $\hat{\eta}_{\text{LS}} = \hat{\eta}_{\text{SVM}}$ in Theorem 1 and Theorem 2, we establish sufficient conditions under which the classification error of hard-margin SVM vanishes as the overparameterization ratio p/n increases. Note that the bi-level ensemble will *not* satisfy the first condition in Theorem 1, hence we focus on the balanced and isotropic ensembles. For later use, define the term in (8) as $\lambda_* := 72(\|\lambda\|_2 \cdot n \sqrt{\log n} + \|\lambda\|_\infty \cdot n \sqrt{n} \log n + 1)$. We first focus on a special case where $\beta = [\beta \ \beta \ \dots \ \beta]^T$ for simplicity.

Corollary 5.1. *Let the same assumption as in Theorem 3 hold with $\tau = 0$ and sufficiently large $n > C/\delta$ for some $C > 1$. Also let $\beta = [\beta \ \beta \ \dots \ \beta]^T$. Then, for large C_i 's > 1 , with probability at least $(1 - \delta)$, $\hat{\eta}_{\text{SVM}}$ linearly interpolates the data and the classification error $\mathcal{R}(\hat{\eta}_{\text{SVM}})$ approaches 0 as $p \rightarrow \infty$ provided the two following sets of conditions on $\|\lambda\|_1$ hold:*

$$\|\lambda\|_1 > \max\{\lambda_*, C_1 \beta^2 n^2 \log(2n)\} \quad \text{and} \quad \max\{\beta^{-2} \|\lambda\|_2^2, \|\lambda\|_1\} \leq C_2 \beta^2 p^\alpha, \quad \text{for } \alpha < 2.$$

²Recall $\Sigma = \mathbf{V} \Lambda \mathbf{V}^T$ and $\eta = \mathbf{V} \beta$. Thus, $\mathbf{X} = \mathbf{y} \eta^T + \mathbf{Q} = (\mathbf{y} \beta^T + \mathbf{Z} \Lambda^{\frac{1}{2}}) \mathbf{V}^T =: \widetilde{\mathbf{X}} \mathbf{V}^T$, where $\mathbf{Z} \in \mathbb{R}^{n \times p}$ has IID standard normal entries. With this, it is not hard to check that $\frac{(\hat{\eta}^T \eta)^2}{\hat{\eta}^T \Sigma \hat{\eta}} = \frac{(\mathbf{y}^T (\mathbf{X} \mathbf{X}^T + \tau \mathbf{I})^{-1} \mathbf{X} \eta)^2}{\mathbf{y}^T (\mathbf{X} \mathbf{X}^T + \tau \mathbf{I})^{-1} \mathbf{X} \Sigma \mathbf{X}^T (\mathbf{X} \mathbf{X}^T + \tau \mathbf{I})^{-1} \mathbf{y}} = \frac{(\mathbf{y}^T (\widetilde{\mathbf{X}} \widetilde{\mathbf{X}}^T + \tau \mathbf{I})^{-1} \widetilde{\mathbf{X}} \beta)^2}{\mathbf{y}^T (\widetilde{\mathbf{X}} \widetilde{\mathbf{X}}^T + \tau \mathbf{I})^{-1} \widetilde{\mathbf{X}} \Lambda \widetilde{\mathbf{X}}^T (\widetilde{\mathbf{X}} \widetilde{\mathbf{X}}^T + \tau \mathbf{I})^{-1} \mathbf{y}}$. Hence, after a change of basis, we can equivalently analyze the simplified model with diagonal covariance: $\widetilde{\mathbf{x}} = \mathbf{y} \beta + \widetilde{\mathbf{q}}, \widetilde{\mathbf{q}} \sim N(\mathbf{0}, \Lambda)$.

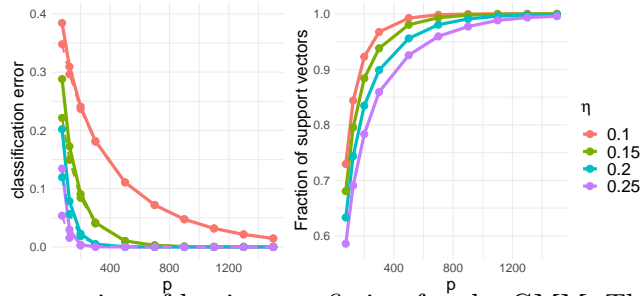


Figure 3: Numerical demonstration of benign overfitting for the GMM. The left plot shows the classification error with $n = 50$ and mean vector $\boldsymbol{\eta}$ with entries $\eta_1 = \dots = \eta_p = \eta$. The solid lines correspond to the LS estimates and the (almost overlapping) dashed lines show the SVM solutions. The error vanishes with $p \rightarrow \infty$ indicating benign overfitting as predicted by Corollary 5.1. The right plot illustrates the proportion of support vectors in the same setting.

The first condition above requires sufficient overparameterization and the second one a large enough SNR. To see that, note for the setting of Corollary 5.1 that $\text{SNR} = p^2 \beta^2 / \|\boldsymbol{\lambda}\|_1$. Thus, the second condition imposes $\text{SNR} \geq cp^{2-\alpha}$ implying that $\text{SNR} \geq cp^\epsilon$ for some $\epsilon > 0$.

Corollary 5.1 assumes that $\boldsymbol{\beta}$ has equal elements. Now we allow the mean vector $\boldsymbol{\eta}$ to have different entry values but let $\boldsymbol{\Sigma} = \mathbf{I}$, then we have the following result.

Corollary 5.2. *Let the same assumptions as in Theorem 4 hold and n sufficiently large such that $n > C/\delta$ for some $C > 1$, thus $\boldsymbol{\Sigma} = \mathbf{I}$. Then, for large enough positive constant C_i 's > 1 , $\hat{\boldsymbol{\eta}}_{\text{SVM}}$ linearly interpolates the data and the classification error $\mathcal{R}(\hat{\boldsymbol{\eta}}_{\text{SVM}})$ approaches zero as $(p/n) \rightarrow \infty$ with probability at least $(1 - \delta)$ provided either of the two following sets of conditions on the number of features p and mean-vector $\boldsymbol{\eta}$ hold:*

(1). *High-SNR regime*

$$\frac{1}{C_1} n \|\boldsymbol{\eta}\|_2^2 > p > \max\{10n \log n + n - 1, C_2 n \sqrt{\log(2n)} \|\boldsymbol{\eta}\|_2\}.$$

(2). *Low-SNR regime*

$$p > \max\{10n \log n + n - 1, C_3 n \sqrt{\log(2n)} \|\boldsymbol{\eta}\|_2, n \|\boldsymbol{\eta}\|_2^2\}, \text{ and } \|\boldsymbol{\eta}\|_2^4 \geq C_4 \left(\frac{p}{n}\right)^\alpha, \text{ for } \alpha > 1.$$

We first compare Corollaries 5.1 and 5.2 assuming both $\boldsymbol{\Sigma} = \mathbf{I}$ and $\boldsymbol{\beta} = [\beta \ \beta \ \dots \ \beta]^T$. Then $\|\boldsymbol{\lambda}\|_1 = \|\boldsymbol{\lambda}\|_2^2 = p$ and $\|\boldsymbol{\eta}\|_2^2 = \|\boldsymbol{\beta}\|_2^2 = p\beta$. It is not hard to check that under those assumptions, they both require $p > Cn^2 \log(2n)$, for sufficiently large constant C . One might expect that a sharper condition can be obtained by Corollary 5.2 when $\boldsymbol{\Sigma} = \mathbf{I}$. Unfortunately, that is not the case because although the first condition in Theorem 2 is sharper than that of Theorem 1, the second conditions become equivalent when $\boldsymbol{\Sigma} = \mathbf{I}$ and $\boldsymbol{\beta} = [\beta \ \beta \ \dots \ \beta]^T$ and are stronger than the first condition.

Remark 1 (Comparison of noiseless conditions to Chatterji and Long [2020]). Using different tools to directly analyze $\hat{\boldsymbol{\eta}}_{\text{SVM}}$ (see Section 9.2.3), Chatterji and Long [2020, Thm. 3.1] proved that for noisy mixtures with possibly adversarial corruptions and with subGaussian features

$$p > C_1 \max\{n \|\boldsymbol{\eta}\|_2^2, n^2 \log(n)\} \text{ and } \|\boldsymbol{\eta}\|_2^4 \geq C_2 p^\alpha, \alpha > 1, \quad (18)$$

suffice for benign overfitting, i.e., for making the classification error asymptotically approach the noise level as $p/n \rightarrow \infty$. Our corollary 5.2 holds for the special case of Gaussian features and *noiseless* labels. Since labels are not corrupted, the noise floor is zero. In this special case, our result relaxes significantly the sufficient conditions for which the risk approaches zero compared to a direct application of their result. To see this note that condition (18) is reminiscent of our ‘low-SNR regime’ condition (2) in Corollary 5.2. First, our condition relaxes the requirement on overparameterization from $p > Cn^2 \log(n)$ in (18) to $p > Cn \sqrt{\log(2n)}$. Second, our condition $\|\boldsymbol{\eta}\|_2^4 = \omega(p/n)$ on the SNR can be equivalent to theirs $\|\boldsymbol{\eta}\|_2^4 = \omega(p)$, for example in a setting of constant n . In order to better

understand different conditions, consider a somewhat concrete setting in which n is fixed and only p and $\|\boldsymbol{\eta}\|_2$ grow large. Then for the classification error to go to 0 as $p \rightarrow \infty$, [Chatterji and Long \[2020\]](#) requires (see (18)) that $\|\boldsymbol{\eta}\|_2 = \Theta(p^\beta)$ for $\beta \in (\frac{1}{4}, \frac{1}{2}]$. Instead, our [Corollary 5.2](#) requires that $\|\boldsymbol{\eta}\|_2 = \Theta(p^\beta)$, $\beta \in (1/4, 1/2]$ (low-SNR) or $\|\boldsymbol{\eta}\|_2 = \Theta(p^\beta)$ for $\beta \in (1/2, 1)$ (high-SNR). We repeat that this improvement is for zero label noise. In [Section 7](#), where we study a noisy GMM, we show that our *sufficient* conditions can indeed change in the noisy case.

Finally, we present numerical illustrations validating [Corollary 5.1](#). In [Fig. 3](#), we let $\eta_1 = \dots = \eta_p = \eta$ with $\eta = 0.1, 0.15, 0.2$ or 0.25 . Thus, $\|\boldsymbol{\eta}\|_2^2 = \eta^2 p$. We also fix $n = 50$. The eigenvalues of $\boldsymbol{\Sigma}$ are generated as follows: $\lambda_1 = 0.005p$, $\lambda_p = 0.2 \cdot \frac{0.995p}{p-1}$ and $\lambda_2 = \dots = \lambda_{p-1} = \frac{p-\lambda_1-\lambda_{p-1}}{p-2}$. This setting is different from the isotropic case, but ensures $\|\boldsymbol{\lambda}\|_1 \leq C_1 p$, $\|\boldsymbol{\lambda}\|_2 \leq C_2 p^{1/2}$ and conditions in [Corollary 5.1](#) are satisfied. In [Fig. 3\(Left\)](#), we plot the classification error as a function of p for both LS estimates (solid lines) and SVM solutions (dashed lines). The solid and dashed curves almost overlap, so it can be hard to distinguish in the figure. We verify that as p increases, the classification error decreases towards zero. Similarly, [Fig. 3\(Right\)](#) reaffirms that all the data points become support vectors for sufficiently large p (cf. [Theorem 2](#)). In addition, [Fig. 3\(Left\)](#) shows that the classification error of SVM solutions is slightly better than that of LS estimates when p is small. The error becomes the same for large p , since then the SVM solutions are the same as LS solutions. Another observation is that the classification error goes to zero very fast when SNR is high (e.g., purple curves), but the probability of interpolation increases at a slow rate. In contrast, when the SNR is low (e.g., red curves), the probability of interpolation increases fast, but the classification error decreases slowly. Intuitively, the harder the classification task (aka lower SNR), the larger the classification error and the more data points become support vectors.

6 On the role of regularization

In this section, we discuss how the ℓ_2 -regularization affects the classification error of $\hat{\boldsymbol{\eta}}_\tau$ under the balanced and bi-level ensembles. For convenience, we start with a brief summary of our findings.

(a). Balanced ensemble:

1. The classification error is decreasing with τ . Thus, it is minimized as $\tau \rightarrow +\infty$.
2. Our bounds verify that in the limit $\tau \rightarrow +\infty$, $\hat{\boldsymbol{\eta}}_\tau$ has the same error as the so-called averaging estimator $\hat{\boldsymbol{\eta}}_{\text{Avg}} = \frac{1}{n} \sum_{i \in [n]} y_i \mathbf{x}_i$, where \mathbf{x}_i^T is the i -th row of \mathbf{X} .
3. The averaging estimator is the best among the ridge-regularized estimator and the LS interpolating estimator.

(b). Bi-level ensemble:

1. Our upper bound on the classification error is *not* monotonically decreasing with τ . Hence regularization might *not* be helpful and the averaging estimator is *not* optimal.
2. There are regimes where $\tau = 0$ is optimal. Specifically, the interpolating estimator performs the best when λ_1 is large enough compared to other eigenvalues of $\boldsymbol{\Sigma}$ and overparameterization is sufficient.

These observations are illustrated in [Figures 4, 5 and 6](#) which are discussed in detail in the next sections.

6.1 Balanced ensemble

We first analyze the bound in (12). Observe that both the terms $\frac{C_1 n \sigma^2}{\tau + \|\boldsymbol{\lambda}\|_1}$ in the numerator and $\frac{n^2 \sigma^2}{(\tau + \|\boldsymbol{\lambda}\|_1)^2}$ in the denominator decrease as the regularization parameter τ becomes larger. This suggests that, under the balanced ensemble, increasing regularization always helps decrease the error. The remaining terms, σ and $\|\boldsymbol{\lambda}\|_2^2$ in (12), that are not affected by changing τ reflect the intrinsic structure of the

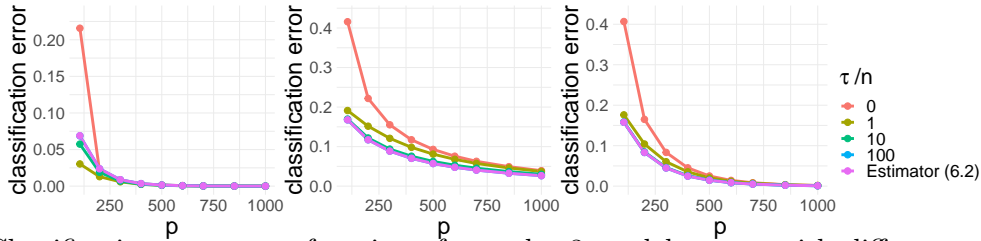


Figure 4: Classification error as a function of p under 3 model setups with different regularization parameter values τ . In the right plot all η_i 's are the same. The middle/left ones correspond to the extreme cases of largest/smallest values σ^2 ; see text for details. Also plotted (in magenta) the averaging estimator defined in (20). As predicted by our theory, for fixed $\|\boldsymbol{\eta}\|_2$ and $\|\boldsymbol{\lambda}\|_2^2$, larger τ and smaller σ^2 lead to better performance and $\hat{\boldsymbol{\eta}}_\tau$ has the same performance as $\hat{\boldsymbol{\eta}}_{\text{Avg}}$ when τ is large.

model and characterize the difficulty of the learning task. As $\tau \rightarrow +\infty$, the “regularization-sensitive” terms vanish and only those “regularization-insensitive” terms remain. Specifically, the upper bound on classification error becomes

$$\exp\left(-\left(\frac{\|\boldsymbol{\eta}\|_2^2}{\sigma} - C_2\right)^2 / \left(C_3 \frac{\|\boldsymbol{\lambda}\|_2^2}{\sigma^2} + C_4\right)\right). \quad (19)$$

In Appendix F we show that the bound in (19) is the same as the bound for the so-called averaging estimator which simply returns

$$\hat{\boldsymbol{\eta}}_{\text{Avg}} = \mathbf{X}^T \mathbf{y} / n. \quad (20)$$

Therefore, under the balanced ensemble, the classification performance of the averaging estimator is superior to that of the ridge and interpolating estimators. A similar finding was recently reported in Mignacco et al. [2020], but in an asymptotic setting and only for the isotropic case.

We now use numerical simulations to validate the above claims. In our simulations in Fig. 4, we fix $n = 100$ and vary p . To check (12), for each p , we set $\|\boldsymbol{\lambda}\|_2$ to be p and $\lambda_1 = \sqrt{0.0125p}$, $\lambda_p = \sqrt{0.000125p}$ and all the rest λ_i 's are $\sqrt{(p - \lambda_1^2 - \lambda_p^2)/(p - 2)}$. This setup makes λ_1 slightly larger than other λ_i 's and λ_p slightly smaller. For example, when $p = 1000$, then $\lambda_1 = 3.53$, $\lambda_p = 0.35$ and all other λ_i 's are 0.99. Note that although λ_i 's are not equal, those settings still satisfy the requirements of the balanced ensemble. Then, we look at different signals $\boldsymbol{\eta}$ with the same strength $\|\boldsymbol{\eta}\|_2^2 = (0.125^2)p$. To make σ^2 in (12) different, we consider 3 cases: all η_i 's are the same, only η_1 nonzero and only η_p nonzero. The right plot in Fig. 4 shows the classification error of the same- η_i case, the middle one shows the nonzero- η_1 case and the left plot shows the nonzero- η_p case. To see the role of regularization, we look at the classification error with different τ values and also include the averaging estimator. We can see that among the three plots, the nonzero- η_p case (left) has the smallest classification error and the nonzero- η_1 case (middle) has the largest classification error. This is in agreement with the fact that the nonzero- η_p case has the smallest σ^2 and the nonzero- η_1 case has the largest σ^2 . For large p , regularization always helps reduce the classification error. When τ is large, the performance of $\hat{\boldsymbol{\eta}}_\tau$ becomes the same as that of $\hat{\boldsymbol{\eta}}_{\text{Avg}}$. All those observations are consistent with Theorem 3.

6.2 Bi-level ensemble

We have seen that regularization is always useful in reducing the classification risk in the balanced ensemble. For the bi-level ensemble, the story is quite different: the classification error is no longer monotonically decreasing as τ increases. Recall that under Assumption 1, with high probability, $\mathcal{R}(\hat{\boldsymbol{\eta}}_\tau)$ is upper bounded by (17). Moreover, when τ goes to infinity, it is not hard to check that this bound matches the corresponding for the averaging estimator (see Appendix F). Thus, in this case the averaging estimator is *not* optimal.

To see why (17) is no longer monotonically decreasing in τ , the term $\frac{\tau + \|\boldsymbol{\lambda}\|_{-1} + C_4 n \sigma}{\tau + \|\boldsymbol{\lambda}\|_{-1} + n \lambda_1}$ in A is increasing in τ and thus A is increasing in τ when $\lambda_1 > C_4 \sigma = C_4 \sqrt{\lambda_k} \eta_k$, i.e., when λ_1 is large enough compared

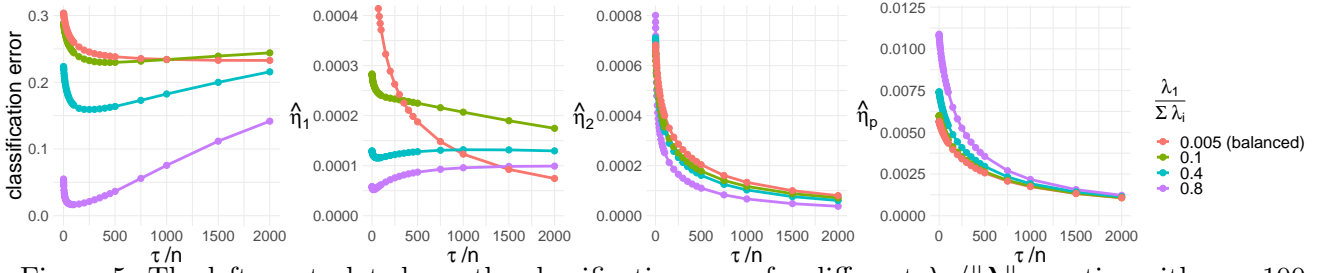


Figure 5: The left-most plot shows the classification error for different $\lambda_1/\|\boldsymbol{\lambda}\|_{-1}$ ratios with $n = 100$ and mean vector $\boldsymbol{\eta}$ with entries $\eta_1 = \dots = \eta_{p-1} = 0$ and $\eta_p = \sqrt{200}$. Other plots show how $\hat{\eta}_i$'s vary with τ . As predicted by the theory, under the balanced ensemble, $\hat{\eta}_1$ and $\hat{\eta}_2$ decrease at similar rates, but have different behaviors when $\boldsymbol{\Sigma}$ has a highly spiky eigen-structure. See text for details.

to λ_k and η_k . Note that (17) is obtained by lower bounding $\frac{(\eta_k \hat{\eta}_k)^2}{\sum_{i=1}^p \lambda_i \hat{\eta}_i^2}$ and A is related to the term $\lambda_1 \hat{\eta}_1^2$, i.e., the estimate in the direction of λ_1 . Since λ_1 is much larger than others, even if the regularization is useful in other directions, the performance won't keep improving as τ increases, because it won't help in the direction with the largest "noise". Term B in (17), on the other hand, is related to $\lambda_i \hat{\eta}_i^2$, for $i \neq 1$ or k , and it becomes smaller as τ becomes larger, thus regularization is useful in these directions. B becomes less important than A if λ_1 becomes larger than other λ_i 's, hence the regularization becomes less helpful in this case. Another observation is that in the numerator of (17), the term $\frac{n\lambda_k}{\tau + \|\boldsymbol{\lambda}\|_{-1}}$ decreases as τ increases. Note that when $\lambda_2 = \dots = \lambda_p$, $\frac{n\lambda_k}{\|\boldsymbol{\lambda}\|_{-1}} = \frac{n}{p-1}$, hence this term measures the sufficiency of overparameterization. When the overparameterization is sufficient, i.e., p is much larger than n , $\frac{n\lambda_k}{\|\boldsymbol{\lambda}\|_{-1}}$ is already very small, hence $\frac{n\lambda_k}{\tau + \|\boldsymbol{\lambda}\|_{-1}}$ won't be much smaller than $\frac{n\lambda_k}{\|\boldsymbol{\lambda}\|_{-1}}$ even for large τ . In other words, strong regularization won't help very much. Summarizing all those observations, we conclude that the regularization becomes less useful in reducing the classification error when λ_1 is large enough relative to other eigenvalues and when overparameterization is sufficient. Under those conditions, $\tau = 0$ minimizes (17), therefore, the interpolating estimator $\hat{\boldsymbol{\eta}}_{\text{LS}}$ has better performance than the regularized estimators. Since small or zero regularization can provide the best estimation in the bi-level setting with Assumption 1 in the overparameterization regime, it seems that the model structure itself provides the implicit regularization. This phenomenon is also discussed in Bartlett et al. [2020], Muthukumar et al. [2020b], Kobak et al. [2018], Muthukumar et al. [2020a], Tsigler and Bartlett [2020].

The following numerical experiments validate our analysis. First in Fig. 5, we illustrate how the ratio $\lambda_1/\|\boldsymbol{\lambda}\|_{-1}$ affects the classification error and the role of regularization. In our simulation, $n = 100$, $p = 200$. $\boldsymbol{\eta} \in \mathbb{R}^{200}$ is one-sparse and only the last element is non-zero, i.e., $\boldsymbol{\eta}^T = [0, 0, \dots, 0, \sqrt{200}]$. For the eigenvalues of $\boldsymbol{\Sigma}$, in the balanced ensemble, the diagonal elements are all equal, i.e., $\lambda_1 = \dots = \lambda_{200} = 150$. In the bi-level ensemble, we fix $\|\boldsymbol{\lambda}\|_1 = 200 \cdot 150$ and let $\lambda_1 = \alpha \|\boldsymbol{\lambda}\|_1$, with $\alpha = 0.1, 0.4$ and 0.8 . Then $\lambda_2 = \dots = \lambda_p = (1 - \alpha) \cdot \|\boldsymbol{\lambda}\|_1 / (p - 1)$. Note that larger α makes $\lambda_1/\|\boldsymbol{\lambda}\|_{-1}$ higher and that $\alpha = 0.005$ in the balanced ensemble. Fig. 5 illustrates how classification error and $\hat{\eta}_i$'s change with the regularization parameter τ . Based on previous analysis, we divide those $\hat{\eta}_i$'s into 3 groups, $\{\hat{\eta}_1; \hat{\eta}_2, \dots, \hat{\eta}_{199}; \hat{\eta}_{200}\}$. $\hat{\eta}_1$ has true value 0 with large noise, $\hat{\eta}_2, \dots, \hat{\eta}_{199}$ have true value 0 with small noise and $\hat{\eta}_{200}$ has non-zero true value with small noise. The figures show $\hat{\eta}_1$, $\hat{\eta}_2$ and $\hat{\eta}_{200}$. We can see that the classification error keeps decreasing as τ increases for the balanced ensemble (red curves). Part of the reason is that $\hat{\eta}_1$, $\hat{\eta}_2$ and $\hat{\eta}_{200}$ decrease at similar rates. In contrast, for the bi-level regime, as τ increases, the classification error decreases first, then increases. $\hat{\eta}_2$ decreases with τ , but $\hat{\eta}_1$ increases slowly with τ for large τ when $\lambda_1/\|\boldsymbol{\lambda}\|_{-1}$ is large. This is consistent with Theorem 5 in which A is increasing in τ when λ_1 is large enough. When λ_1 is not large enough, as the green curve shows, $\hat{\eta}_1$ decreases at a similar rate as $\hat{\eta}_2$ and all the curves are closer to those of the balanced ensemble.

Finally, we illustrate how the overparameterization ratio p/n affects the role of regularization in Fig. 6 (a). Here to guarantee p/n sufficiently large, we fix $n = 30$. We plot how the classification error changes with τ for $p = 75, 100, 200, 300$ and 500 . $\boldsymbol{\eta}$ is one-sparse with $\eta_p = 25$. For eigenvalues of $\boldsymbol{\Sigma}$, to make $\lambda_1/\|\boldsymbol{\lambda}\|_{-1}$ sufficiently large, we set $\lambda_2 = \dots = \lambda_p = 50$ and $\lambda_1 = 10\|\boldsymbol{\lambda}\|_{-1}$. We observe from

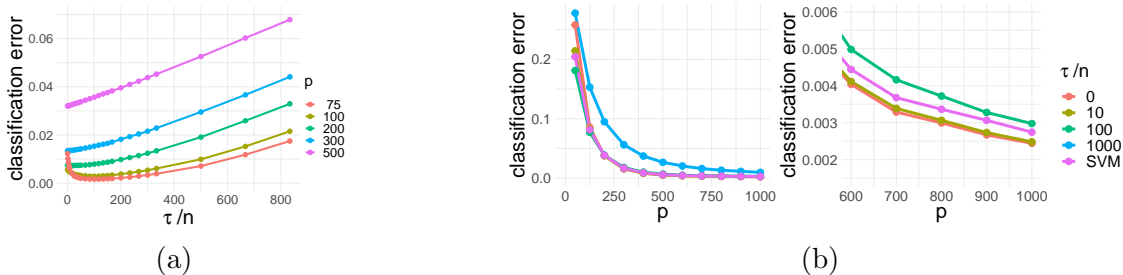


Figure 6: For all the plots here, we fix $n = 30$, $\lambda_2 = \dots = \lambda_p = 50$ and $\lambda_1/\|\boldsymbol{\lambda}\|_{-1} = 10$ (corresponding to the bi-level ensemble). (a) Classification error versus τ/n for different p and fixed $\eta_p = 25$. Observe that the classification error increases monotonically with τ for large p . (b) A regime where $\hat{\boldsymbol{\eta}}_{\text{LS}}$ performs the best and its classification error approaches 0 as $p \rightarrow \infty$. Specifically, we set here $\eta_p = 0.1\sqrt{50}p^{0.6}$. See text for details.

Fig. 6 (a) that when p is large, the classification error increases with τ , thus $\tau = 0$ performs the best. The optimal choice of τ is larger than 0 when p is not large enough (e.g., $p = 75$ and 100). In Fig. 6 (b), we show a regime where $\hat{\boldsymbol{\eta}}_{\text{LS}}$ performs better than $\hat{\boldsymbol{\eta}}_{\tau}$ and $\hat{\boldsymbol{\eta}}_{\text{SVM}}$ when p is large. Again we fix $n = 30$ to ensure sufficient overparameterization. Same as before, we set $\lambda_2 = \dots = \lambda_p = 50$ and $\lambda_1 = 10\|\boldsymbol{\lambda}\|_{-1}$. To make the classification error approach 0 as $p \rightarrow \infty$, according to Corollary 7.2 in Appendix, we set $\eta_p = 0.1\sqrt{50}p^{0.6}$. Fig. 6 (b)(Left) shows the classification error over different p for various τ . We also added the curve for $\hat{\boldsymbol{\eta}}_{\text{SVM}}$. Fig. 6 (b)(Right) zooms in to $p \geq 600$. The classification error for the case with the largest τ is too large to be shown. We can see that the interpolating estimator $\hat{\boldsymbol{\eta}}_{\text{LS}}$ performs better than the regularized estimators when p is sufficiently large.

7 Noisy GMM: Interpolation and Benign Overfitting

We extend our results to a probabilistic label-noise Gaussian mixture model.

7.1 Model and assumptions

We formally define the noisy model below; note that this is a special case of the adversarial noise model studied in Chatterji and Long [2020].

Definition 7.1 (Noisy GMM). A data pair $(\boldsymbol{x}, y_c) \in \mathbb{R}^p \times \{\pm 1\}$ is generated from the noisy Gaussian mixture model (GMM) with mean vector $\boldsymbol{\eta}$, covariance matrix $\boldsymbol{\Sigma}$ and corruption probability γ as follows. First, the clean data pair (\boldsymbol{x}, y) is generated according to (1). Then the label y_c is generated by flipping the correct label y with probability γ . We assume that γ is independent of everything else (i.e., independent of the label y and the Gaussian noise term \boldsymbol{q}). Also, we assume that $0 \leq \gamma \leq 1/C$ for a large constant C .

We define the label vector with clean/corrupted labels as $\boldsymbol{y}/\boldsymbol{y}_c$. For brevity, we focus here on the isotropic case $\boldsymbol{\Sigma} = \boldsymbol{I}$ and we derive analogues of Theorems 2, 4 and of Corollary 5.2. Throughout this section, we let $\hat{\boldsymbol{\eta}}_{\text{LS}}/\hat{\boldsymbol{\eta}}_{\text{SVM}}$ be the LS and SVM solutions obtained by solving minimizations (4) and (5) but with the unobserved clean label vector \boldsymbol{y} substituted by the observed corrupted vector \boldsymbol{y}_c .

7.2 Interpolation

Our first result establishes the equivalence between SVM and LS solutions for high enough effective overparameterization for noisy GMM data. As we will see, the required overparameterization conditions are now stronger compared to the noiseless case.

Theorem 6. Assume n training samples following the noisy GMM with $\boldsymbol{\Sigma} = \boldsymbol{I}$. There exist large constants C_i 's > 1 such that, if the following conditions on the number of features p and the mean-vector $\boldsymbol{\eta}$ hold:

$$p > C_1 n \log n + n - 1 \quad \text{and} \quad p > C_2 \max\{n\sqrt{\log(2n)}\|\boldsymbol{\eta}\|_2, n\|\boldsymbol{\eta}\|_2^2\}, \quad (21)$$

then, the SVM-solution $\hat{\boldsymbol{\eta}}_{\text{SVM}}$ satisfies the linear interpolation constraint with probability at least $(1 - \frac{C_3}{n})$.

Note the extra term $n\|\boldsymbol{\eta}\|_2^2$ in the second condition above compared to Theorem 2. When $\text{SNR} = \|\boldsymbol{\eta}\|_2^2 = \Omega(\log^{1/2}(n))$, this new condition becomes dominant and the overparameterization ratio p/n should exceed SNR to guarantee interpolation. In Corollary 4.1, we called the regime $p/n \geq \text{SNR}$ the low-noise regime. Hence, in the noisy case, we can guarantee equivalence of the SVM and LS solutions only in the low-SNR regime.

7.3 Error bounds

Our next result upper bounds the risk of the LS estimator. The bound holds in a regime where $\hat{\boldsymbol{\eta}}_{\text{LS}} = \hat{\boldsymbol{\eta}}_{\text{SVM}}$, so it also applies to the risk of the SVM solution.

Theorem 7. *Assume that conditions in (21) hold for noisy GMM data with $\boldsymbol{\Sigma} = \mathbf{I}$. Fix $\delta \in (0, 1)$ and suppose n is large enough such that $n > c/\delta$ for some $c > 1$. Then, there exist constants $C, b > 1$ such that with probability at least $1 - \delta$, $\hat{\boldsymbol{\eta}}_{\text{LS}}^T \boldsymbol{\eta} > 0$ provided that $p > b \cdot n$ and $(1 - \frac{n}{p})\|\boldsymbol{\eta}\|_2 > C$. Further assume that these two conditions hold for $C, b > 1$. Then, there exist constants $C_1, C_2 > 1$ such that with probability at least $1 - \delta$:*

$$\mathcal{R}(\hat{\boldsymbol{\eta}}_{\text{LS}}) \leq \gamma + \exp\left(-C_2 \cdot \|\boldsymbol{\eta}\|_2^4 \frac{((1 - \frac{n}{p}) - C_1 \frac{1}{\|\boldsymbol{\eta}\|_2})^2}{p/n}\right). \quad (22)$$

Since the conditions in (21) hold, we operate here again in the low-SNR regime. The bound has two additive terms. The first term is the noise-level γ which we cannot beat due to the corruptions. The exponential term is the same as the bound for noiseless GMM in the low-SNR regime presented in Corollary 4.1.

Remark 2 (Comparison of risk bounds to Chatterji and Long [2020]). For an adversarial noise model and subGaussian features Chatterji and Long [2020] prove that

$$\mathcal{R}(\hat{\boldsymbol{\eta}}_{\text{SVM}}) \leq \gamma + \exp\left(-C \frac{\|\boldsymbol{\eta}\|_2^4}{p}\right), \quad (23)$$

in the following regime:

$$p > C \max\{n^2 \log(n), n\|\boldsymbol{\eta}\|_2^2\}, \quad \|\boldsymbol{\eta}\|_2^2 \geq C \log(n) \quad \text{and} \quad n \geq C. \quad (24)$$

While our model is a special case of theirs, note that Theorem 7 holds under relaxed assumptions. Specifically, we relax (24) to

$$p > C \max\{n \log(n), n\|\boldsymbol{\eta}\|_2^2\}, \quad \|\boldsymbol{\eta}\|_2^2 \geq C \quad \text{and} \quad n \geq C. \quad (25)$$

Also, assuming the special case (24) of Chatterji and Long [2020] our bound in Theorem 7 reduces to the one in (23).

7.4 Benign overfitting

Paralleling the exposition in Section 5, we use the results above to show that both the SVM and LS solutions approach the Bayes error as overparameterization increases. The requirements for this to happen are now stronger. However, the conclusion is somewhat more surprising in the noisy case: interpolating solutions nearly achieve optimal Bayes error despite perfectly fitting to corrupted labels. Borrowing the terminology introduced by Bartlett et al. [2020], our result establishes “benign overfitting” for noisy GMM data.

Corollary 7.1. *Let the same assumptions as in Theorem 7 hold and n sufficiently large such that $n > C/\delta$ for some $C > 1$. Then, for large enough positive constant C_i 's > 1 , $\hat{\boldsymbol{\eta}}_{\text{SVM}}$ linearly interpolates the data and the classification error $\mathcal{R}(\hat{\boldsymbol{\eta}}_{\text{SVM}})$ approaches γ as $p/n \rightarrow \infty$ with probability at least $(1 - \delta)$ provided the following sets of conditions on the number of features p and mean-vector $\boldsymbol{\eta}$ hold:*

$$p > \max\{C_2 n \log n + n - 1, C_3 n \sqrt{\log(2n)} \|\boldsymbol{\eta}\|_2, n\|\boldsymbol{\eta}\|_2^2\}, \quad \text{and} \quad \|\boldsymbol{\eta}\|_2^4 \geq C_4 \left(\frac{p}{n}\right)^\alpha, \quad \text{for } \alpha > 1.$$

Note that the benign overfitting condition above is identical to the condition of Corollary 5.2 for the Low-SNR regime in the noiseless case. However, instead of $\|\boldsymbol{\eta}\|_2 = \Theta(p^\beta)$ with $\beta \in (\frac{1}{4}, 1)$ in the noiseless case, the conclusion of Corollary 7.1 holds under the stronger condition $\|\boldsymbol{\eta}\|_2 = \Theta(p^\beta)$ for $\beta \in (\frac{1}{4}, \frac{1}{2}]$. We remark that (according also to the discussion in Remark 2), our conditions for benign overfitting of noisy GMM coincide with the conditions derived by Chatterji and Long [2020].

8 Proofs outline

The complete proofs are given in the Appendix. Here, we provide an outline. For simplicity, we focus on the noiseless GMM in (1). At a high-level, the proofs for the noisy model remain the same with some more care needed to account for the mismatch between the clean and the corrupted labels (see Appendix H for details).

8.1 Reductions to quadratic forms

We first show that the proofs of all theorems reduce to establishing lower/upper bounds on quadratic forms of the Gram matrix $(\mathbf{X}\mathbf{X}^T + \tau\mathbf{I})^{-1}$.

Link between SVM solution and LS solution. We start with Theorems 1 and 2. As in Muthukumar et al. [2020a, Theorem 1], it suffices to derive conditions under which the following complementary slackness condition of (5) is satisfied with high probability:

$$y_i \mathbf{e}_i^T (\mathbf{X}\mathbf{X}^T)^{-1} \mathbf{y} > 0, \text{ for all } i \in [n]. \quad (26)$$

Note that the LHS of (26) is a quadratic form involving $(\mathbf{X}\mathbf{X}^T)^{-1}$.

Classification error. When deriving upper bounds on the classification error, it suffices from Lemma 1 that we lower bound the ratio

$$\frac{(\hat{\boldsymbol{\eta}}_\tau^T \boldsymbol{\eta})^2}{\hat{\boldsymbol{\eta}}_\tau^T \boldsymbol{\Sigma} \hat{\boldsymbol{\eta}}_\tau} = \frac{(\mathbf{y}^T (\mathbf{X}\mathbf{X}^T + \tau\mathbf{I})^{-1} \mathbf{X}\boldsymbol{\eta})^2}{\mathbf{y}^T (\mathbf{X}\mathbf{X}^T + \tau\mathbf{I})^{-1} \mathbf{X}\boldsymbol{\Sigma}\mathbf{X}^T (\mathbf{X}\mathbf{X}^T + \tau\mathbf{I})^{-1} \mathbf{y}}. \quad (27)$$

Specifically, when $\tau = 0$ and $\boldsymbol{\Sigma} = \mathbf{I}$, we have

$$\frac{(\hat{\boldsymbol{\eta}}_{\text{LS}}^T \boldsymbol{\eta})^2}{\hat{\boldsymbol{\eta}}_{\text{LS}}^T \boldsymbol{\Sigma} \hat{\boldsymbol{\eta}}_{\text{LS}}} = \frac{(\mathbf{y}^T (\mathbf{X}\mathbf{X}^T)^{-1} \mathbf{X}\boldsymbol{\eta})^2}{\mathbf{y}^T (\mathbf{X}\mathbf{X}^T)^{-1} \mathbf{y}}. \quad (28)$$

Note that both the numerator and denominator above include terms such as $\mathbf{y}^T (\mathbf{X}\mathbf{X}^T + \tau\mathbf{I})^{-1}$ and $\mathbf{y}^T (\mathbf{X}\mathbf{X}^T)^{-1} \mathbf{y}$. Our key technical contribution is bounding those for GMM data.

Challenge. Bounding quadratic forms of $(\mathbf{X}\mathbf{X}^T + \tau\mathbf{I})^{-1}$ is challenging for GMM data, since $\mathbf{X}\mathbf{X}^T = (\mathbf{y}\boldsymbol{\eta}^T + \mathbf{Q})(\mathbf{y}\boldsymbol{\eta}^T + \mathbf{Q})^T$, i.e. the Gram matrix ‘‘includes’’ both \mathbf{y} and $\boldsymbol{\eta}$. Specifically, this is different to Muthukumar et al. [2020a], Bartlett et al. [2020], Tsigler and Bartlett [2020], since in their setting $\mathbf{X}\mathbf{X}^T = \mathbf{Q}\mathbf{Q}^T$ and their results on quadratic forms of inverse Wishart matrices do not directly apply here.

Our approach. For concreteness, consider the problem of bounding the quadratic form $T_1 := \mathbf{y}^T (\mathbf{X}\mathbf{X}^T + \tau\mathbf{I})^{-1} \mathbf{y}$. A possible approach is to start from bounds on the eigenvalues of $\mathbf{X}\mathbf{X}^T + \tau\mathbf{I}$ and then obtain bounds for the eigenvalues of its inverse. Specifically, this turned out to be appropriate in the setting of Bartlett et al. [2020], Muthukumar et al. [2020a]. The situation is different here: the same eigenvalue approach fails to capture the dependence of \mathbf{X} on \mathbf{y} when bounding T_1 and results in suboptimal bounds. Instead of decoupling \mathbf{y} and the inverse Gram matrix that appear in T_1 , we consider both terms simultaneously. To make this possible we begin with the following decomposition of the Gram matrix:

$$\mathbf{X}\mathbf{X}^T + \tau\mathbf{I} = (\mathbf{Q}\mathbf{Q}^T + \tau\mathbf{I}) + \begin{bmatrix} \|\boldsymbol{\eta}\|_2 \mathbf{y} & \mathbf{Q}\boldsymbol{\eta} & \mathbf{y} \end{bmatrix} \begin{bmatrix} \|\boldsymbol{\eta}\|_2 \mathbf{y}^T \\ \mathbf{y}^T \\ (\mathbf{Q}\boldsymbol{\eta})^T \end{bmatrix},$$

which already isolates the (translated) Wishart matrix $(\mathbf{Q}\mathbf{Q}^T + \tau\mathbf{I})$ from the terms $\boldsymbol{\eta}$ and \mathbf{y} . Once decomposed in this form, our observation is that with an appropriate application of the matrix inversion lemma we can now express quadratic forms of interest (such as T_1) in terms of five more primitive quadratic forms. This idea is materialized in the following key lemma.

Lemma 3. *Let $\mathbf{U}_\tau := \mathbf{Q}\mathbf{Q}^T + \tau\mathbf{I}$ (thus, $\mathbf{U}_0 = \mathbf{Q}\mathbf{Q}^T$) and $\mathbf{d} := \mathbf{Q}\boldsymbol{\eta}$. Further define the following five primitive quadratic forms*

$$s := \mathbf{y}^T \mathbf{U}_\tau^{-1} \mathbf{y}, \quad t := \mathbf{d}^T \mathbf{U}_\tau^{-1} \mathbf{d}, \quad h := \mathbf{y}^T \mathbf{U}_\tau^{-1} \mathbf{d}, \quad g_i := \mathbf{y}^T \mathbf{U}_0^{-1} \mathbf{e}_i, \quad f_i := \mathbf{d}^T \mathbf{U}_0^{-1} \mathbf{e}_i, \quad i \in [n], \quad (29)$$

and denote $D := s(\|\boldsymbol{\eta}\|_2^2 - t) + (h + 1)^2$. With this notation, the following identity is true:

$$\mathbf{y}^T (\mathbf{X}\mathbf{X}^T + \tau\mathbf{I})^{-1} = \mathbf{y}^T \mathbf{U}_\tau^{-1} - \frac{1}{D} \left[\|\boldsymbol{\eta}\|_2 s, h^2 + h - st, s \right] \begin{bmatrix} \|\boldsymbol{\eta}\|_2 \mathbf{y}^T \\ \mathbf{y}^T \\ \mathbf{d}^T \end{bmatrix} \mathbf{U}_\tau^{-1}. \quad (30)$$

The five quadratic forms defined in (29) involve now the inverse of the Wishart matrix $\mathbf{Q}\mathbf{Q}^T$ rather than of the original Gram matrix $\mathbf{X}\mathbf{X}^T$; this is why we call them ‘‘primitive’’. Despite that feature, bounding these terms still does *not* follow by mere application of results appearing in previous works [Bartlett et al., 2020, Tsigler and Bartlett, 2020, Muthukumar et al., 2020a]. Moreover, observe in identity (30) that the five primitive forms appear with mixed signs each and both in the numerator/denominator. Thus, it is critical to obtain both lower and upper bounds for them. We derive these in the two lemmas below, which together with Lemma 3 form key technical contributions of our work.

Lemma 4 (Balanced). *Recall that $\sigma^2 = \sum_{i=1}^p \lambda_i \beta_i^2$. Assume that $\boldsymbol{\Sigma}$ follows the balanced ensemble defined in Definition 2.1. Fix $\delta \in (0, 1)$ and suppose n is large enough such that $n > c \log(1/\delta)$ for some $c > 1$. Then, there exists constants $C_1, C_2, C_3, C_6 > 1$, $C_5 > C_4 > 0$ such that with probability at least $1 - \delta$, the following results hold:*

$$\begin{aligned} \frac{n}{C_1(\tau + \|\boldsymbol{\lambda}\|_1)} \leq s \leq C_1 \frac{n}{(\tau + \|\boldsymbol{\lambda}\|_1)}, \quad C_4 \frac{n\sigma^2}{(\tau + \|\boldsymbol{\lambda}\|_1)} \leq t \leq C_5 \frac{n\sigma^2}{(\tau + \|\boldsymbol{\lambda}\|_1)}, \\ -C_2 \frac{n\sigma}{(\tau + \|\boldsymbol{\lambda}\|_1)} \leq h \leq C_2 \frac{n\sigma}{(\tau + \|\boldsymbol{\lambda}\|_1)}, \quad \|\mathbf{d}\|_2^2 \leq C_3 n\sigma^2, \quad \|\mathbf{y}^T \mathbf{U}_\tau^{-1}\|_2 \leq C_6 \frac{\sqrt{n}}{(\tau + \|\boldsymbol{\lambda}\|_1)}. \end{aligned}$$

We state our finding on $f_i, i \in [n]$ separately since it requires extra technical work to yield a bound that is uniform over $[n]$ and dimension independent. See Appendix G.3.3 for details.

Lemma 5. *Assume the condition in (8) is satisfied, Fix $\delta \in (0, 1)$ and suppose large enough $n > c/\delta, c > 1$. There exists constant $C > 1$ such that with probability at least $1 - \delta$,*

$$\max_{i \in [n]} |f_i| \leq \frac{C\sqrt{\log(2n)}\sigma}{\|\boldsymbol{\lambda}\|_1}. \quad (31)$$

8.2 Proof sketch of Theorems 1 and 2

With the technical lemmas above, we are now ready to sketch the proof of Theorem 1. For simplicity here, consider the unregularized estimator ($\tau = 0$). As mentioned previously, it suffices to derive conditions under which (26) holds with high probability. Thanks to our Lemma 3, we derive the following decomposition in terms of the primitive terms defined in (29) (with $\tau = 0$ therein):

$$\mathbf{y}^T (\mathbf{X}\mathbf{X}^T)^{-1} \mathbf{e}_i = \frac{g_i + hg_i - sf_i}{s(\|\boldsymbol{\eta}\|_2^2 - t) + (h + 1)^2}. \quad (32)$$

The denominator above is positive with high probability. Thus, we only need to ensure that $y_i(g_i + hg_i - sf_i) > 0$. For this, we use Lemmas 4 and 5 (see also (42) for a lower bound on $y_i g_i$). Detailed proof is in Appendix B.1.

The proof of Theorem 2 is similar, except that the bounds on quadratic forms of the Wishart matrix are used when $\boldsymbol{\Sigma} = \mathbf{I}$, thus providing a sharper result. Specifically, when lower bounding $y_i g_i$, less overparameterization is needed, i.e., the first condition in (10) is sharper than (9).

8.3 Proof sketch of Theorems 3 and 4

As per Section 8.1, we will lower bound the ratio in (27). First, work with the denominator. Observe that $\mathbf{X}\Sigma\mathbf{X}^T = (\mathbf{y}\beta^T + \mathbf{Z}\Lambda^{\frac{1}{2}})\mathbf{A}(\mathbf{y}\beta^T + \mathbf{Z}\Lambda^{\frac{1}{2}})^T$. Further let $\mathbf{A} := (\mathbf{X}\mathbf{X}^T + \tau\mathbf{I})^{-1}\mathbf{y}\mathbf{y}^T(\mathbf{X}\mathbf{X}^T + \tau\mathbf{I})^{-1}$ and \mathbf{z}_i denote the i -th column of \mathbf{Z} . Then, we show the following by applying the cyclic property of trace and the inequality $\mathbf{v}^T\mathbf{M}\mathbf{u} \leq \frac{1}{2}(\mathbf{v}^T\mathbf{M}\mathbf{v} + \mathbf{u}^T\mathbf{M}\mathbf{u})$, true for any PSD matrix \mathbf{M} :

$$\begin{aligned} \text{Tr}\left(\mathbf{y}^T(\mathbf{X}\mathbf{X}^T + \tau\mathbf{I})^{-1}\mathbf{X}\Sigma\mathbf{X}^T(\mathbf{X}\mathbf{X}^T + \tau\mathbf{I})^{-1}\mathbf{y}\right) &= \text{Tr}\left((\mathbf{y}\beta^T + \mathbf{Z}\Lambda^{\frac{1}{2}})\mathbf{A}(\mathbf{y}\beta^T + \mathbf{Z}\Lambda^{\frac{1}{2}})^T\mathbf{A}\right) \\ &\leq 2\left(\sum_{i=1}^p \lambda_i^2 \|\mathbf{A}\|_2 \|\mathbf{z}_i\|_2^2 + \sigma^2(\mathbf{y}^T(\mathbf{X}\mathbf{X}^T + \tau\mathbf{I})^{-1}\mathbf{y})^2\right), \end{aligned}$$

Now, to upper bound $\sum_{i=1}^p \lambda_i^2 \|\mathbf{A}\|_2 \|\mathbf{z}_i\|_2^2$, note $\|\mathbf{z}_i\|_2^2$'s are independent sub-exponentials; thus, for fixed $B > 0$, we can bound $\sum_{i=1}^p \lambda_i^2 B \|\mathbf{z}_i\|_2^2$ using the Bernstein's inequality. Specifically, we choose B as an upper bound on $\|\mathbf{A}\|_2 = \|\mathbf{y}^T(\mathbf{X}\mathbf{X}^T + \tau\mathbf{I})^{-1}\|_2^2$, which we obtain thanks to Lemma 4 after the following decomposition as per Lemma 3: $\mathbf{y}^T(\mathbf{X}\mathbf{X}^T + \tau\mathbf{I})^{-1} = ((1+h)\mathbf{y}^T\mathbf{U}_\tau^{-1} - s\mathbf{d}^T\mathbf{U}_\tau^{-1})/D$. Similarly, we can upper bound $\sigma^2(\mathbf{y}^T(\mathbf{X}\mathbf{X}^T + \tau\mathbf{I})^{-1}\mathbf{y})^2$ since again by Lemma 3 $\mathbf{y}^T(\mathbf{X}\mathbf{X}^T + \tau\mathbf{I})^{-1}\mathbf{y} = s/D$.

Next, focus on the numerator in (27). Thanks to Lemma 3, we have the decomposition

$$\mathbf{y}^T(\mathbf{X}\mathbf{X}^T + \tau\mathbf{I})^{-1}\mathbf{X}\boldsymbol{\eta} = \frac{s(\|\boldsymbol{\eta}\|_2^2 - t) + h^2 + h}{D}, \quad (33)$$

and the desired bound is obtained by a careful application of Lemma 4 that bounds the primitive quadratic appearing above. See Appendix C for details and proof steps for Theorems 3 and 4.

8.4 Proof sketch of Theorem 5

We need to lower bound the ratio $\frac{(\hat{\boldsymbol{\eta}}_\tau^T \boldsymbol{\eta})^2}{\hat{\boldsymbol{\eta}}_\tau^T \Sigma \hat{\boldsymbol{\eta}}_\tau} = \frac{(\eta_k \hat{\eta}_k)^2}{\sum_{i=1}^p \lambda_i \hat{\eta}_i^2}$. To do this, we divide $\hat{\eta}_i$'s into 3 groups ($\hat{\eta}_1$, $\hat{\eta}_k$ and the rest) and upper bound the following:

$$\frac{\lambda_1 \hat{\eta}_1^2}{(\eta_k \hat{\eta}_k)^2}, \quad \frac{\sum_{i \neq 1, k} \lambda_i \hat{\eta}_i^2}{(\eta_k \hat{\eta}_k)^2} \quad \text{and} \quad \frac{\lambda_k \hat{\eta}_k^2}{(\eta_k \hat{\eta}_k)^2},$$

where note from $\hat{\eta}_i = \mathbf{e}_i^T \hat{\boldsymbol{\eta}}$ that $\hat{\eta}_i = \sqrt{\lambda_i} \mathbf{z}_i^T (\mathbf{X}\mathbf{X}^T + \tau\mathbf{I})^{-1} \mathbf{y}$, for $i \neq k$, and $\hat{\eta}_k = (\eta_k \mathbf{y}^T + \sqrt{\lambda_k} \mathbf{z}_k^T) (\mathbf{X}\mathbf{X}^T + \tau\mathbf{I})^{-1} \mathbf{y}$. As before, thanks to Lemma 3 this reduces to upper/lower bounding quadratic forms involving $\mathbf{U}_\tau^{-1} = (\mathbf{Q}\mathbf{Q}^T + \tau\mathbf{I})^{-1}$. However, because here λ_1 is much larger than other eigenvalues of Σ , instead of directly bounding the eigenvalues of \mathbf{U}_τ , we leverage the leave-one-out trick introduced in Bartlett et al. [2020] and first separate λ_1 from the other eigenvalues. Specifically, by Woodbury's identity, \mathbf{U}_τ^{-1} is expressed as

$$\mathbf{U}_\tau^{-1} = (\tau\mathbf{I} + \sum_{i=2}^p \lambda_i \mathbf{z}_i \mathbf{z}_i^T + \lambda_1 \mathbf{z}_1 \mathbf{z}_1^T)^{-1} = \mathbf{U}_{-1, \tau}^{-1} - \frac{\lambda_1 \mathbf{U}_{-1, \tau}^{-1} \mathbf{z}_1 \mathbf{z}_1^T \mathbf{U}_{-1, \tau}^{-1}}{1 + \lambda_1 \mathbf{z}_1^T \mathbf{U}_{-1, \tau}^{-1} \mathbf{z}_1},$$

where $\mathbf{U}_{-1, \tau} = \tau\mathbf{I} + \sum_{i=2}^p \lambda_i \mathbf{z}_i \mathbf{z}_i^T$. Now, we first bound the eigenvalues of $\mathbf{U}_{-1, \tau}$, and then use these results to bound the eigenvalues of \mathbf{U}_τ and \mathbf{U}_τ^{-1} . See Appendix G.4 for details.

9 Discussion

Here, we include further details on how our results fit in the related literature.

9.1 Comparison to classical margin-based bounds

We start by arguing that classical bounds on the generalization of SVM are uninformative in the highly overparameterized settings of GMM data that we focus on. We do this by quantitatively comparing our results with classical margin-based bounds applied to GMM data.

First, consider the following well-known bound.

Proposition 7.1. [Shalev-Shwartz and Ben-David, 2014, Theorem 26.13]. Consider a distribution \mathcal{D} over $\mathcal{X} \times \{\pm 1\}$ such that there exists some vector $\boldsymbol{\eta}^*$ with $\mathbf{P}_{(\mathbf{x}, y) \sim \mathcal{D}}(y \cdot \boldsymbol{\eta}^{*T} \mathbf{x} \geq 1) = 1$ and such that $\|\mathbf{x}\|_2 \leq R$ with probability 1. Let $\hat{\boldsymbol{\eta}}_{\text{SVM}}$ be the SVM solution. Then with probability at least $1 - \delta$, we have that

$$\mathcal{R}(\hat{\boldsymbol{\eta}}_{\text{SVM}}) \leq \frac{2R\|\boldsymbol{\eta}^*\|_2}{\sqrt{n}} + (1 + R\|\boldsymbol{\eta}^*\|_2) \sqrt{\frac{2 \log(2/\delta)}{n}}. \quad (34)$$

We apply Proposition 7.1 to the setting studied in Corollary 5.2. Specifically, we will apply the bound for $\boldsymbol{\eta}^* \leftarrow \boldsymbol{\eta}$. But, first we need to show that this choice satisfies the conditions of the proposition. To this end, by definition of \mathbf{x} , we have $y \cdot \boldsymbol{\eta}^T \mathbf{x} = \|\boldsymbol{\eta}\|_2^2 + \boldsymbol{\eta}^T(y\mathbf{q})$ with $\mathbf{q} \sim \mathcal{N}(0, \mathbf{I}_p)$. Therefore,

$$\begin{aligned} \mathbf{P}(y \cdot \boldsymbol{\eta}^T \mathbf{x} \leq 1) &= \mathbf{P}(\boldsymbol{\eta}^T(y\mathbf{q}) \leq 1 - \|\boldsymbol{\eta}\|_2^2) = \mathbf{P}(\boldsymbol{\eta}^T(y\mathbf{q}) \geq \|\boldsymbol{\eta}\|_2^2 - 1) \\ &\leq \exp\left(-\frac{(\|\boldsymbol{\eta}\|_2^2 - 1)^2}{2\|\boldsymbol{\eta}\|_2^2}\right) \leq \exp\left(-\frac{\|\boldsymbol{\eta}\|_2^2}{2} + 1\right) \\ &\leq \exp(-C(p/n)^{2\alpha}) \xrightarrow{p/n \rightarrow \infty} 0. \end{aligned}$$

The inequalities in the second line used Hoeffding's tail bound. In the third line, we used the conditions of Corollary 5.2 that $\|\boldsymbol{\eta}\|_2 \geq C_2(p/n)^\alpha$ for some $\alpha > 1/4$. Now, we compute the upper bound R . Bernstein's inequality gives with probability at least $1 - 2e^{-p/c}$,

$$\|\boldsymbol{\eta}\|_2^2 + (1 - (1/C))p \leq \|\mathbf{x}\|_2^2 \leq \|\boldsymbol{\eta}\|_2^2 + (1 + (1/C))p.$$

Thus, in our setting with probability 1, $\|\mathbf{x}\|_2 \leq \|\boldsymbol{\eta}\|_2 + C\sqrt{p} =: R$. Plugging this in (34) we see that

$$R\|\boldsymbol{\eta}^*\|_2/\sqrt{n} = \Theta\left(\|\boldsymbol{\eta}\|_2^2/\sqrt{n} + \sqrt{p/n}\|\boldsymbol{\eta}\|_2\right).$$

This bound becomes vacuous in the setting of Corollary 5.2. Indeed, by using $\|\boldsymbol{\eta}\|_2 \geq C_2(p/n)^\alpha$, we find that $\sqrt{p/n}\|\boldsymbol{\eta}\|_2 \rightarrow \infty$ as $p/n \rightarrow \infty$.

One might wonder if the conclusion would be different have we instead used a margin-based bound. We show that such bounds are also *not* able to explain why SVM nearly achieves Bayes optimal (aka zero) error in the highly overparameterized regime of Corollary 5.2.

Proposition 7.2. [Shalev-Shwartz and Ben-David, 2014, Theorem 26.14]. Assume the conditions of Proposition 7.1. Then, with probability at least $1 - \delta$, we have that

$$\mathcal{R}(\hat{\boldsymbol{\eta}}_{\text{SVM}}) \leq \frac{4R\|\hat{\boldsymbol{\eta}}_{\text{SVM}}\|_2}{\sqrt{n}} + \sqrt{\frac{\log(4 \log_2(\|\hat{\boldsymbol{\eta}}_{\text{SVM}}\|_2)/\delta)}{n}}. \quad (35)$$

In order to analytically evaluate the bound above, we need a means to control the inverse margin $\|\hat{\boldsymbol{\eta}}_{\text{SVM}}\|_2$. While it is not a-priori clear how to do this, our analysis establishes an upper bound on $\|\hat{\boldsymbol{\eta}}_{\text{SVM}}\|_2$ in the sufficiently overparameterized regime. Specifically, we do this as part of the proof of Theorem 3 in the process of upper bounding the correlation of the LS solution in Section C.2 (see Equation 49). But in the setting of Corollary 5.2 $\|\hat{\boldsymbol{\eta}}_{\text{SVM}}\|_2 = \|\hat{\boldsymbol{\eta}}_{\text{LS}}\|_2$. Thus, (50) and (52) show that $\|\hat{\boldsymbol{\eta}}_{\text{SVM}}\|_2^2 \leq \frac{C}{(1-n/p)\|\boldsymbol{\eta}\|_2^2}$. Recalling from above that $R = \|\boldsymbol{\eta}\|_2 + C\sqrt{p}$ and putting things together proves that

$$\frac{R\|\hat{\boldsymbol{\eta}}_{\text{SVM}}\|_2}{\sqrt{n}} = O\left(\frac{1}{\sqrt{n}} + \sqrt{\frac{p}{n\|\boldsymbol{\eta}\|_2^2}}\right). \quad (36)$$

In the High-SNR regime of Corollary 5.2 recall that $p < n\|\boldsymbol{\eta}\|_2^2/C$, thus the value in (36) is $O(1 + 1/\sqrt{n})$. We see that (at least in the High-SNR regime) the bound we obtained by combining Proposition 7.2 with our upper bound of $\|\hat{\boldsymbol{\eta}}_{\text{SVM}}\|_2$ is indeed improved compared to that of Proposition 7.1. However, it still fails to predict the fact that the error goes to zero with increasing overparameterization (as predicted by Proposition 7.2). The bound is similarly inconclusive about the Low-SNR regime.

We end this section by noting that the fact that margin-based bounds are loose in the overparameterized regime has been previously also discussed in Montanari et al. [2019], Deng et al. [2019] and Muthukumar et al. [2020a]. Specifically, Montanari et al. [2019], Deng et al. [2019] showed that Proposition 7.2 fails to predict the exact double-descent behavior of the risk in linear models even if the inverse margin $\|\hat{\boldsymbol{\eta}}_{\text{SVM}}\|_2$ in (35) is evaluated using sharp asymptotic formulas. Here, we have used our non-asymptotic bound for $\|\hat{\boldsymbol{\eta}}_{\text{SVM}}\|_2$ and showed that a margin-based argument is insufficient to yield the conclusions on Section 5. Finally, see also the discussion in [Muthukumar et al., 2020a, Sec. 6] where the authors demonstrate the deficiency of margin-based explanations in classification of signed data via numerical simulations. Here, we have arrived at the same conclusion, this time for GMM data, via an analytic study.

9.2 Comparison to previous works

We have already discussed how our results are motivated and how they differ from previous works in the Introduction. Here, we focus on the three most closely related papers [Bartlett et al., 2020, Muthukumar et al., 2020a, Chatterji and Long, 2020] and provide a more detailed discussion.

9.2.1 Bartlett et al. [2020]

As mentioned in the Introduction Bartlett et al. [2020] is amongst the first to analytically study generalization principles under overparameterization. Our work is inspired by them, but otherwise differs in four important aspects as outlined next.

(i) First, unlike linear regression, we study a linear classification model in which labels y are binary and covariates are of the form $\mathbf{x} = y\boldsymbol{\eta} + \mathbf{q}$. As discussed in Section 2 this implies that $y = \mathbf{x}^T \bar{\boldsymbol{\eta}} + z$ with $\bar{\boldsymbol{\eta}} := \boldsymbol{\eta} / \|\boldsymbol{\eta}\|_2^2$ and $z = \mathbf{q}^T \bar{\boldsymbol{\eta}}$. While this latter formulation resembles the linear regression model, where noise is additive, note here that the additive “noise” term z is highly signal dependent. The analysis of Bartlett et al. [2020] makes heavy use of the assumption that noise is signal independent, hence their techniques *cannot* be directly applied to the GMM (see why in point (iii) below).

(ii) Second, our model is also different in that the feature vectors, although still Gaussian, are now signal dependent. Again, this does not allow a direct application of the technical results in [Bartlett et al., 2020] in our setting. Specifically, Bartlett et al. [2020] show that in their setting bounding generalization can be mapped to a question about controlling the rate of decay of eigenvalues of inverse Wishart matrices. Instead, as explained in Section 8.1, in our setting we first express the generalization metric of interest as a non-trivial function of a number of simpler quadratic forms. While these quadratic forms involve inverse Wishart matrices, their statistics are not solely governed by the eigenstructure of the latter, but they also involve the mean vector $\boldsymbol{\eta}$.

(iii) Third, beyond the model itself what differs fundamentally in classification is the measure of generalization performance. Instead of the squared prediction risk studied by Bartlett et al. [2020], relevant for us is the expected error as measured by the 0/1 loss. For Gaussian covariates, the former essentially reduces to the mean-squared error and the authors show that it suffices controlling a quantity $\boldsymbol{\epsilon}^T \mathbf{C} \boldsymbol{\epsilon}$, where $\mathbf{C} = (\mathbf{X}\mathbf{X}^T)^{-1} \mathbf{X} \boldsymbol{\Sigma} \mathbf{X}^T (\mathbf{X}\mathbf{X}^T)^{-1}$ and $\boldsymbol{\epsilon}$ is the additive noise in the linear regression model [Bartlett et al., 2020, Lemma 7]. To do this, they exploit the assumption that $\boldsymbol{\epsilon}$ is independent of \mathbf{X} and sub-Gaussian, which reduces the problem to upper bounding $\text{Tr}(\mathbf{C})$ [Bartlett et al., 2020, Lemma 8]. Their subsequent analysis is tailored to this term. Instead, Lemma 1 shows that controlling the 0/1 risk requires bounding the estimator’s correlation. For the latter, we show that one needs to *both* upper bound $\mathbf{y}^T \mathbf{C} \mathbf{y}$ and lower bound $\mathbf{y}^T (\mathbf{X}\mathbf{X}^T)^{-1} \mathbf{X} \boldsymbol{\eta}$ (see (27)). Our goal is now more complicated compared to the situation faced in linear regression because: (a) In the first term \mathbf{y} is not random (unlike $\boldsymbol{\epsilon}$). (b) The second quadratic form involves a matrix other than \mathbf{C} and both vectors \mathbf{y} and $\boldsymbol{\eta}$. (c) The feature matrix \mathbf{X} is a non-centered Gaussian matrix whose mean involves both the response \mathbf{y} and the mean vector $\boldsymbol{\eta}$.

(iv) The fourth difference is that in our setting, we are interested in the generalization performance of the SVM solution rather than the minimum-norm interpolator. The challenge is that the former is *not* given in closed form in terms of the label vector \mathbf{y} and the feature matrix \mathbf{X} . The key innovation to circumvent this challenge is attributed to Muthukumar et al. [2020a] who realized that under

sufficient overparameterization SVM becomes equivalent to LS. We remark though that identifying the appropriate conditions for this to happen for GMM data is key contribution of our work (see Section 9.2.2). Following the above discussion emphasizing differences to the setting of [Bartlett et al., 2020] it should not be surprising that our error bounds in Section 4 are of different nature to those in [Bartlett et al., 2020]. The first key difference is that our bounds involve not only the eigenstructure of the covariance matrix, but also the mean vector of the GMM. Second, as a natural follow up, our conditions in Section 5 for which the classifier’s error approaches the Bayes error are different to those in [Bartlett et al., 2020]. Despite the differences, it might be interesting to the reader noting that the two ensembles introduced in Definitions 2 and 3 can be expressed in terms of the notions of “effective ranks” defined by Bartlett et al. [2020], i.e. $r_k := (\sum_{i>k}^p \lambda_i)/\lambda_{k+1}$. To see the relationship, let $\tilde{r}_k := (\sum_{i>k+1}^p \lambda_i)/\lambda_{k+1} = r_k - 1$. With this notation, in the balanced ensemble, $\tilde{r}_0 \geq bn$, which directly implies $r_0 \geq bn$. For large enough n , the reverse direction of implication is also true. In the bi-level ensemble, the first condition $\tilde{r}_0 \leq bn$ implies again $r_0 \leq b'n$ for large enough n . Similarly, the second condition $\tilde{r}_1 \geq b_1n$ implies $r_1 \geq b_1n$.

9.2.2 Muthukumar et al. [2020a]

The paper by Muthukumar et al. [2020a] is the most closely related to this work in terms of the approach that we follow. We complement the discussion in the Introduction regarding the different setting between the two works with a more detailed exposition of our key technical differences. For concreteness, we focus on the proof of equivalence between SVM and LS in Theorems 1 and 2, since the same differences apply to the error analysis in Theorems 3, 4 and 5.

There are two main steps in proving Theorems 1 and 2. The first step involves a deterministic sufficient condition guaranteeing that the constraints of the SVM optimization in (5) are active. The second step involves a probabilistic analysis of this deterministic condition using the generative statistical model at hand. The first part of our proof is same as in Muthukumar et al. [2020a] and Hsu et al. [2020]. Specifically, we use their deterministic condition (26). On the other hand, the second part of our analysis is technically challenging. The reason is that unlike previous work where the covariates are zero mean Gaussians, in our case, $\mathbf{X} = \mathbf{Q} + \mathbf{y}\boldsymbol{\eta}^T$ for a zero-mean Gaussian matrix \mathbf{Q} . Note that the deterministic condition (26) to be checked involves the inverse Gram matrix. The key relevant technical argument in Muthukumar et al. [2020a] (i.e., Lemma 1 therein) controls how far the inverse Wishart matrix $(\mathbf{Q}\mathbf{Q}^T)^{-1}$ is from $(\sum_{i \in [p]} |\lambda_i|) \mathbf{I}_d$. This result is clearly not sufficient in our case as $(\mathbf{X}\mathbf{X}^T)^{-1}$ involves more terms. We repeat our strategy at circumventing this challenge as also sketched in Section 8.1. We start by expanding the terms in $(\mathbf{X}\mathbf{X}^T)$ and recognizing that after appropriate application of the matrix inversion lemma together with some algebra we can express the LHS of (26) as a function of five quadratic forms of either of two random matrices, $(\mathbf{Q}\mathbf{Q}^T)^{-1}$ or $\mathbf{Q}^T(\mathbf{Q}\mathbf{Q}^T)^{-1}$. It should be noted that this function involves the five quadratic forms in a convoluted way making it necessary to provide both upper and lower bounds for those forms (see Equation (32)). Besides lower bounding one of the first two terms that involves $(\mathbf{Q}\mathbf{Q}^T)^{-1}$ using Lemma 1 in Muthukumar et al. [2020a], none of the remaining quadratic forms appear in the analysis of Muthukumar et al. [2020a]. Lemmas 7 and 8, where we obtain lower/upper bounds for them, form a main technical contribution of our work (see Appendix G for details). Finally, the delicate piece of putting together those bounds to guarantee a positive quantity overall is also new compared to previous works (see Appendix B).

As we have highlighted in the previous sections, differences to [Muthukumar et al., 2020a] are not only technical. Most importantly, the differences extend to the conclusions regarding the conditions playing a key role for interpolation of the SVM solution and for the classification error of SVM to approach the Bayes error. See discussions in Sections 3 and 4. As a side technical note here, we have here relaxed the one-sparse assumption [Muthukumar et al., 2020a, Assumption 1] on the parameter vector $\boldsymbol{\eta}$ in the balanced ensemble. Finally, unlike Muthukumar et al. [2020a], our bounds further apply to regularized LS and are extended to a model with label corruptions.

As a last note, we discuss the nice follow-up to Muthukumar et al. [2020a] by Hsu et al. [2020], which involves two key contributions. The first concerns conditions for interpolation. The first step in their analysis (aka the deterministic condition (26) discussed above) is the same as in Muthukumar

et al. [2020a], but (26) is eventually expressed in a different equivalent form that allows tightening the probabilistic analysis that follows in the case of anisotropic covariance. Their second novelty involves relaxing the requirement for Gaussianity of the features to subGaussianity and Haar distribution. These improvements still only apply to the discriminative model, thus they are not directly applicable here.

9.2.3 Chatterji and Long [2020]

We now compare our work to Chatterji and Long [2020], who also derive non-asymptotic error bounds on the classification error of GMM data.

First, there are certain differences in the problem setting. On the one hand, Chatterji and Long [2020] relaxes the assumption on Gaussianity by studying the case where \mathbf{q} in (1) has subGaussian entries³. On the other hand, while we require that \mathbf{q} is Gaussian, our results capture explicitly the role of the data covariance matrix and its interplay with the mean vector via the key parameter $\sigma^2 = \boldsymbol{\eta}^T \boldsymbol{\Sigma} \boldsymbol{\eta}$. As we have seen in Sections 4, 5 and 6, the error behavior can differ substantially for different covariance structures (e.g., balanced vs bi-level ensembles). This phenomenon is *not* revealed by Chatterji and Long [2020, Thm. 3.1]⁴. Another distinguishing feature of the results in Chatterji and Long [2020] is that they apply to a noisy model that allows for (bounded number of) adversarial label corruptions. Our main focus is the noiseless GMM, but we also extended our results to a special case of their model in Section 7.

In terms of analysis, our techniques are very different. As mentioned we follow the high-level recipe of Muthukumar et al. [2020a] (also adapted by Hsu et al. [2020]), that is first showing equivalence of SVM to LS and then deriving error bounds for the latter. Instead, Chatterji and Long [2020] analyze the SVM solution by viewing it as the limit of gradient-descent updates on logistic loss minimization with sufficiently small step-size [Soudry et al., 2018]. Specifically, they produce a recursive argument that at each iteration lower bounds the the expected margin of the current gradient-descent iterate on a clean point with respect to the margin of the previous iterate [Chatterji and Long, 2020, Lem. 4.4]. We believe that both techniques are of interest. Via the connection to logistic loss minimization, their approach also yields insights on the degree to which one example (possibly a noisy one) can affect the quality of the learnt classifier [Chatterji and Long, 2020, Lem. 4.8]. It also allows the study of subGaussian features (rather than Gaussian) rather naturally. On the other hand, the approach followed here leads to Theorems 1 and 2 on equivalence of SVM to LS under sufficient effective overparameterization, which is a result of its own interest. Besides, as mentioned, our technique allows us to capture the effect of data covariance.

We already discussed in Sections 5 and 7 how our findings compare to those in Chatterji and Long [2020]. In summary, for the noiseless case, we show that interpolating solutions asymptotically achieve the Bayes error under relaxed assumptions compared to the noisy model (see Remark 1. For the noisy model, our benign-overfitting conditions are identical, but our risk bounds hold under relaxed assumptions (see Remark 2). Finally, in addition to the risk bounds for SVM derived by Chatterji and Long [2020], we also derive conditions for which SVM solution interpolates the data and we investigate regularized LS.

9.3 Contemporaneous and follow-up work

While the current version of our paper was undergoing review and after an earlier version of our paper [Wang and Thrampoulidis, 2021], we became aware of contemporaneous independent work by Cao et al. [2021]. Compared to our setting, Cao et al. [2021] only requires sub-Gaussian features. Similar to us their results capture the key role of the spectrum of the data covariance. Their proofs for the correlated case build on ideas developed in our earlier version [Wang and Thrampoulidis, 2021] for the isotropic case. Compared to them, we also derived bounds for regularized LS in our paper.

³This is interesting as for example it includes a Boolean noisy version of the rare-weak model by Jin [2009], for which our results do not directly apply.

⁴We note that the key role played by data covariance in double-decent and benign overfitting has been also emphasized in several related works, e.g., Hastie et al. [2019], Bartlett et al. [2020], Muthukumar et al. [2020a], Montanari et al. [2019], Chang et al. [2020]

A more detailed technical comparison between the two paper is as follows. First, Cao et al. [2021] obtains a sharper first condition $\|\boldsymbol{\lambda}\|_1 \geq \max\{n\sqrt{n}\|\boldsymbol{\lambda}\|_\infty, n\|\boldsymbol{\lambda}\|_2\}$ for equivalence of SVM to LS in Theorem 1, by invoking stronger concentration arguments. Their second condition is the same as Theorem 1. For this, we further present insightful simulation results suggesting its tightness (see Figure 1). Regarding the classification error, Cao et al. [2021] provides both upper and the lower bound for $\mathcal{R}(\hat{\boldsymbol{\eta}}_{\text{SVM}})$. However, note that their results only apply to the balanced ensemble. For the anisotropic balanced setting, compared to Theorem 1, Cao et al. [2021, Theorem 3.1] proved that $\mathcal{R}(\hat{\boldsymbol{\eta}}_{\text{LS}}) \leq \exp\left(\frac{-C\|\boldsymbol{\eta}\|_2^4}{\|\boldsymbol{\lambda}\|_\infty + (\|\boldsymbol{\lambda}\|_1^2/n + \sigma^2)}\right)$. Under the same assumptions in Theorem 1, Cao et al. [2021, Theorem 3.1], the numerator of our corresponding bound in (13) can be simplified to the same as the result in Cao et al. [2021]. However, the denominators are slightly different, where instead of $\|\boldsymbol{\lambda}\|_2^2/n$ in Cao et al. [2021], we obtain $\|\boldsymbol{\lambda}\|_2^2$ and an additional $\|\boldsymbol{\lambda}\|_\infty$ term. For the isotropic setting, after some simplification, the bound on $\mathcal{R}(\hat{\boldsymbol{\eta}}_{\text{LS}})$ in Cao et al. [2021, Corollary 3.3] is the same as Theorem 4. Therefore, the benign overfitting condition ($\|\boldsymbol{\eta}\|_2 = \Theta(p^\beta), \beta \in (1/4, 1)$) is matching for finite n in the isotropic setting. As mentioned, we also investigate regularized LS in this paper. Additionally, in Section 7 we extend our results to a probabilistic label-noise model and derive conditions for benign overfitting that are not studied in Cao et al. [2021].

More recently, Ardeshir et al. [2021] derived lower bounds for the conditions required to make SVM and LS solutions equivalent for discriminative models. For unconditional Gaussian covariates they show a sharp phase-transition characterizing the equivalence phenomenon. It is interesting to extend their analyses focusing on lower bounds to GMM data as studied in our paper. Finally, it is worth mentioning exciting related work Zou et al. [2021], Varre et al. [2021] that explores benign overfitting of *stochastic* gradient descent (SGD) (instead, note in Section 2 that our motivation for studying SVM or the minimum-norm interpolator comes from implicit bias of GD rather than SGD).

10 Future work

We established a connection between the SVM and the LS solutions in the overparameterized regime for GMMs. We then proved a non-asymptotic bound for the classification error, which we used to study generalization of SVM in the highly overparameterized regime. We also discussed the role of regularization and illustrated a regime that interpolation estimators perform better than the regularized estimators. We then show that our analysis and results (both on equivalence of SVM to LS and on risk bounds) extend naturally to a probabilistic label-noise model. For this model, we derive conditions for benign overfitting. We are interested in extending our analysis to adversarial corruptions and misspecified models. Another possible direction is deriving lower bounds to investigate whether our conditions in Theorems 1 and 2 are tight (as suggested by Figure 1). Possible extensions to more complex nonlinear settings are naturally very important. Finally, we are particularly interested in extensions to multiclass settings for which the GMM studied here serves as a natural model.

Acknowledgments

This work is partially supported by the NSF under Grant Number CCF-2009030 and by a research grant from KAUST. The authors would like to thank Dr. Vidya Muthukumar from the Georgia Institute of Technology for very helpful discussions and the anonymous reviewers for helpful suggestions that helped improve the presentation of our results.

References

- N. Ardeshir, C. Sanford, and D. Hsu. Support vector machines and linear regression coincide with very high-dimensional features. *arXiv preprint arXiv:2105.14084*, 2021.
- J. Ba, M. Erdogdu, T. Suzuki, D. Wu, and T. Zhang. Generalization of two-layer neural networks: An asymptotic viewpoint. In *International Conference on Learning Representations*, 2019.

- P. L. Bartlett, P. M. Long, G. Lugosi, and A. Tsigler. Benign overfitting in linear regression. *Proceedings of the National Academy of Sciences*, 2020.
- M. Belkin, D. Hsu, S. Ma, and S. Mandal. Reconciling modern machine learning and the bias-variance trade-off. *stat*, 1050:28, 2018a.
- M. Belkin, D. J. Hsu, and P. Mitra. Overfitting or perfect fitting? risk bounds for classification and regression rules that interpolate. In *Advances in neural information processing systems*, pages 2300–2311, 2018b.
- M. Belkin, S. Ma, and S. Mandal. To understand deep learning we need to understand kernel learning. *arXiv preprint arXiv:1802.01396*, 2018c.
- M. Belkin, D. Hsu, and J. Xu. Two models of double descent for weak features. *arXiv preprint arXiv:1903.07571*, 2019.
- Y. Cao, Q. Gu, and M. Belkin. Risk bounds for over-parameterized maximum margin classification on sub-gaussian mixtures. *arXiv preprint arXiv:2104.13628*, 2021.
- X. Chang, Y. Li, S. Oymak, and C. Thrampoulidis. Provable benefits of overparameterization in model compression: From double descent to pruning neural networks. *arXiv preprint arXiv:2012.08749*, 2020.
- N. S. Chatterji and P. M. Long. Finite-sample analysis of interpolating linear classifiers in the over-parameterized regime. *arXiv preprint arXiv:2004.12019*, 2020.
- N. S. Chatterji, P. M. Long, and P. L. Bartlett. When does gradient descent with logistic loss find interpolating two-layer networks? *arXiv preprint arXiv:2012.02409*, 2020.
- T. H. Cormen, C. E. Leiserson, R. L. Rivest, and C. Stein. *Introduction to algorithms*. MIT press, 2009.
- Z. Deng, A. Kammoun, and C. Thrampoulidis. A model of double descent for high-dimensional binary linear classification. *arXiv preprint arXiv:1911.05822*, 2019.
- R. P. Duin. Classifiers in almost empty spaces. In *Proceedings 15th International Conference on Pattern Recognition. ICPR-2000*, volume 2, pages 1–7. IEEE, 2000.
- I. Goodfellow, Y. Bengio, A. Courville, and Y. Bengio. *Deep learning*, volume 1. MIT press Cambridge, 2016.
- Y. Gordon. Some inequalities for gaussian processes and applications. *Israel Journal of Mathematics*, 50(4):265–289, 1985.
- T. Hastie, R. Tibshirani, and J. Friedman. *The elements of statistical learning: data mining, inference, and prediction*. Springer Science & Business Media, 2009.
- T. Hastie, A. Montanari, S. Rosset, and R. J. Tibshirani. Surprises in high-dimensional ridgeless least squares interpolation. *arXiv preprint arXiv:1903.08560*, 2019.
- R. A. Horn and C. R. Johnson. *Matrix analysis*. Cambridge university press, 2012.
- D. Hsu, V. Muthukumar, and J. Xu. On the proliferation of support vectors in high dimensions. *arXiv preprint arXiv:2009.10670*, 2020.
- Z. Ji and M. Telgarsky. The implicit bias of gradient descent on nonseparable data. In *Conference on Learning Theory*, pages 1772–1798, 2019.
- J. Jin. Impossibility of successful classification when useful features are rare and weak. *Proceedings of the National Academy of Sciences*, 106(22):8859–8864, 2009.

- A. Kammoun and M.-S. Alouini. On the precise error analysis of support vector machines. *arXiv preprint arXiv:2003.12972*, 2020.
- G. Kini and C. Thrampoulidis. Analytic study of double descent in binary classification: The impact of loss. *arXiv preprint arXiv:2001.11572*, 2020.
- D. Kobak, J. Lomond, and B. Sanchez. Optimal ridge penalty for real-world high-dimensional data can be zero or negative due to the implicit ridge regularization. *arXiv preprint arXiv:1805.10939*, 2018.
- A. Krizhevsky, I. Sutskever, and G. E. Hinton. Imagenet classification with deep convolutional neural networks. *Advances in neural information processing systems*, 25:1097–1105, 2012.
- T. Liang, A. Rakhlin, and X. Zhai. On the risk of minimum-norm interpolants and restricted lower isometry of kernels. *arXiv preprint arXiv:1908.10292*, 2019.
- Z. Liao, R. Couillet, and M. W. Mahoney. A random matrix analysis of random fourier features: beyond the gaussian kernel, a precise phase transition, and the corresponding double descent. *arXiv preprint arXiv:2006.05013*, 2020.
- M. Loog, T. Viering, A. Mey, J. H. Krijthe, and D. M. Tax. A brief prehistory of double descent. *Proceedings of the National Academy of Sciences*, 117(20):10625–10626, 2020.
- S. Mei and A. Montanari. The generalization error of random features regression: Precise asymptotics and double descent curve. *arXiv preprint arXiv:1908.05355*, 2019.
- F. Mignacco, F. Krzakala, Y. M. Lu, and L. Zdeborová. The role of regularization in classification of high-dimensional noisy gaussian mixture. *arXiv preprint arXiv:2002.11544*, 2020.
- A. Montanari, F. Ruan, Y. Sohn, and J. Yan. The generalization error of max-margin linear classifiers: High-dimensional asymptotics in the overparametrized regime. *arXiv preprint arXiv:1911.01544*, 2019.
- G. F. Montufar, R. Pascanu, K. Cho, and Y. Bengio. On the number of linear regions of deep neural networks. In *Advances in neural information processing systems*, pages 2924–2932, 2014.
- V. Muthukumar, A. Narang, V. Subramanian, M. Belkin, D. Hsu, and A. Sahai. Classification vs regression in overparameterized regimes: Does the loss function matter? *arXiv preprint arXiv:2005.08054*, 2020a.
- V. Muthukumar, K. Vodrahalli, V. Subramanian, and A. Sahai. Harmless interpolation of noisy data in regression. *IEEE Journal on Selected Areas in Information Theory*, 2020b.
- P. Nakkiran, G. Kaplun, Y. Bansal, T. Yang, B. Barak, and I. Sutskever. Deep double descent: Where bigger models and more data hurt. *arXiv preprint arXiv:1912.02292*, 2019.
- M. Opper, W. Kinzel, J. Kleinz, and R. Nehl. On the ability of the optimal perceptron to generalise. *Journal of Physics A: Mathematical and General*, 23(11):L581, 1990.
- S. Oymak, C. Thrampoulidis, and B. Hassibi. The squared-error of generalized lasso: A precise analysis. In *2013 51st Annual Allerton Conference on Communication, Control, and Computing (Allerton)*, pages 1002–1009. IEEE, 2013.
- T. Poggio, H. Mhaskar, L. Rosasco, B. Miranda, and Q. Liao. Why and when can deep-but not shallow-networks avoid the curse of dimensionality: a review. *International Journal of Automation and Computing*, 14(5):503–519, 2017.
- S. Rosset, J. Zhu, and T. Hastie. Margin maximizing loss functions. In *NIPS*, pages 1237–1244, 2003.

- M. Rudelson, R. Vershynin, et al. Hanson-wright inequality and sub-gaussian concentration. *Electronic Communications in Probability*, 18, 2013.
- F. Salehi, E. Abbasi, and B. Hassibi. The impact of regularization on high-dimensional logistic regression. *arXiv preprint arXiv:1906.03761*, 2019.
- F. Salehi, E. Abbasi, and B. Hassibi. The performance analysis of generalized margin maximizer (gmm) on separable data. *arXiv preprint arXiv:2010.15379*, 2020.
- S. Shalev-Shwartz and S. Ben-David. *Understanding machine learning: From theory to algorithms*. Cambridge university press, 2014.
- D. Soudry, E. Hoffer, M. S. Nacson, S. Gunasekar, and N. Srebro. The implicit bias of gradient descent on separable data. *The Journal of Machine Learning Research*, 19(1):2822–2878, 2018.
- M. Stojnic. A framework to characterize performance of lasso algorithms. *arXiv preprint arXiv:1303.7291*, 2013.
- P. Sur and E. J. Candès. A modern maximum-likelihood theory for high-dimensional logistic regression. *Proceedings of the National Academy of Sciences*, 116(29):14516–14525, 2019.
- C. Thrampoulidis, S. Oymak, and B. Hassibi. Regularized linear regression: A precise analysis of the estimation error. *Proceedings of Machine Learning Research*, 40:1683–1709, 2015.
- C. Thrampoulidis, E. Abbasi, and B. Hassibi. Precise error analysis of regularized m -estimators in high dimensions. *IEEE Transactions on Information Theory*, 64(8):5592–5628, 2018.
- A. Tsigler and P. L. Bartlett. Benign overfitting in ridge regression. *arXiv preprint arXiv:2009.14286*, 2020.
- F. Vallet, J.-G. Cailton, and P. Refregier. Linear and nonlinear extension of the pseudo-inverse solution for learning boolean functions. *EPL (Europhysics Letters)*, 9(4):315, 1989.
- A. Varre, L. Pillaud-Vivien, and N. Flammarion. Last iterate convergence of sgd for least-squares in the interpolation regime. *arXiv preprint arXiv:2102.03183*, 2021.
- R. Vershynin. *High-dimensional probability: An introduction with applications in data science*, volume 47. Cambridge university press, 2018.
- M. J. Wainwright. *High-dimensional statistics: A non-asymptotic viewpoint*, volume 48. Cambridge University Press, 2019.
- K. Wang and C. Thrampoulidis. Benign overfitting in binary classification of gaussian mixtures. In *2021 IEEE International Conference on Acoustics, Speech and Signal Processing (ICASSP)*. IEEE, 2021.
- Z. Yang, Y. Yu, C. You, J. Steinhardt, and Y. Ma. Rethinking bias-variance trade-off for generalization of neural networks. In *International Conference on Machine Learning*, pages 10767–10777. PMLR, 2020.
- C. Zhang, S. Bengio, M. Hardt, B. Recht, and O. Vinyals. Understanding deep learning requires rethinking generalization. *arXiv preprint arXiv:1611.03530*, 2016.
- D. Zou, J. Wu, V. Braverman, Q. Gu, and S. M. Kakade. Benign overfitting of constant-stepsize sgd for linear regression. *arXiv preprint arXiv:2103.12692*, 2021.

A Key Technical Lemmas

For the reader's convenience, we repeat here some definitions and lemmas that were previously stated in Section 8.2. Define $\mathbf{U}_\tau := \mathbf{Q}\mathbf{Q}^T + \tau\mathbf{I}$ and $\mathbf{d} := \mathbf{Q}\boldsymbol{\eta}$; thus $\mathbf{U}_0 = \mathbf{Q}\mathbf{Q}^T$. The lemma below expresses $\mathbf{y}^T(\mathbf{X}\mathbf{X}^T + \tau\mathbf{I})^{-1}$ in terms of the following quadratic forms:

$$\begin{aligned} s &= \mathbf{y}^T \mathbf{U}_\tau^{-1} \mathbf{y}, \\ t &= \mathbf{d}^T \mathbf{U}_\tau^{-1} \mathbf{d}, \\ h &= \mathbf{y}^T \mathbf{U}_\tau^{-1} \mathbf{d}, \\ g_i &= \mathbf{y}^T \mathbf{U}_0^{-1} \mathbf{e}_i, \quad i \in [n], \\ f_i &= \mathbf{d}^T \mathbf{U}_0^{-1} \mathbf{e}_i, \quad i \in [n]. \end{aligned}$$

Lemma 6. Define $D := s(\|\boldsymbol{\eta}\|_2^2 - t) + (h + 1)^2$, then

$$\mathbf{y}^T(\mathbf{X}\mathbf{X}^T + \tau\mathbf{I})^{-1} = \mathbf{y}^T \mathbf{U}_\tau^{-1} - \frac{1}{D} \left[\|\boldsymbol{\eta}\|_{2s}, h^2 + h - st, s \right] \begin{bmatrix} \|\boldsymbol{\eta}\|_{2\mathbf{y}^T} \\ \mathbf{y}^T \\ \mathbf{d}^T \end{bmatrix} \mathbf{U}_\tau^{-1}. \quad (37)$$

The lemma below derives upper/lower bounds for those quadratic forms involving the inverse Gram matrix \mathbf{U}_τ^{-1} .

Lemma 7 (Balanced). Recall that $\sigma^2 = \sum_{i=1}^p \lambda_i \beta_i^2$. Assume the $\boldsymbol{\Sigma}$ follows the balanced ensemble defined in Definition 2.1. Fix $\delta \in (0, 1)$ and suppose n is large enough such that $n > c \log(1/\delta)$ for some $c > 1$. Then, there exists constants $C_1, C_2, C_3, C_6, C_7 > 1$, $C_5 > C_4 > 0$ such that with probability at least $1 - \delta$, the following results hold:

$$\begin{aligned} \frac{n}{C_1(\tau + \|\boldsymbol{\lambda}\|_1)} &\leq s \leq C_1 \frac{n}{(\tau + \|\boldsymbol{\lambda}\|_1)}, \\ C_4 \frac{n\sigma^2}{(\tau + \|\boldsymbol{\lambda}\|_1)} &\leq t \leq C_5 \frac{n\sigma^2}{(\tau + \|\boldsymbol{\lambda}\|_1)}, \\ -C_2 \frac{n\sigma}{(\tau + \|\boldsymbol{\lambda}\|_1)} &\leq h \leq C_2 \frac{n\sigma}{(\tau + \|\boldsymbol{\lambda}\|_1)}, \\ \|\mathbf{d}\|_2^2 &\leq C_3 n\sigma^2, \\ \|\mathbf{y}^T \mathbf{U}_\tau^{-1}\|_2 &\leq C_6 \frac{\sqrt{n}}{(\tau + \|\boldsymbol{\lambda}\|_1)}, \\ \|\mathbf{d}^T \mathbf{U}_\tau^{-1}\|_2 &\leq C_7 \frac{\sqrt{n}\sigma}{(\tau + \|\boldsymbol{\lambda}\|_1)}. \end{aligned}$$

To bound the term f_i , we need some additional work, which leads to the following result.

Lemma 8. Assume that the condition in (8) is satisfied, Fix $\delta \in (0, 1)$ and suppose n is large enough such that $n > c/\delta$ for some $c > 1$. Then, there exists a constant $C > 1$ such that with probability at least $1 - \delta$,

$$\max_{i \in [n]} |f_i| \leq \frac{C\sqrt{\log(2n)\sigma}}{\|\boldsymbol{\lambda}\|_1}. \quad (38)$$

The proofs of Lemmas 6, 7 and 8 are given in Section G. We will also need the following lemmas adapted from Muthukumar et al. [2020a, Proof of Theorem 1].

Lemma 9. Let $\mathbf{E} = \mathbf{Q}\mathbf{Q}^T - \|\boldsymbol{\lambda}\|_1 \cdot \mathbf{I}$ and $\mathbf{E}' = \frac{1}{\|\boldsymbol{\lambda}\|_1} \cdot (\mathbf{Q}\mathbf{Q}^T)^{-1} \mathbf{E}$. Assume that the condition in (8) is satisfied, then there exists a constant $C > 1$ such that with probability at least $(1 - \frac{C}{n})$,

$$\|\mathbf{E}'\|_2 \leq \frac{1}{2\sqrt{n}\|\boldsymbol{\lambda}\|_1}. \quad (39)$$

Lemma 10. Let $d'(n) := (p - n + 1)$. With probability at least $(1 - \frac{2}{n^2})$,

$$y_i g_i = y_i (\mathbf{e}_i^T \mathbf{U}_0^{-1} \mathbf{y}) \geq \frac{1}{4\sqrt{n}} \frac{2\sqrt{n}d'(n) - 2n\sqrt{4\log(n)d'(n)} - 4n\log(n)}{(d'(n) + \sqrt{4\log(n)d'(n)})(d'(n) - \sqrt{4\log(n)d'(n)}), \quad \text{for } i \in [n].$$

B Proof of Theorem 1 and Theorem 2

B.1 Proof of Theorem 1

Now we are ready to prove Theorem 1. In this section, we only consider the unregularized estimator, i.e., $\tau = 0$. Define $\gamma^* := (\mathbf{X}\mathbf{X}^T)^{-1}\mathbf{y}$. Using duality (see Muthukumar et al. [2020a, Appendix C.1]), all the constraints in (5) hold with equality provided that

$$y_i\gamma_i^* > 0, \text{ for all } i \in [n]. \quad (40)$$

Hence it suffices to derive conditions under which (40) holds with high probability. Note that $\gamma_i^* = \mathbf{y}^T(\mathbf{X}\mathbf{X}^T)^{-1}\mathbf{e}_i$, for all $i \in [n]$. Using (37) and some algebra steps, it can be checked that:

$$\begin{aligned} \mathbf{y}^T(\mathbf{X}\mathbf{X}^T)^{-1}\mathbf{e}_i &= \mathbf{y}^T\mathbf{U}_0^{-1}\mathbf{e}_i - \frac{1}{D} \begin{bmatrix} \|\boldsymbol{\eta}\|_2 s & h^2 + h - st & s \end{bmatrix} \begin{bmatrix} \|\boldsymbol{\eta}\|_2 \mathbf{y}^T \mathbf{U}_0^{-1} \mathbf{e}_i \\ \mathbf{y}^T \mathbf{U}_0^{-1} \mathbf{e}_i \\ \mathbf{d}^T \mathbf{U}_0^{-1} \mathbf{e}_i \end{bmatrix} \\ &= g_i - \frac{1}{D} \begin{bmatrix} \|\boldsymbol{\eta}\|_2 s & h^2 + h - st & s \end{bmatrix} \begin{bmatrix} \|\boldsymbol{\eta}\|_2 g_i \\ g_i \\ f_i \end{bmatrix} \\ &= \frac{g_i(s(\|\boldsymbol{\eta}\|_2^2 - t) + (h+1)^2) - \|\boldsymbol{\eta}\|_2^2 s g_i - (h^2 + h - st)g_i - s f_i}{D} \\ &= \frac{g_i + h g_i - s f_i}{s(\|\boldsymbol{\eta}\|_2^2 - t) + (h+1)^2}. \end{aligned} \quad (41)$$

Here, s, h, t, g_i and f_i are as defined in Section A with $\tau = 0$. The denominator of (41) is non-negative, thus to make $\gamma_i > 0$, we only need to study the numerator:

$$y_i(g_i + h g_i - s f_i) = (1 + \mathbf{y}^T \mathbf{U}_0^{-1} \mathbf{d}) y_i (\mathbf{e}_i^T \mathbf{U}_0^{-1} \mathbf{y}) - y_i (\mathbf{e}_i^T \mathbf{U}_0^{-1} \mathbf{d}) \mathbf{y}^T \mathbf{U}_0^{-1} \mathbf{y}.$$

First, consider the term $y_i(\mathbf{e}_i^T \mathbf{U}_0^{-1} \mathbf{y})$. By the proof of Muthukumar et al. [2020a, Theorem 1], if (8) is satisfied, then with probability at least $(1 - \frac{C}{n})$,

$$y_i g_i \geq \frac{1}{2\|\boldsymbol{\lambda}\|_1}. \quad (42)$$

We know that $\mathbf{U}_0^{-1} = \frac{1}{\|\boldsymbol{\lambda}\|_1} \mathbf{I} - \mathbf{E}'$. Thus for $\mathbf{y}^T \mathbf{U}_0^{-1} \mathbf{d}$, by Lemma 7 and 9, with probability at least $(1 - \frac{C}{n})$,

$$\mathbf{y}^T \mathbf{U}_0^{-1} \mathbf{d} = \mathbf{y}^T \left(\frac{1}{\|\boldsymbol{\lambda}\|_1} \mathbf{I} - \mathbf{E}' \right) \mathbf{d} \geq -\frac{C_1 n \sigma}{\|\boldsymbol{\lambda}\|_1} - \frac{C_2 \sqrt{n} \sigma}{\|\boldsymbol{\lambda}\|_1} \geq -\frac{C_3 n \sigma}{\|\boldsymbol{\lambda}\|_1},$$

where the first inequality above follows from the fact $\mathbf{v}^T \mathbf{M} \mathbf{u} \geq -\|\mathbf{v}\|_2 \|\mathbf{u}\|_2 \|\mathbf{M}\|_2$. Lemma 8 gives for every $i \in [n]$, with the same high probability,

$$y_i \mathbf{e}_i^T \mathbf{U}_0^{-1} \mathbf{d} = y_i f_i \geq -\max_{i \in [n]} |f_i| \geq -\frac{C_4 \sqrt{\log(2n)} \sigma}{\|\boldsymbol{\lambda}\|_1}.$$

Similarly, the fact $\mathbf{v}^T \mathbf{M} \mathbf{u} \leq \|\mathbf{v}\|_2 \|\mathbf{u}\|_2 \|\mathbf{M}\|_2$ gives with probability at least $1 - \delta$,

$$\mathbf{y}^T \mathbf{U}_0^{-1} \mathbf{y} = \mathbf{y}^T \left(\frac{1}{\|\boldsymbol{\lambda}\|_1} \mathbf{I} - \mathbf{E}' \right) \mathbf{y} \leq \mathbf{y}^T \frac{1}{\|\boldsymbol{\lambda}\|_1} \mathbf{y} \leq \frac{C_5 n}{\|\boldsymbol{\lambda}\|_1}.$$

Combining the results above gives

$$\begin{aligned} y_i(g_i + h g_i - s f_i) &\geq \left(\frac{\|\boldsymbol{\lambda}\|_1 - C_1 n \sigma}{\|\boldsymbol{\lambda}\|_1} \right) \frac{1}{2\|\boldsymbol{\lambda}\|_1} - \frac{C_2 n \sqrt{\log(2n)} \sigma}{\|\boldsymbol{\lambda}\|_1^2} \\ &\geq \frac{\|\boldsymbol{\lambda}\|_1 - C_1 n \sigma - 2C_2 n \sqrt{\log(2n)} \sigma}{2\|\boldsymbol{\lambda}\|_1^2}. \end{aligned}$$

To make the expression above positive, it suffices to have $\|\boldsymbol{\lambda}\|_1 \geq C n \sqrt{\log(2n)} \sigma$. This completes the proof.

B.2 Proof of Theorem 2

According to section B.1, we need to study:

$$y_i(g_i + hg_i - sf_i) = (1 + \mathbf{y}^T \mathbf{U}_0^{-1} \mathbf{d}) y_i (\mathbf{e}_i^T \mathbf{U}_0^{-1} \mathbf{y}) - y_i (\mathbf{e}_i^T \mathbf{U}_0^{-1} \mathbf{d}) \mathbf{y}^T \mathbf{U}_0^{-1} \mathbf{y}.$$

First, consider the term $y_i (\mathbf{e}_i^T \mathbf{U}_0^{-1} \mathbf{y})$. By Lemma 10, if $d'(n) = p - n + 1 > 9n \log(n)$, then, $4n \log(n) < \frac{4}{9} d'(n)$ gives

$$\begin{aligned} y_i g_i = y_i (\mathbf{e}_i^T \mathbf{U}_0^{-1} \mathbf{y}) &> \frac{1}{4\sqrt{n}} \frac{2\sqrt{nd'}(n) - \frac{4}{3}\sqrt{nd'}(n) - \frac{4}{9}d'(n)}{(d'(n) + \sqrt{4/(9n)d'(n)})d'(n)} \\ &> \frac{1}{4\sqrt{n}} \frac{2\sqrt{nd'}(n) - \frac{4}{3}\sqrt{nd'}(n) - \frac{4}{9}\sqrt{nd'}(n)}{2d'(n)^2} \\ &> \frac{1}{4\sqrt{n}} \frac{(2 - \frac{4}{3} - \frac{4}{9})\sqrt{n}}{2p} \\ &> \frac{1}{36p}. \end{aligned} \tag{43}$$

Second, by Lemmas 7, 8 and (43), we find that for large enough constants C_i 's > 1 , with probability at least $1 - \frac{C_1}{n^2}$,

$$\begin{aligned} y_i(g_i + hg_i - sf_i) &= (1 + h)y_i g_i - y_i s f_i \\ &\geq (1 - |h|) \frac{1}{36p} - \max_{i \in [n]} |f_i| s \\ &\geq (1 - \frac{C_2 n}{p} \|\boldsymbol{\eta}\|_2) \frac{1}{36p} - \frac{C_3 \sqrt{\log(2n)}}{p} \|\boldsymbol{\eta}\|_2 \frac{n}{p} \\ &\geq \frac{p - C_2 n \|\boldsymbol{\eta}\|_2 - 36C_3 \sqrt{2 \log(2n)n} \|\boldsymbol{\eta}\|_2}{36p^2} \\ &\geq \frac{p - 36C_4 \sqrt{2 \log(2n)n} \|\boldsymbol{\eta}\|_2}{36p^2}. \end{aligned}$$

To make the expression above positive, it suffices to have $p > C_5 n \sqrt{\log(2n)} \|\boldsymbol{\eta}\|_2$, for large enough $C_5 > 1$. The result above holds for every γ_i^* , $i \in [n]$ with probability $1 - \frac{C_1}{n^2}$ each (by Lemma 9). Applying union bound over all n training data points, we conclude that $y_i \gamma_i^* > 0$ for all i with probability at least $1 - \frac{C_1}{n}$. This completes the proof.

C Proof of Theorem 3 and Theorem 4

C.1 Proof of Theorem 3

From Section 8, we need to lower bound the ratio

$$\frac{(\mathbf{y}^T (\mathbf{X}\mathbf{X}^T + \tau\mathbf{I})^{-1} \mathbf{X}\boldsymbol{\eta})^2}{\mathbf{y}^T (\mathbf{X}\mathbf{X}^T + \tau\mathbf{I})^{-1} \mathbf{X}\boldsymbol{\Sigma}\mathbf{X}^T (\mathbf{X}\mathbf{X}^T + \tau\mathbf{I})^{-1} \mathbf{y}}. \tag{44}$$

We will upper bound the denominator and lower bound the numerator. We first look at the denominator. We know $\mathbf{X}\boldsymbol{\Sigma}\mathbf{X}^T = (\mathbf{y}\boldsymbol{\beta}^T + \mathbf{Z}\boldsymbol{\Lambda}^{\frac{1}{2}})\boldsymbol{\Lambda}(\mathbf{y}\boldsymbol{\beta}^T + \mathbf{Z}\boldsymbol{\Lambda}^{\frac{1}{2}})^T$. Define $\mathbf{A} := (\mathbf{X}\mathbf{X}^T + \tau\mathbf{I})^{-1} \mathbf{y}\mathbf{y}^T (\mathbf{X}\mathbf{X}^T +$

$\tau \mathbf{I}$)⁻¹. Then by the cyclic property of trace, the denominator of (44) can be expressed as

$$\begin{aligned}
& \text{Tr}\left(\mathbf{y}^T(\mathbf{X}\mathbf{X}^T + \tau\mathbf{I})^{-1}\mathbf{X}\Sigma\mathbf{X}^T(\mathbf{X}\mathbf{X}^T + \tau\mathbf{I})^{-1}\mathbf{y}\right) \\
&= \text{Tr}\left((\mathbf{y}\boldsymbol{\beta}^T + \mathbf{Z}\boldsymbol{\Lambda}^{\frac{1}{2}})\boldsymbol{\Lambda}(\mathbf{y}\boldsymbol{\beta}^T + \mathbf{Z}\boldsymbol{\Lambda}^{\frac{1}{2}})^T\mathbf{A}\right) \\
&= \sum_{i=1}^p \lambda_i^2 \mathbf{z}_i^T \mathbf{A} \mathbf{z}_i + \sum_{i=1}^p \lambda_i \beta_i^2 (\mathbf{y}^T \mathbf{A} \mathbf{y}) + 2 \sum_{i=1}^p \lambda_i^{1.5} \beta_i \mathbf{z}_i^T \mathbf{A} \mathbf{y} \\
&\leq 2 \left(\sum_{i=1}^p \lambda_i^2 \mathbf{z}_i^T \mathbf{A} \mathbf{z}_i + \sigma^2 \mathbf{y}^T \mathbf{A} \mathbf{y} \right) \\
&\leq 2 \left(\sum_{i=1}^p \lambda_i^2 \|\mathbf{A}\|_2 \|\mathbf{z}_i\|_2^2 + \sigma^2 (\mathbf{y}^T (\mathbf{X}\mathbf{X}^T + \tau\mathbf{I})^{-1} \mathbf{y})^2 \right),
\end{aligned}$$

where the first inequality follows from the inequality $\mathbf{v}^T \mathbf{M} \mathbf{u} \leq \frac{1}{2}(\mathbf{v}^T \mathbf{M} \mathbf{v} + \mathbf{u}^T \mathbf{M} \mathbf{u})$ for positive semidefinite matrix \mathbf{M} and \mathbf{z}_i is the i -th column of matrix \mathbf{Z} . Thus, we need to upper bound $\sum_{i=1}^p \lambda_i^2 \|\mathbf{A}\|_2 \|\mathbf{z}_i\|_2^2$ and $\sigma^2 (\mathbf{y}^T (\mathbf{X}\mathbf{X}^T + \tau\mathbf{I})^{-1} \mathbf{y})^2$. For $\sum_{i=1}^p \lambda_i^2 \|\mathbf{A}\|_2 \|\mathbf{z}_i\|_2^2$, note that $\|\mathbf{z}_i\|_2^2$'s are independent sub-exponential random variables [Vershynin, 2018, Chapter 2], thus for a fixed number $B > 0$, $\sum_{i=1}^p \lambda_i^2 B \|\mathbf{z}_i\|_2^2$ is the weighted sum of sub-exponential random variables, with the weights given by $B \lambda_i^2$ in blocks of size n [Bartlett et al., 2020, Lemma 7 and Corollary 1]. By Lemma 8.1, with probability at least $1 - 2e^{-x}$,

$$\begin{aligned}
\sum_{i=1}^p \lambda_i^2 B \|\mathbf{z}_i\|_2^2 &\leq Bn \sum_{i=1}^p \lambda_i^2 + Bc \max\left(\lambda_1^2 x, \sqrt{xn \sum_{i=1}^p \lambda_i^4}\right) \\
&\leq Bn \sum_{i=1}^p \lambda_i^2 + Bc \max\left(x \sum_{i=1}^p \lambda_i^2, \sqrt{xn \sum_{i=1}^p \lambda_i^2}\right) \\
&\leq CnB \sum_{i=1}^p \lambda_i^2,
\end{aligned}$$

for $x < n/c_0$. The number B above should be replaced by the upper bound of $\|\mathbf{A}\|_2$. Recall $\mathbf{A} := (\mathbf{X}\mathbf{X}^T + \tau\mathbf{I})^{-1} \mathbf{y} \mathbf{y}^T (\mathbf{X}\mathbf{X}^T + \tau\mathbf{I})^{-1}$, thus $\|\mathbf{A}\|_2 = \|\mathbf{y}^T (\mathbf{X}\mathbf{X}^T + \tau\mathbf{I})^{-1}\|_2^2$. Further recalling $D := s(\|\boldsymbol{\eta}\|_2^2 - t) + (h+1)^2$, by Lemma 6,

$$\begin{aligned}
\mathbf{y}^T (\mathbf{X}\mathbf{X}^T + \tau\mathbf{I})^{-1} &= \mathbf{y}^T \mathbf{U}_\tau^{-1} - \frac{1}{D} \begin{bmatrix} \|\boldsymbol{\eta}\|_2 s & h^2 + h - st & s \end{bmatrix} \begin{bmatrix} \|\boldsymbol{\eta}\|_2 \mathbf{y}^T \\ \mathbf{y}^T \\ \mathbf{d}^T \end{bmatrix} \mathbf{U}_\tau^{-1} \\
&= \frac{1}{D} \left((1+h) \mathbf{y}^T \mathbf{U}_\tau^{-1} - s \mathbf{d}^T \mathbf{U}_\tau^{-1} \right).
\end{aligned}$$

Therefore, by Lemma 7, with probability at least $1 - \delta$,

$$\begin{aligned}
\|\mathbf{y}^T (\mathbf{X}\mathbf{X}^T + \tau\mathbf{I})^{-1}\|_2 &\leq \frac{1}{D} \left((1+|h|) \|\mathbf{y}\|_2 \|\mathbf{U}_\tau^{-1}\|_2 + s \|\mathbf{d}\|_2 \|\mathbf{U}_\tau^{-1}\|_2 \right) \\
&\leq \frac{1}{D} \left(\left(1 + \frac{C_1 n \sigma}{(\tau + \|\boldsymbol{\lambda}\|_1)}\right) \frac{C_2 \sqrt{n}}{(\tau + \|\boldsymbol{\lambda}\|_1)} + \frac{C_3 n \sqrt{n} \sigma}{(\tau + \|\boldsymbol{\lambda}\|_1)^2} \right).
\end{aligned}$$

The above result can be further simplified. If $1 \leq \frac{n\sigma}{\tau + \|\boldsymbol{\lambda}\|_1}$, then,

$$\|\mathbf{y}^T (\mathbf{X}\mathbf{X}^T + \tau\mathbf{I})^{-1}\|_2 \leq \frac{1}{D} \frac{C_4 n \sqrt{n} \sigma}{(\tau + \|\boldsymbol{\lambda}\|_1)^2}.$$

If $1 > \frac{n\sigma}{\tau + \|\boldsymbol{\lambda}\|_1}$, then,

$$\|\mathbf{y}^T (\mathbf{X}\mathbf{X}^T + \tau\mathbf{I})^{-1}\|_2 \leq \frac{1}{D} \frac{C_5 \sqrt{n}}{(\tau + \|\boldsymbol{\lambda}\|_1)}.$$

Combining the above gives, with probability at least $1 - \delta$,

$$\sum_{i=1}^p \lambda_i^2 \|\mathbf{A}\|_2 \|\mathbf{z}_i\|_2^2 \leq \frac{C}{D^2} \frac{n^2}{(\tau + \|\boldsymbol{\lambda}\|_1)^2} \max\left\{1, \frac{n^2 \sigma^2}{(\tau + \|\boldsymbol{\lambda}\|_1)^2}\right\} \|\boldsymbol{\lambda}\|_2^2. \quad (45)$$

Now we look at $\sigma^2 (\mathbf{y}^T (\mathbf{X} \mathbf{X}^T + \tau \mathbf{I})^{-1} \mathbf{y})^2$. We need to upper bound $\mathbf{y}^T (\mathbf{X} \mathbf{X}^T + \tau \mathbf{I})^{-1} \mathbf{y}$. Using Lemma 7 gives with probability at least $1 - \delta$,

$$\begin{aligned} \mathbf{y}^T (\mathbf{X} \mathbf{X}^T + \tau \mathbf{I})^{-1} \mathbf{y} &= s - \frac{\|\boldsymbol{\eta}\|_2^2 s^2 + sh^2 + 2sh - s^2 t}{s(\|\boldsymbol{\eta}\|_2^2 - t) + (h+1)^2} \\ &= \frac{s}{s(\|\boldsymbol{\eta}\|_2^2 - t) + (h+1)^2} \\ &= \frac{s}{D} \leq \frac{1}{D} \frac{Cn}{(\tau + \|\boldsymbol{\lambda}\|_1)}. \end{aligned}$$

Therefore, $\sigma^2 \mathbf{y}^T \mathbf{A} \mathbf{y} \leq \frac{C}{D^2} \frac{n^2 \sigma^2}{(\tau + \|\boldsymbol{\lambda}\|_1)^2}$. Hence the denominator of (44) is upper bounded by

$$\frac{1}{D^2} \frac{n^2}{(\tau + \|\boldsymbol{\lambda}\|_1)^2} \left(C_1 \max\left\{1, \frac{n^2 \sigma^2}{(\tau + \|\boldsymbol{\lambda}\|_1)^2}\right\} \|\boldsymbol{\lambda}\|_2 + C_2 \sigma^2 \right). \quad (46)$$

Now we look at the numerator of (44). By Lemma 6,

$$\begin{aligned} \mathbf{y}^T (\mathbf{X} \mathbf{X}^T + \tau \mathbf{I})^{-1} \mathbf{X} \boldsymbol{\eta} &= \|\boldsymbol{\eta}\|_2^2 \mathbf{y}^T (\mathbf{X} \mathbf{X}^T + \tau \mathbf{I})^{-1} \mathbf{y} + \mathbf{y}^T (\mathbf{X} \mathbf{X}^T + \tau \mathbf{I})^{-1} \mathbf{Q} \boldsymbol{\eta} \\ &= \frac{s(\|\boldsymbol{\eta}\|_2^2 - t) + h^2 + h}{D}. \end{aligned}$$

The numerator needs to be lower bounded and Lemma 7 gives with probability at least $1 - \delta$,

$$s(\|\boldsymbol{\eta}\|_2^2 - t) + h^2 + h \geq s(\|\boldsymbol{\eta}\|_2^2 - t) + h \geq \frac{n}{C(\tau + \|\boldsymbol{\lambda}\|_1)} \left(\|\boldsymbol{\eta}\|_2^2 - \frac{C_1 n \sigma^2}{\tau + \|\boldsymbol{\lambda}\|_1} - C_2 \sigma \right). \quad (47)$$

Combining (46) and (47) gives with probability at least $1 - \delta$, (44) is lower bounded by

$$\frac{\left(\|\boldsymbol{\eta}\|_2^2 - \frac{C_1 n \sigma^2}{\tau + \|\boldsymbol{\lambda}\|_1} - C_2 \sigma \right)^2}{C_3 \max\left\{1, \frac{n^2 \sigma^2}{(\tau + \|\boldsymbol{\lambda}\|_1)^2}\right\} \|\boldsymbol{\lambda}\|_2^2 + C_4 \sigma^2}. \quad (48)$$

This completes the proof of the theorem.

C.2 Proof of Theorem 4

We need to lower bound the ratio

$$\frac{(\mathbf{y}^T (\mathbf{X} \mathbf{X}^T)^{-1} \mathbf{X} \boldsymbol{\eta})^2}{\mathbf{y}^T (\mathbf{X} \mathbf{X}^T)^{-1} \mathbf{y}}. \quad (49)$$

Here we will lower bound $\mathbf{y}^T (\mathbf{X} \mathbf{X}^T)^{-1} \mathbf{X} \boldsymbol{\eta}$ and upper bound $\mathbf{y}^T (\mathbf{X} \mathbf{X}^T)^{-1} \mathbf{y}$. By Lemma 1, we know that the bound is not useful if $\mathbf{y}^T (\mathbf{X} \mathbf{X}^T)^{-1} \mathbf{X} \boldsymbol{\eta} < 0$, hence we need the conditions that ensure $\mathbf{y}^T (\mathbf{X} \mathbf{X}^T)^{-1} \mathbf{X} \boldsymbol{\eta} \geq 0$ with high probability. Using (37) and some algebra steps, it can be checked that:

$$\mathbf{y}^T (\mathbf{X} \mathbf{X}^T)^{-1} \mathbf{y} = s - \frac{\|\boldsymbol{\eta}\|_2^2 s^2 + sh^2 + 2sh - s^2 t}{s(\|\boldsymbol{\eta}\|_2^2 - t) + (h+1)^2} = \frac{s}{s(\|\boldsymbol{\eta}\|_2^2 - t) + (h+1)^2}. \quad (50)$$

Similarly,

$$\mathbf{y}^T (\mathbf{X} \mathbf{X}^T)^{-1} \mathbf{X} \boldsymbol{\eta} = \|\boldsymbol{\eta}\|_2^2 \mathbf{y}^T (\mathbf{X} \mathbf{X}^T)^{-1} \mathbf{y} + \mathbf{y}^T (\mathbf{X} \mathbf{X}^T)^{-1} \mathbf{Q} \boldsymbol{\eta} = \frac{s \|\boldsymbol{\eta}\|_2^2 - st + h^2 + h}{s(\|\boldsymbol{\eta}\|_2^2 - t) + (h+1)^2}.$$

Combining the above gives

$$\frac{(\mathbf{y}^T(\mathbf{X}\mathbf{X}^T)^{-1}\mathbf{X}\boldsymbol{\eta})^2}{\mathbf{y}^T(\mathbf{X}\mathbf{X}^T)^{-1}\mathbf{y}} = \frac{\left(s(\|\boldsymbol{\eta}\|_2^2 - t) + h^2 + h\right)^2}{s\left(s(\|\boldsymbol{\eta}\|_2^2 - t) + (h+1)^2\right)}. \quad (51)$$

The numerator needs to be lower bounded and Lemma 7 gives with probability at least $1 - \delta$,

$$\begin{aligned} s(\|\boldsymbol{\eta}\|_2^2 - t) + h^2 + h &\geq s(\|\boldsymbol{\eta}\|_2^2 - t) + h \\ &\geq \frac{n}{C_1 p} \left(1 - \frac{n}{p}\right) \|\boldsymbol{\eta}\|_2^2 - C_2 \frac{n}{p} \|\boldsymbol{\eta}\|_2 \\ &\geq \frac{n}{C_1 p} \left(\left(1 - \frac{n}{p}\right) \|\boldsymbol{\eta}\|_2^2 - C_3 \|\boldsymbol{\eta}\|_2\right). \end{aligned} \quad (52)$$

Similarly, the denominator is upper bounded by:

$$\begin{aligned} s\left(s(\|\boldsymbol{\eta}\|_2^2 - t) + (h+1)^2\right) &\leq s\left(s\|\boldsymbol{\eta}\|_2^2 + (1+|h|)^2\right) \\ &\leq C_1 \frac{n}{p} \left(C_1 \frac{n}{p} \|\boldsymbol{\eta}\|_2^2 + (1+C_2 \frac{n}{p} \|\boldsymbol{\eta}\|_2)^2\right) \\ &\leq C_1 \frac{n}{p} \left(C_3 \frac{n}{p} \|\boldsymbol{\eta}\|_2^2 + C_4\right) \\ &\leq C_5 \frac{n^2}{p^2} \left(\|\boldsymbol{\eta}\|_2^2 + \frac{p}{n}\right), \end{aligned}$$

where we also use the fact $(a+b)^2 \leq 2(a^2 + b^2)$ and $n < p$. Combining the above results gives with probability at least $1 - \delta$,

$$\frac{(\mathbf{y}^T(\mathbf{X}\mathbf{X}^T)^{-1}\mathbf{X}\boldsymbol{\eta})^2}{\mathbf{y}^T(\mathbf{X}\mathbf{X}^T)^{-1}\mathbf{y}} \geq \|\boldsymbol{\eta}\|_2^2 \frac{\left(\left(1 - \frac{n}{p}\right) \|\boldsymbol{\eta}\|_2 - C_3\right)^2}{C_6 \left(\frac{p}{n} + \|\boldsymbol{\eta}\|_2^2\right)}. \quad (53)$$

To ensure the classification error is smaller than 0.5, we need $p > b \cdot n$ and $\left(1 - \frac{n}{p}\right) \|\boldsymbol{\eta}\|_2 > C_3$ for $b > 1$ to make $\hat{\boldsymbol{\eta}}_{\text{LS}}^T \boldsymbol{\eta} > 0$ with high probability. This completes the proof of the theorem.

D Proof of Theorem 5 and benign overfitting for the bi-level ensemble

D.1 Proof of Theorem 5

We first introduce some new notations. Following Assumption 1, we assume that the covariance matrix $\boldsymbol{\Sigma}$ is diagonal and the mean vector $\boldsymbol{\eta}$ is one-sparse ($\eta_k \neq 0$ and $k \neq 1$). Hence the data matrix \mathbf{X} can be written as

$$\mathbf{X} = \mathbf{y}\boldsymbol{\eta}^T + \mathbf{Q} = \mathbf{y}\boldsymbol{\eta}^T + \mathbf{Z}\boldsymbol{\Lambda}^{\frac{1}{2}}.$$

Let \mathbf{z}_i be the i -th column of the matrix \mathbf{Z} above whose elements are IID standard Gaussian. Recall $\mathbf{U}_\tau := \mathbf{Q}\mathbf{Q}^T + \tau\mathbf{I}$, define

$$\begin{aligned} s &:= \mathbf{y}^T \mathbf{U}_\tau^{-1} \mathbf{y}, \\ t_k &:= \mathbf{z}_k^T \mathbf{U}_\tau^{-1} \mathbf{z}_k, \\ f_1 &:= \mathbf{y}^T \mathbf{U}_\tau^{-1} \mathbf{z}_1, \\ f_k &:= \mathbf{y}^T \mathbf{U}_\tau^{-1} \mathbf{z}_k, \\ g_1 &:= \mathbf{z}_1^T \mathbf{U}_\tau^{-1} \mathbf{z}_k. \end{aligned}$$

Lemma 11 (Bi-level). *Assume that Σ follows the bi-level ensemble defined in Definition 2. Fix $\delta \in (0, 1)$ and suppose n is large enough such that $n > c \log(1/\delta)$ for some $c > 1$. Then, there exists constants C_i 's > 1 such that with probability at least $1 - \delta$, the following results hold:*

$$\begin{aligned} \frac{n}{C_1(\tau + \|\boldsymbol{\lambda}\|_{-1})} &\leq s \leq \frac{C_2 n}{(\tau + \|\boldsymbol{\lambda}\|_{-1})}, \\ -\frac{C_3 n}{(\tau + \|\boldsymbol{\lambda}\|_{-1})} &\leq f_k \leq \frac{C_3 n}{(\tau + \|\boldsymbol{\lambda}\|_{-1})}, \\ \frac{n}{C_4(\tau + \|\boldsymbol{\lambda}\|_{-1})} &\leq t_k \leq \frac{C_5 n}{(\tau + \|\boldsymbol{\lambda}\|_{-1})}, \\ -\frac{C_6 n}{(\tau + \|\boldsymbol{\lambda}\|_{-1} + n\lambda_1)} &\leq f_1 \leq \frac{C_6 n}{(\tau + \|\boldsymbol{\lambda}\|_{-1} + n\lambda_1)}, \\ -\frac{C_7 n}{(\tau + \|\boldsymbol{\lambda}\|_{-1} + n\lambda_1)} &\leq g_1 \leq \frac{C_7 n}{(\tau + \|\boldsymbol{\lambda}\|_{-1} + n\lambda_1)}, \\ \|\mathbf{y}^T \mathbf{U}_\tau^{-1}\|_2 &\leq \frac{C_8 \sqrt{n}}{(\tau + \|\boldsymbol{\lambda}\|_{-1})}, \\ \|\mathbf{z}_k^T \mathbf{U}_\tau^{-1}\|_2 &\leq \frac{C_9 \sqrt{n}}{(\tau + \|\boldsymbol{\lambda}\|_{-1})}. \end{aligned}$$

Now we are ready to prove Theorem 5. We know from the proof outline that we need to lower bound

$$\frac{(\hat{\boldsymbol{\eta}}_\tau^T \boldsymbol{\eta})^2}{\hat{\boldsymbol{\eta}}_\tau^T \Sigma \hat{\boldsymbol{\eta}}_\tau} = \frac{(\eta_k \hat{\eta}_k)^2}{\sum_{i=1}^p \lambda_i \hat{\eta}_i^2}. \quad (54)$$

We divide $\hat{\eta}_i$'s into 3 groups: $\hat{\eta}_1$, $\hat{\eta}_k$ and the rest. Rather than lower bounding (54), we will upper bound its reciprocal. Specifically, we will upper bound

$$\frac{\lambda_1 \hat{\eta}_1^2}{(\eta_k \hat{\eta}_k)^2}, \quad \frac{\sum_{i \neq 1, k} \lambda_i \hat{\eta}_i^2}{(\eta_k \hat{\eta}_k)^2} \quad \text{and} \quad \frac{\lambda_k \hat{\eta}_k^2}{(\eta_k \hat{\eta}_k)^2}, \quad (55)$$

then reverse the sum of the upper bounds of the three ratios above to obtain the lower bound of (54).

Following the fact that $\hat{\eta}_i = \mathbf{e}_i^T \hat{\boldsymbol{\eta}}$, we have

$$\hat{\eta}_i = \sqrt{\lambda_i} \mathbf{z}_i^T (\mathbf{X} \mathbf{X}^T + \tau \mathbf{I})^{-1} \mathbf{y}, \quad \text{for } i \neq k, \quad (56)$$

$$\hat{\eta}_k = \eta_k \mathbf{y}^T (\mathbf{X} \mathbf{X}^T + \tau \mathbf{I})^{-1} \mathbf{y} + \sqrt{\lambda_k} \mathbf{z}_k^T (\mathbf{X} \mathbf{X}^T + \tau \mathbf{I})^{-1} \mathbf{y}. \quad (57)$$

To upper bound the 3 terms in (55), we need to lower bound $(\eta_k \hat{\eta}_k)^2$. Recall that under Assumption 1, σ^2 is $\lambda_k \eta_k^2$. By Lemma 6 and using our newly defined notations, we have

$$\begin{aligned} \eta_k \hat{\eta}_k &= \frac{\eta_k^2 s}{D} + \sqrt{\lambda_k} \eta_k \left(f_k - \frac{\|\boldsymbol{\eta}\|_2^2 s f_k + ((\sqrt{\lambda_k} \eta_k f_k)^2 + \sqrt{\lambda_k} \eta_k f_k - s(\lambda_k \eta_k^2 t_k)) f_k + \sqrt{\lambda_k} \eta_k t_k s}{D} \right) \\ &= \frac{1}{D} \left(\eta_k^2 s (1 - \lambda_k t_k) + \sigma f_k + \sigma^2 f_k^2 \right), \end{aligned}$$

where D becomes $(\sigma f_k + 1)^2 + s(\eta_k^2 - \sigma^2 t_k)$. Lemma 11 gives with probability at least $1 - \delta$,

$$\eta_k \hat{\eta}_k \geq \frac{1}{D} \frac{n}{C_1(\tau + \|\boldsymbol{\lambda}\|_{-1})} \left(\eta_k^2 \left(1 - \frac{C_2 n \lambda_k}{\tau + \|\boldsymbol{\lambda}\|_{-1}} \right) - \sigma \right). \quad (58)$$

Now we upper bound $\sum_{i \neq 1, k} \lambda_i \hat{\eta}_i^2$. From the proof of Theorem 3, we know

$$\sum_{i \neq 1, k} \lambda_i \hat{\eta}_i^2 = \sum_{i \neq 1, k} \lambda_i^2 \mathbf{z}_i^T \mathbf{A} \mathbf{z}_i \leq \sum_{i \neq 1, k} \lambda_i^2 \|\mathbf{z}_i\|_2^2 \|\mathbf{A}\|_2,$$

where $\mathbf{A} = (\mathbf{X}\mathbf{X}^T + \tau\mathbf{I})^{-1}\mathbf{y}\mathbf{y}^T(\mathbf{X}\mathbf{X}^T + \tau\mathbf{I})^{-1}$. Then we need to upper bound $\|\mathbf{y}^T(\mathbf{X}\mathbf{X}^T + \tau\mathbf{I})^{-1}\|_2$. Following Lemmas 6 and 11, we have

$$\begin{aligned}\|\mathbf{y}^T(\mathbf{X}\mathbf{X}^T + \tau\mathbf{I})^{-1}\|_2 &= \left\| \frac{1}{D} \left(\mathbf{y}^T \mathbf{U}_\tau^{-1} (1 + \sigma f_k) - \mathbf{z}_k^T \mathbf{U}_\tau^{-1} (\sigma s) \right) \right\|_2 \\ &\leq \frac{1}{D} \left((1 + \sigma f_k) \|\mathbf{y}^T \mathbf{U}_\tau^{-1}\|_2 + (\sigma s) \|\mathbf{z}_k^T \mathbf{U}_\tau^{-1}\|_2 \right) \\ &\leq \frac{1}{D} \frac{C_1 \sqrt{n}}{(\tau + \|\boldsymbol{\lambda}\|_{-1})} \left(1 + \frac{C_2 n \sigma}{(\tau + \|\boldsymbol{\lambda}\|_{-1})} \right).\end{aligned}$$

Note for a fixed number $B > 0$, $\sum_{i \neq 1, k} \lambda_i^2 \|\mathbf{z}_i\|_2^2 B$ is the weighted sum of sub-exponential random variables. By Bartlett et al. [2020, Lemma 7], with probability at least $1 - 2e^{-x}$,

$$\sum_{i=1}^p \lambda_i^2 B \|\mathbf{z}_i\|_2^2 \leq Cn \sum_{i=1}^p \lambda_i^2 B,$$

for $x < n/c_0$. Combining (58) and bounds above with B replaced by the upper bound of \mathbf{A} gives with probability at least $1 - \delta$,

$$\frac{\sum_{i \neq 1, k} \lambda_i \hat{\eta}_i^2}{(\eta_k \hat{\eta}_k)^2} \leq \frac{C_1 \sum_{i \neq 1, k} \lambda_i^2}{\left(\eta_k^2 \left(1 - \frac{C_2 n \lambda_k}{\tau + \|\boldsymbol{\lambda}\|_{-1}} \right) - \sigma \right)^2} \left(1 + \frac{C_3 n \sigma}{(\tau + \|\boldsymbol{\lambda}\|_{-1})} \right)^2. \quad (59)$$

Next we upper bound $\lambda_1 \hat{\eta}_1^2$. (56) gives

$$\begin{aligned}\hat{\eta}_1 &= \sqrt{\lambda_1} \mathbf{z}_1^T (\mathbf{X}\mathbf{X}^T + \tau\mathbf{I})^{-1} \mathbf{y} \\ &= \frac{\sqrt{\lambda_1}}{D} (f_1 + \sigma f_1 f_k - \sigma g_1 s) \\ &\leq \frac{\sqrt{\lambda_1}}{D} \frac{C_6 n}{(\tau + \|\boldsymbol{\lambda}\|_{-1} + n \lambda_1)} \left(1 + \frac{C_3 n \sigma}{(\tau + \|\boldsymbol{\lambda}\|_{-1})} \right).\end{aligned}$$

Combining the result above and (58) gives with probability at least $1 - \delta$,

$$\frac{\lambda_1 \hat{\eta}_1^2}{(\eta_k \hat{\eta}_k)^2} \leq \frac{C_1 \lambda_1^2}{\left(\eta_k^2 \left(1 - \frac{C_2 n \lambda_k}{\tau + \|\boldsymbol{\lambda}\|_{-1}} \right) - \sigma \right)^2} \frac{(\tau + \|\boldsymbol{\lambda}\|_{-1})^2}{(\tau + \|\boldsymbol{\lambda}\|_{-1} + n \lambda_1)^2} \left(1 + \frac{C_3 n \sigma}{(\tau + \|\boldsymbol{\lambda}\|_{-1})} \right)^2. \quad (60)$$

In addition, $\frac{\lambda_k \hat{\eta}_k^2}{(\eta_k \hat{\eta}_k)^2}$ in (55) is $\frac{\lambda_k}{\eta_k^2}$. Then the sum of (59), (60) and $\frac{\lambda_k}{\eta_k^2}$ is

$$\frac{A + B + \lambda_k \left(\eta_k \left(1 - \frac{C_2 n \lambda_k}{\tau + \|\boldsymbol{\lambda}\|_{-1}} \right) - \sqrt{\lambda_k} \right)^2}{\left(\eta_k^2 \left(1 - \frac{C_2 n \lambda_k}{\tau + \|\boldsymbol{\lambda}\|_{-1}} \right) - \sigma \right)^2} \leq \frac{A + B + \lambda_k \left(\eta_k^2 + \lambda_k \right)}{\left(\eta_k^2 \left(1 - \frac{C_2 n \lambda_k}{\tau + \|\boldsymbol{\lambda}\|_{-1}} \right) - \sigma \right)^2},$$

where we use $(a - b)^2 \leq a^2 + b^2$ for $a, b > 0$ and with

$$\begin{aligned}A &= C_3 \lambda_1^2 \left(\frac{\tau + \|\boldsymbol{\lambda}\|_{-1}}{\tau + n \lambda_1 + \|\boldsymbol{\lambda}\|_{-1}} \right)^2 \left(1 + \frac{C_4 n \sigma}{\tau + \|\boldsymbol{\lambda}\|_{-1}} \right)^2, \\ B &= C_5 \left(\sum_{i \neq 1, k} \lambda_i^2 \right) \left(1 + \frac{C_4 n \sigma}{\tau + \|\boldsymbol{\lambda}\|_{-1}} \right)^2,\end{aligned}$$

for large constants C_i 's. The inverse of the upper bound of $\frac{\lambda_k}{\eta_k^2}$ gives the lower bound of (54). To ensure $\hat{\boldsymbol{\eta}}_\tau^T \boldsymbol{\eta} > 0$ with high probability, we need $\eta_k^2 > \frac{c_1 n \sigma^2}{\tau + \|\boldsymbol{\lambda}\|_{-1}} + c_2 \sigma$ for $c_1, c_2 > 1$.

D.2 Benign overfitting for the bi-level ensemble

For the bi-level ensemble, the first condition in Theorem 1 is not satisfied, hence we can no longer analyze $\hat{\eta}_{\text{SVM}}$ by studying $\hat{\eta}_{\text{LS}}$. We show a regime that suffices to make the classification error of $\hat{\eta}_{\text{LS}}$ vanish as p increase to $+\infty$. Consider the setting:

$$\lambda_2 = \dots = \lambda_p = \lambda \quad \text{and} \quad \lambda_1 = \alpha p \lambda, \quad \text{for } \alpha > 1. \quad (61)$$

For large enough p , the setting above can ensure the bi-level ensemble condition in (3) is satisfied.

Corollary 7.2. *Assume that the data generating process follows Assumption 1 and (61). Fix $\delta \in (0, 1)$ and suppose n is finite but large enough such that $n > c \log(1/\delta)$ for some $c > 1$. Then for large enough $C > 1$, with probability at least $1 - \delta$, $\mathcal{R}(\hat{\eta}_{\text{LS}})$, the expected 0-1 loss of the least squares estimator $\hat{\eta}_{\text{LS}}$, approaches 0 as $p \rightarrow \infty$, provided that $\eta_k > C\sqrt{\lambda}p^r$, for $r > \frac{1}{2}$.*

Proof. First, the bound on the unregularized estimator $\hat{\eta}_{\text{LS}}$ can be obtained by setting $\tau = 0$ in (17). Thus, with probability at least $1 - \delta$, $\mathcal{R}(\hat{\eta}_{\text{LS}})$ is upper bounded by

$$\exp\left(\frac{-\left(\eta_k^2\left(1 - \frac{C_1 n \lambda_k}{\|\boldsymbol{\lambda}\|_{-1}}\right) - C_2 \sigma\right)^2}{A + B + C_6(\lambda_k^2 + \sigma^2)}\right), \quad (62)$$

with $A = C_3 \lambda_1^2 \left(\frac{\|\boldsymbol{\lambda}\|_{-1} + C_4 n \sigma}{\|\boldsymbol{\lambda}\|_{-1} + n \lambda_1}\right)^2$, $B = C_5 \left(\sum_{i \neq 1, k} \lambda_i^2\right) \left(1 + \frac{C_4 n \sigma}{\|\boldsymbol{\lambda}\|_{-1}}\right)^2$.

Note from (61) that $\|\boldsymbol{\lambda}\|_{-1} = (p-1)\lambda$. We first look at the denominator of the exponent of (62). Assuming $n\eta_k \leq p\sqrt{\lambda}$, we have

$$\begin{aligned} A &= C_1 \lambda_1^2 \left(\frac{\|\boldsymbol{\lambda}\|_{-1} + C_2 n \sigma}{n \lambda_1 + \|\boldsymbol{\lambda}\|_{-1}}\right)^2 \\ &= C_1 \alpha^2 p^2 \lambda^2 \left(\frac{(p-1)\lambda + C_2 n \sigma}{n \alpha p \lambda + (p-1)\lambda}\right)^2 \\ &\leq C_3 \alpha^2 p^2 \lambda^2 \left(\frac{p \lambda}{n \alpha p \lambda + (p-1)\lambda}\right)^2 \\ &\leq C_4 \alpha^2 p^2 \lambda^2 \left(\frac{p \lambda}{n \alpha p \lambda}\right)^2, \quad \text{by } n \alpha p \gg 1 \\ &\leq C_4 \frac{p^2 \lambda^2}{n^2}. \end{aligned}$$

Moreover,

$$\begin{aligned} B &= C_5 \left(\sum_{i \neq 1, k} \lambda_i^2\right) \left(1 + \frac{C_6 n \sigma}{\|\boldsymbol{\lambda}\|_{-1}}\right)^2 \\ &= C_5 (p-2) \lambda^2 \left(1 + \frac{C_6 n \sigma}{\|\boldsymbol{\lambda}\|_{-1}}\right)^2 \\ &\leq C_7 (p-2) \left(\lambda^2 + \frac{n^2 \sigma^2}{(p-1)^2}\right) \\ &\leq C_8 (p-2) \lambda^2, \end{aligned}$$

where the last inequality comes from $n\eta_k \leq p\sqrt{\lambda}$. Combining the results above, we have the denominator of the exponent of (62) is upper bounded by

$$C_4 \frac{p^2 \lambda^2}{n^2} + C_8 (p-2) \lambda^2 + C_9 (\lambda^2 + \sigma^2) \leq C_{10} \left(\frac{p^2}{n^2} \lambda^2 + p \lambda^2\right). \quad (63)$$

Now we look at the numerator.

$$\begin{aligned} \left(\eta_k^2 \left(1 - \frac{C_0 n \lambda_k}{\|\boldsymbol{\lambda}\|_{-1}} \right) - C_2 \sigma \right)^2 &\geq \eta_k^4 \left(1 - C \frac{n}{p} \right)^2 - C_9 \sqrt{\lambda} \eta_k^3 \\ &\geq \eta_k^4 - 2C \eta_k^4 \frac{n}{p} - C_9 \sqrt{\lambda} \eta_k^3. \end{aligned} \quad (64)$$

Let $\eta_k = C\sqrt{\lambda}p^r$, for some $C > 1$. Combining (63) and (64), if $p > n^2$, in (63), $\frac{p^2}{n^2} > p$, then the negative exponent of (62) is lower bounded by

$$\frac{\eta_k^4 n^2}{\lambda^2 p^2} - C_{10} \frac{\eta_k^4 n^3}{\lambda^2 p^3} - C_{11} \frac{\eta_k^3 n^2 \sqrt{\lambda}}{\lambda^2 p^2}. \quad (65)$$

Then

$$\begin{aligned} (65) &\geq n^2 p^{4r-2} - C_{10} n^3 p^{4r-3} - C_{11} n^2 p^{3r-2} \\ &\geq n^2 p^{4r-2} - C_{10} n p^{4r-2} - C_{11} n^2 p^{3r-2}, \end{aligned}$$

where we use $\frac{p^2}{n^2} > p$ in the last inequality. Thus to make the bound above approach $+\infty$ as $p \rightarrow \infty$, it suffices to have $r > \frac{1}{2}$.

If $p \leq n^2$, then the negative exponent of (62) is lower bounded by

$$\frac{\eta_k^4}{\lambda^2 p} - C_{10} \frac{\eta_k^4 n}{\lambda^2 p^2} - C_{11} \frac{\eta_k^3 \sqrt{\lambda}}{\lambda^2 p} \geq p^{4r-1} - C_{10} \frac{n}{p} p^{4r-1} - C_{11} p^{3r-1}.$$

It suffices to have $r > \frac{1}{4}$ to make the bound above approach $+\infty$ as $p \rightarrow \infty$. Combing previous results, it suffices to have $\eta_k = C\sqrt{\lambda}p^r$, for $r > \frac{1}{2}$ and some $C > 1$. Recall that we assume $n\eta_k \leq p\sqrt{\lambda}$, and actually $n\eta_k > p\sqrt{\lambda}$ is stronger than the condition $\eta_k > C\sqrt{\lambda}p^r$, for $r > \frac{1}{2}$ and some $C > 1$ for finite n , hence the later condition is sufficient to make the classification error approach 0 as $p \rightarrow \infty$. \square

E Proof of Corollaries 5.1 and 5.2

E.1 Proof of Corollary 5.1

We need to find the conditions that make the negative exponent of (13) vanish as p increases when conditions in Theorem 1 hold. Recall Theorem 1 requires

$$\|\boldsymbol{\lambda}\|_1 > \max\{\lambda_*, C_1 n \sqrt{\log(2n)} \sigma\}, \quad (66)$$

for some $C_1, C_2 > 1$ and $\lambda_* = 72 \left(\|\boldsymbol{\lambda}\|_2 \cdot n \sqrt{\log n} + \|\boldsymbol{\lambda}\|_\infty \cdot n \sqrt{n} \log n + 1 \right)$. It is not hard to check that (66) implies that $\frac{n^2 \sigma^2}{\|\boldsymbol{\lambda}\|_1^2} < 1$. Then the negative exponent of (13) is lower bounded by

$$\begin{aligned} \frac{\left(\|\boldsymbol{\eta}\|_2^2 - \frac{C_1 n \sigma^2}{\|\boldsymbol{\lambda}\|_1} - C_2 \sigma \right)^2}{C_3 \max\{1, \frac{n^2 \sigma^2}{\|\boldsymbol{\lambda}\|_1^2}\} \sum_{i=1}^p \lambda_i^2 + C_4 \sigma^2} &\geq \frac{\left(\|\boldsymbol{\eta}\|_2^2 - \frac{C_1 n \sigma^2}{\|\boldsymbol{\lambda}\|_1} - C_2 \sigma \right)^2}{C_5 \left(\sum_{i=1}^p \lambda_i^2 + \sigma^2 \right)} \\ &\geq \frac{\left(\|\boldsymbol{\eta}\|_2^2 - C_1 \frac{\|\boldsymbol{\lambda}\|_1}{n \sqrt{\log(2n)}} \frac{n \sigma}{\|\boldsymbol{\lambda}\|_1} - C_2 \sigma \right)^2}{C_5 \left(\sum_{i=1}^p \lambda_i^2 + \sigma^2 \right)} \\ &\geq \frac{\left(\|\boldsymbol{\eta}\|_2^2 - C_1 \frac{\sigma}{\sqrt{\log(2n)}} - C_2 \sigma \right)^2}{C_5 \left(\sum_{i=1}^p \lambda_i^2 + \sigma^2 \right)} \\ &\geq \frac{\left(\|\boldsymbol{\eta}\|_2^2 - C_6 \sigma \right)^2}{C_5 \left(\sum_{i=1}^p \lambda_i^2 + \sigma^2 \right)} \\ &\geq \frac{\|\boldsymbol{\eta}\|_2^4 - C_7 \|\boldsymbol{\eta}\|_2^2 \sigma}{C_5 \left(\sum_{i=1}^p \lambda_i^2 + \sigma^2 \right)}. \end{aligned} \quad (67)$$

Note that $\boldsymbol{\beta} = [\beta \ \beta \ \dots \ \beta]^T$, hence $\sigma = \beta\sqrt{\|\boldsymbol{\lambda}\|_1}$. Looking at the denominator of (67), when $\sum_{i=1}^p \lambda_i^2 \leq \sigma^2$, i.e. $\|\boldsymbol{\lambda}\|_2^2 \leq \beta^2\|\boldsymbol{\lambda}\|_1$,

$$\begin{aligned}
(67) &\geq \frac{\|\boldsymbol{\eta}\|_2^4 - C_7\|\boldsymbol{\eta}\|_2^2\sigma}{C_8\sigma^2} \\
&\geq \frac{(p\beta^2)^2 - C_7(p\beta^2)\sqrt{\beta^2\|\boldsymbol{\lambda}\|_1}}{C_8(\beta^2\|\boldsymbol{\lambda}\|_1)} \\
&\geq \left(\frac{p\beta}{\sqrt{\|\boldsymbol{\lambda}\|_1}}\right)^2 - \frac{C_9p\beta}{\sqrt{\|\boldsymbol{\lambda}\|_1}}.
\end{aligned} \tag{68}$$

To guarantee (68) $\rightarrow \infty$ as $p \rightarrow \infty$, it suffices to have $\|\boldsymbol{\lambda}\|_1 \leq C\beta^2p^\alpha$, for $\alpha < 2$. Note that the second condition in Theorem 1 becomes

$$\|\boldsymbol{\lambda}\|_1 > Cn\sqrt{\log(2n)}\beta\sqrt{\|\boldsymbol{\lambda}\|_1} \iff \|\boldsymbol{\lambda}\|_1 > C^2n^2\log(2n)\beta^2.$$

Combing the conditions above, the SVM solution goes to 0 with $p \rightarrow \infty$ provided the assumptions of Theorem 3 with $\tau = 0$ hold and

$$\max\{\lambda_*, C_1\beta^2n^2\log(2n)\} < \|\boldsymbol{\lambda}\|_1 \leq C_2\beta^2p^\alpha, \quad \text{for } \alpha < 2. \tag{69}$$

When $\sum_{i=1}^p \lambda_i^2 > \sigma^2$, i.e. $\|\boldsymbol{\lambda}\|_2^2 > \beta^2\|\boldsymbol{\lambda}\|_1$,

$$\begin{aligned}
(67) &\geq \frac{\|\boldsymbol{\eta}\|_2^4 - C_7\|\boldsymbol{\eta}\|_2^2\sigma}{C_8\left(\sum_{i=1}^p \lambda_i^2\right)} \\
&\geq \left(\frac{p\beta^2}{\sqrt{\sum_{i=1}^p \lambda_i^2}}\right)^2 - \frac{C_9p\beta^2}{\sqrt{\sum_{i=1}^p \lambda_i^2}}.
\end{aligned} \tag{70}$$

To guarantee (70) $\rightarrow \infty$ as $p \rightarrow \infty$, it suffices to have $\sum_{i=1}^p \lambda_i^2 \leq C\beta^4p^\alpha$, for $\alpha < 2$, which is equivalent to $\|\boldsymbol{\lambda}\|_2 \leq C\beta^2p^\alpha$, for $\alpha < 1$. Combing the conditions in Theorem 1, the SVM solution goes to 0 with $p \rightarrow \infty$ provided the assumptions of Theorem 3 with $\tau = 0$ hold and

$$\|\boldsymbol{\lambda}\|_1 > \max\{\lambda_*, C_1\beta^2n^2\log(2n)\} \quad \text{and} \quad \|\boldsymbol{\lambda}\|_2 \leq C\beta^2p^\alpha, \quad \text{for } \alpha < 1. \tag{71}$$

Combining (69) and (71) completes the proof.

E.2 Proof of Corollary 5.2

We start from the high-SNR regime. In fact, we can assume a bit stronger that

$$\|\boldsymbol{\eta}\|_2^2 > C\frac{p}{n}, \quad \text{for some large } C > 1. \tag{72}$$

Then the exponent in (15) becomes:

$$\begin{aligned}
\|\boldsymbol{\eta}\|_2^2\left(1 - \frac{n}{p}\right)^2 + C_1 - 2C_1\left(1 - \frac{n}{p}\right)\|\boldsymbol{\eta}\|_2 &> \|\boldsymbol{\eta}\|_2^2 - 2\|\boldsymbol{\eta}\|_2^2\frac{n}{p} - 2C_1\|\boldsymbol{\eta}\|_2 \\
&> C\frac{p}{n} - 2\|\boldsymbol{\eta}\|_2^2\frac{n}{p} - 2C_1\|\boldsymbol{\eta}\|_2,
\end{aligned} \tag{73}$$

where the last inequality comes from (72). Following Theorem 2, we further assume that

$$p > 10n\log n + n - 1 \quad \text{and} \quad p > C_2n\sqrt{\log(2n)}\|\boldsymbol{\eta}\|_2, \tag{74}$$

for some constant $C_2 > 1$. Then combining the relationships above gives

$$\begin{aligned}
(73) &> C\frac{p}{n} - 2\left(\frac{p}{C_2n\sqrt{\log(2n)}}\right)^2\frac{n}{p} - 2C_1\frac{p}{n\sqrt{\log(2n)}} \\
&= C\frac{p}{n} - \frac{2p}{C_2n\log(2n)} - \frac{2C_1p}{n\sqrt{\log(2n)}} \\
&= \frac{p}{n}\left(C - \frac{2C_1}{\sqrt{\log(2n)}} - \frac{2}{C_2\log(2n)}\right).
\end{aligned} \tag{75}$$

Notice that (75) $\rightarrow \infty$ as $(p/n) \rightarrow \infty$ for sufficiently large C and n . Thus we have proved that in the high-SNR regime, the error of SVM solution goes to 0 with $(p/n) \rightarrow \infty$ provided that the assumptions of Theorem 4 hold and

$$\frac{1}{C}n\|\boldsymbol{\eta}\|_2^2 > p > \max\{10n \log n + n - 1, C_1n\sqrt{\log(2n)}\|\boldsymbol{\eta}\|_2\},$$

for sufficiently large constants $C, C_1 > 1$.

For the low-SNR regime, assume that

$$p > 10n \log n + n - 1, \quad p > C_1n\sqrt{\log(2n)}\|\boldsymbol{\eta}\|_2, \quad (76)$$

$$\text{and } \|\boldsymbol{\eta}\|_2^2 \leq \frac{p}{n}, \quad \|\boldsymbol{\eta}\|_2^4 = C_2\left(\frac{p}{n}\right)^\alpha, \quad \text{for } \alpha > 1. \quad (77)$$

Then the exponent in (16) becomes:

$$\begin{aligned} \frac{n}{p}\|\boldsymbol{\eta}\|_2^4 \left(1 - \frac{n}{p} - C_3 \frac{1}{\|\boldsymbol{\eta}\|_2}\right)^2 &> \frac{n}{p}\|\boldsymbol{\eta}\|_2^4 - 2\frac{n^2}{p^2}\|\boldsymbol{\eta}\|_2^4 - 2\frac{n}{p}C_3\|\boldsymbol{\eta}\|_2^3 \\ &\geq C_2\left(\frac{p}{n}\right)^{\alpha-1} - 2C_2\left(\frac{p}{n}\right)^{\alpha-2} - 2C_3C_2\left(\frac{p}{n}\right)^{0.75\alpha-1}, \end{aligned} \quad (78)$$

where the last inequality comes from (76) and (77). (78) will go to $+\infty$ as $(p/n) \rightarrow \infty$ provided that $\alpha > 1$. Overall in the low-SNR regime, we need the assumptions of Theorem 3 plus

$$\begin{aligned} p &> \max\{10n \log n + n - 1, C_1n\sqrt{\log(2n)}\|\boldsymbol{\eta}\|_2, n\|\boldsymbol{\eta}\|_2^2\}, \\ \text{and } \|\boldsymbol{\eta}\|_2^4 &\geq C_2\left(\frac{p}{n}\right)^\alpha, \quad \text{for } \alpha \in (1, 2]. \end{aligned}$$

F Results for the averaging estimator

The theorem below shows an upper bound on the classification error for the averaging estimator $\hat{\boldsymbol{\eta}}_{\text{Avg}}$. Note the result below is for general $\boldsymbol{\Sigma}$, i.e. no balanced or bi-level structure is required.

Theorem 8. *Assume that the data are generated with the GMM model. Fix $\delta \in (0, 1)$ and suppose n is large enough such that $n > c \log(1/\delta)$ for some $c > 1$. Then, there exist a constant $c_1 > 1$ such that with probability at least $1 - \delta$, $\hat{\boldsymbol{\eta}}_{\text{Avg}}^T \boldsymbol{\eta} > 0$ provided that $\|\boldsymbol{\eta}\|_2^2 > c_1\sigma$. Then, there exists constants C_i 's > 1 such that with probability at least $1 - \delta$,*

$$\mathcal{R}(\hat{\boldsymbol{\eta}}_{\text{Avg}}) \leq \exp\left(\frac{-\left(\|\boldsymbol{\eta}\|_2^2 - C_1\sigma\right)^2}{C_2\|\boldsymbol{\lambda}\|_2^2 + C_3\sigma^2}\right). \quad (79)$$

The bound above is the same as (19).

Proof. We need to lower bound $\frac{(\hat{\boldsymbol{\eta}}_{\text{Avg}}^T \boldsymbol{\eta})^2}{\hat{\boldsymbol{\eta}}_{\text{Avg}}^T \boldsymbol{\Sigma} \hat{\boldsymbol{\eta}}_{\text{Avg}}}$. Recall that $\hat{\boldsymbol{\eta}}_{\text{Avg}} = \frac{1}{n} \mathbf{X}^T \mathbf{y}$. For the denominator,

$$\hat{\boldsymbol{\eta}}_{\text{Avg}}^T \boldsymbol{\Sigma} \hat{\boldsymbol{\eta}}_{\text{Avg}} \leq \frac{2}{n^2} \left(n^2 \boldsymbol{\eta}^T \boldsymbol{\Sigma} \boldsymbol{\eta} + \mathbf{y}^T \mathbf{Q} \boldsymbol{\Sigma} \mathbf{Q}^T \mathbf{y} \right),$$

where we use the fact $\mathbf{v}^T \mathbf{u} \leq \frac{1}{2}(\mathbf{v}^T \mathbf{v} + \mathbf{u}^T \mathbf{u})$. Then we need to upper bound $\mathbf{y}^T \mathbf{Q} \boldsymbol{\Sigma} \mathbf{Q}^T \mathbf{y}$. Following what we show in the proof of Theorem 3, with probability at least $1 - \delta$,

$$\mathbf{y}^T \mathbf{Q} \boldsymbol{\Sigma} \mathbf{Q}^T \mathbf{y} = \text{Tr} \left(\sum_{i=1}^p \lambda_i^2 \mathbf{z}_i^T (\mathbf{y} \mathbf{y}^T) \mathbf{z}_i \right) \leq \sum_{i=1}^p \lambda_i^2 \|\mathbf{y} \mathbf{y}^T\|_2 \|\mathbf{z}_i\|_2^2 \leq Cn \sum_{i=1}^p \lambda_i^2 \|\mathbf{z}_i\|_2^2 \leq Cn^2 \|\boldsymbol{\lambda}\|_2^2,$$

where the last inequality follows the fact that $\sum_{i=1}^p \lambda_i^2 \|\mathbf{z}_i\|_2^2$ is the weighted sum of sub-exponential variables. Next we lower bound the numerator $\hat{\boldsymbol{\eta}}_{\text{Avg}}^T \boldsymbol{\eta}$, Lemma 7 gives with probability at least $1 - \delta$,

$$\hat{\boldsymbol{\eta}}_{\text{Avg}}^T \boldsymbol{\eta} = \frac{1}{n} \mathbf{y}^T \mathbf{y} \|\boldsymbol{\eta}\|_2^2 + \frac{1}{n} \mathbf{y}^T \mathbf{d} \geq \|\boldsymbol{\eta}\|_2^2 - C\sigma.$$

We need $\|\boldsymbol{\eta}\|_2^2 - C\sigma > 0$ to guarantee $\hat{\boldsymbol{\eta}}_{\text{Avg}}^T \boldsymbol{\eta} > 0$ with high probability. Combining results above completes the proof. \square

G Proof of Lemmas

G.1 Proof of Lemmas 2

For Lemma 2, the proof of Theorem 3 gives

$$\hat{\boldsymbol{\eta}}_\tau^T \boldsymbol{\eta} = \frac{s(\|\boldsymbol{\eta}\|_2^2 - t) + h^2 + h}{D},$$

for $D > 0$. Then we proceed by directly applying (47).

G.2 Proof of Lemma 6

Recall

$$\mathbf{X}\mathbf{X}^T + \tau\mathbf{I} = \mathbf{Q}\mathbf{Q}^T + \tau\mathbf{I} + \|\boldsymbol{\eta}\|_2^2 \mathbf{y}\mathbf{y}^T + \mathbf{Q}\boldsymbol{\eta}\mathbf{y}^T + (\mathbf{Q}\boldsymbol{\eta}\mathbf{y}^T)^T = \mathbf{U}_\tau + \begin{bmatrix} \|\boldsymbol{\eta}\|_2 \mathbf{y} & \mathbf{d} & \mathbf{y} \end{bmatrix} \begin{bmatrix} \|\boldsymbol{\eta}\|_2 \mathbf{y}^T \\ \mathbf{y}^T \\ \mathbf{d}^T \end{bmatrix}.$$

Thus, by Woodbury identity [Horn and Johnson, 2012], $(\mathbf{X}\mathbf{X}^T)^{-1}$ can be expressed as:

$$\mathbf{U}_\tau^{-1} - \mathbf{U}_\tau^{-1} \begin{bmatrix} \|\boldsymbol{\eta}\|_2 \mathbf{y} & \mathbf{d} & \mathbf{y} \end{bmatrix} \left[\mathbf{I} + \begin{bmatrix} \|\boldsymbol{\eta}\|_2 \mathbf{y}^T \\ \mathbf{y}^T \\ \mathbf{d}^T \end{bmatrix} \mathbf{U}_\tau^{-1} \begin{bmatrix} \|\boldsymbol{\eta}\|_2 \mathbf{y} & \mathbf{d} & \mathbf{y} \end{bmatrix} \right]^{-1} \begin{bmatrix} \|\boldsymbol{\eta}\|_2 \mathbf{y}^T \\ \mathbf{y}^T \\ \mathbf{d}^T \end{bmatrix} \mathbf{U}_\tau^{-1}. \quad (80)$$

We first compute the inverse of the 3×3 matrix $\mathbf{A} := \begin{bmatrix} \mathbf{I} + \begin{bmatrix} \|\boldsymbol{\eta}\|_2 \mathbf{y}^T \\ \mathbf{y}^T \\ \mathbf{d}^T \end{bmatrix} \mathbf{U}_\tau^{-1} \begin{bmatrix} \|\boldsymbol{\eta}\|_2 \mathbf{y} & \mathbf{d} & \mathbf{y} \end{bmatrix} \end{bmatrix}$. By our definitions of s, h and t in Section A:

$$\mathbf{A} = \begin{bmatrix} 1 + \|\boldsymbol{\eta}\|_2^2 s & \|\boldsymbol{\eta}\|_2 h & \|\boldsymbol{\eta}\|_2 s \\ \|\boldsymbol{\eta}\|_2 s & 1 + h & s \\ \|\boldsymbol{\eta}\|_2 h & t & 1 + h \end{bmatrix}.$$

Recalling $\mathbf{A}^{-1} = \frac{1}{\det(\mathbf{A})} \text{adj}(\mathbf{A})$, where $\det(\mathbf{A})$ is the determinant of \mathbf{A} and $\text{adj}(\mathbf{A})$ is the adjoint of \mathbf{A} , it can be checked that:

$$\det(\mathbf{A}) = D = s(\|\boldsymbol{\eta}\|_2^2 - t) + (h + 1)^2,$$

and

$$\text{adj}(\mathbf{A}) = \begin{bmatrix} (h + 1)^2 - st & \|\boldsymbol{\eta}\|_2(st - h - h^2) & -\|\boldsymbol{\eta}\|_2 s \\ -\|\boldsymbol{\eta}\|_2 s & h + 1 + \|\boldsymbol{\eta}\|_2^2 s & -s \\ \|\boldsymbol{\eta}\|_2(st - h - h^2) & \|\boldsymbol{\eta}\|_2^2 h^2 - t(1 + \|\boldsymbol{\eta}\|_2^2 s) & h + 1 + \|\boldsymbol{\eta}\|_2^2 s \end{bmatrix}.$$

Combining the above gives

$$\begin{aligned} \mathbf{y}^T (\mathbf{X}\mathbf{X}^T + \tau\mathbf{I})^{-1} &= \mathbf{y}^T \mathbf{U}_\tau^{-1} - \begin{bmatrix} \|\boldsymbol{\eta}\|_2 s & h & s \end{bmatrix} \mathbf{A}^{-1} \begin{bmatrix} \|\boldsymbol{\eta}\|_2 \mathbf{y}^T \\ \mathbf{y}^T \\ \mathbf{d}^T \end{bmatrix} \mathbf{U}_\tau^{-1} \\ &= \mathbf{y}^T \mathbf{U}_\tau^{-1} - \frac{1}{D} \begin{bmatrix} \|\boldsymbol{\eta}\|_2 s & h^2 + h - st & s \end{bmatrix} \begin{bmatrix} \|\boldsymbol{\eta}\|_2 \mathbf{y}^T \\ \mathbf{y}^T \\ \mathbf{d}^T \end{bmatrix} \mathbf{U}_\tau^{-1}. \end{aligned}$$

This completes the proof of the lemma.

G.3 Proof of Lemma 7 and Lemma 8

To prove Lemma 7, we need to bound the eigenvalues of \mathbf{U}_τ . Recall $\mathbf{U}_0 = \mathbf{Q}\mathbf{Q}^T = \sum_{i=1}^p \lambda_i \mathbf{z}_i \mathbf{z}_i^T$, where $\mathbf{z}_i \in \mathbb{R}^n$ are independent vectors with IID standard normal elements. Let $\lambda_k(\mathbf{M})$ represent the k -th eigenvalue of matrix \mathbf{M} . We start from Bartlett et al. [2020, Lemma 5 (3)]:

Lemma 12. *There are constants $b, c \geq 1$ such that, for any $k \geq 0$, with probability at least $1 - 2e^{-n/c}$, if $\frac{\sum_{i>k} \lambda_i}{\lambda_{k+1}} \geq bn$, then*

$$\frac{1}{c} \sum_{i>k} \lambda_i \leq \lambda_n \left(\sum_{i>k} \lambda_i \mathbf{z}_i \mathbf{z}_i^T \right) \leq \lambda_1 \left(\sum_{i>k} \lambda_i \mathbf{z}_i \mathbf{z}_i^T \right) \leq c \sum_{i>k} \lambda_i.$$

First note that the balanced ensemble requirement $bn\lambda_1 \leq \|\boldsymbol{\lambda}\|_{-1}$ implies $bn\lambda_1 \leq \|\boldsymbol{\lambda}\|_1$. We can then obtain the bounds for eigenvalues of \mathbf{U}_0 by letting $k = 0$ in Lemma 12. Then the eigenvalues of \mathbf{U}_τ are bounded as follows.

Lemma 13. *Assume the balanced Σ assumption is satisfied. Suppose that $\delta < 1$ with $\log(1/\delta) < n/c$ for some $c > 1$. There is a constant $C > 1$ such that with probability at least $1 - \delta$, the largest and smallest eigenvalues of \mathbf{U}_τ satisfy:*

$$\frac{1}{C} \left(\tau + \sum_{i=1}^p \lambda_i \right) \leq \tau + \frac{1}{C} \sum_{i=1}^p \lambda_i \leq \lambda_n(\mathbf{U}_\tau) \leq \lambda_1(\mathbf{U}_\tau) \leq \tau + C \sum_{i=1}^p \lambda_i \leq C \left(\tau + \sum_{i=1}^p \lambda_i \right). \quad (81)$$

Now we are ready to prove Lemma 7.

G.3.1 Bounds for \mathbf{s}

For $\mathbf{s} = \mathbf{y}^T \mathbf{U}_\tau^{-1} \mathbf{y}$, from (81) and $\|\mathbf{y}\|_2^2 = n$, the variational characterization of eigenvalues gives:

$$\mathbf{s} = \mathbf{y}^T \mathbf{U}_\tau^{-1} \mathbf{y} \leq \|\mathbf{y}\|_2^2 \lambda_1(\mathbf{U}_\tau^{-1}) \leq n \frac{1}{\lambda_n(\mathbf{U}_\tau)} \leq C_1 \frac{n}{\tau + \|\boldsymbol{\lambda}\|_1}.$$

The lower bound can be derived in a similar way and is omitted for brevity.

G.3.2 Bounds for \mathbf{t} and \mathbf{h}

We begin by presenting the definitions of sub-Gaussian and sub-exponential norms. For a detailed discussion of sub-Gaussian and sub-exponential variables, we refer the readers to Vershynin [2018, Chapter 2].

Definition G.1. For a sub-Gaussian variable X defined in Vershynin [2018, 2.5], the sub-Gaussian norm of X , denoted by $\|X\|_{\psi_2}$, is defined as

$$\|X\|_{\psi_2} = \inf\{t > 0 : \mathbb{E}[e^{X^2/t^2}] < 2\}.$$

Then Vershynin [2018, Example 2.5.8 (a)] states that if $X \sim \mathcal{N}(0, \sigma^2)$, then X is sub-Gaussian with $\|X\|_{\psi_2} < C\sigma$, where C is an absolute constant.

Definition G.2. For a sub-exponential variable X defined in Vershynin [2018, 2.7], the sub-exponential norm of X , denoted by $\|X\|_{\psi_1}$, is defined as

$$\|X\|_{\psi_1} = \inf\{t > 0 : \mathbb{E}[e^{|X|/t}] < 2\}.$$

Vershynin [2018, Lemma 2.7.6] shows that sub-exponential is sub-Gaussian squared.

Lemma 14. *A random variable X is sub-Gaussian if and only if X^2 is sub-exponential. Moreover,*

$$\|X^2\|_{\psi_1} = \|X\|_{\psi_2}^2.$$

We now look at $\|\mathbf{d}\|_2$. Recall $\mathbf{d} = \mathbf{Q}\boldsymbol{\eta} = \mathbf{Z}\boldsymbol{\Lambda}^{\frac{1}{2}}\boldsymbol{\beta}$. $\|\mathbf{d}\|_2^2 = \sum_{j=1}^n d_j^2$, where $d_j = \sum_{i=1}^p \sqrt{\lambda_i} \beta_i z_{ji}$ and z_{ji} 's are IID standard Gaussian variable. Hence d_j is Gaussian with mean zero and variance $\sum_{i=1}^p \lambda_i \beta_i^2$ and d_j^2 is sub-exponential with $\|d_j^2\|_{\psi_1} < c \sum_{i=1}^p \lambda_i \beta_i^2$ and mean $\sum_{i=1}^p \lambda_i \beta_i^2$. To bound $\|\mathbf{d}\|_2$, we need the Bernstein's inequality [Vershynin, 2018, Theorem 2.8.2]:

Lemma 15. *Let ξ_1, \dots, ξ_n be independent, mean zero, sub-exponential random variables with sub-exponential norm $\|\xi\|_{\psi_1}$, and $a = (a_1, \dots, a_n) \in \mathbb{R}^n$. Then for every $t \geq 0$, we have*

$$\mathbb{P}\left(\left|\sum_{i=1}^n a_i \xi_i\right| \geq t\right) \leq 2 \exp\left\{-c \min\left(\frac{t^2}{\|\xi\|_{\psi_1}^2 \cdot \sum_{i=1}^n a_i^2}, \frac{t}{\|\xi\|_{\psi_1} \cdot \max_{i \in [n]} |a_i|}\right)\right\}.$$

Corollary 8.1. *Suppose $\{a_i\}$ is a non-increasing sequence of non-negative numbers such that $\sum_i a_i < \infty$. Then there is a constant c such that for any sequence of independent, zero-mean sub-exponential random variables $\{\xi_i\}$ with sub-exponential norm $\|\xi\|_{\psi_1}$, and any $x > 0$, with probability at least $1 - 2e^{-x}$,*

$$\left|\sum_{i=1}^n a_i \xi_i\right| \leq c \|\xi\|_{\psi_1} \cdot \max\left(a_1 x, \sqrt{x \sum_i a_i^2}\right).$$

Let fix the length of the sequence as n and let $a_i = 1$, for $i \in [n]$. Then combing the inequality above with $x = n/c$ and the fact that d_j^2 's are sub-exponential gives with probability at least $1 - 2e^{-\frac{n}{c}}$,

$$\|\mathbf{d}\|_2 \leq C \sqrt{n \sum_{i=1}^p \lambda_i \beta_i^2} = C \sqrt{n} \sigma. \quad (82)$$

Recall $t = \mathbf{d}^T \mathbf{U}_\tau^{-1} \mathbf{d}$ and $h = \mathbf{y}^T \mathbf{U}_\tau^{-1} \mathbf{d}$, we can obtain the upper and lower bounds of t by the variational characterization of eigenvalues. The bounds of h can be derived from the fact $-\|\mathbf{d}\|_2 \|\mathbf{y}\|_2 \|\mathbf{U}_\tau^{-1}\|_2 \leq h \leq \|\mathbf{d}\|_2 \|\mathbf{y}\|_2 \|\mathbf{U}_\tau^{-1}\|_2$. The bounds for $\|\mathbf{y}^T \mathbf{U}_\tau^{-1}\|_2$ and $\|\mathbf{d}^T \mathbf{U}_\tau^{-1}\|_2$ can be obtained from Cauchy-Schwarz for matrices.

G.3.3 Proof of Lemma 8

Now we prove Lemma 8. Recall

$$f_i = \mathbf{e}_i^T \mathbf{U}_0^{-1} \mathbf{d} = \mathbf{e}_i^T \left(\frac{1}{\|\boldsymbol{\lambda}\|_1} \mathbf{I} - \mathbf{E}' \right) \mathbf{d},$$

thus,

$$\begin{aligned} \max_{i \in [n]} |f_i| &\leq \frac{1}{\|\boldsymbol{\lambda}\|_1} \|\mathbf{d}\|_\infty + \|\mathbf{e}_i^T \mathbf{E}' \mathbf{d}\|_\infty \\ &\leq \frac{1}{\|\boldsymbol{\lambda}\|_1} \|\mathbf{d}\|_\infty + \|\mathbf{e}_i^T \mathbf{E}' \mathbf{d}\|_2, \end{aligned}$$

where the last equality comes from the fact that the ℓ_2 norm of a vector won't be smaller than its infinity norm. By Markov's inequality [Wainwright, 2019, 2.1.1], for sufficiently large constant $C > 1$,

$$\mathbb{P}(\max_{i \in [n]} |d_i| \geq C \mathbb{E}[\max_{i \in [n]} |d_i|]) \leq \delta.$$

Thus it suffices to bound $\mathbb{E}[\max_{i \in [n]} |d_i|]$. We know that the elements of \mathbf{d} are IID zero-mean Gaussian variables with variance $\sum_{i=1}^p \lambda_i \beta_i^2$. By Wainwright [2019, Exercise 2.11],

$$\mathbb{E}[\max_{i \in [n]} |d_i|] \leq \sqrt{\sum_{i=1}^p \lambda_i \beta_i^2} \sqrt{2 \log(2n)} = \sqrt{2 \log(2n)} \sigma.$$

Thus with probability at least $1 - \delta$,

$$\|\mathbf{d}\|_\infty \leq C\sqrt{2\log(2n)}\sigma.$$

To bound $\|\mathbf{e}_i^T \mathbf{E}' \mathbf{d}\|_2$, using $\mathbf{v}^T \mathbf{M} \mathbf{u} \leq \|\mathbf{v}\|_2 \|\mathbf{u}\|_2 \|\mathbf{M}\|_2$ and the bound on $\|\mathbf{d}\|_2$ in (82) and the bound on $\|\mathbf{E}'\|_2$ in (39) give, for $n > c/\delta$ and for every $i \in [n]$,

$$\begin{aligned} \|\mathbf{e}_i^T \mathbf{E}' \mathbf{d}\|_2 &\leq \|\mathbf{e}_i\|_2 \|\mathbf{d}\|_2 \|\mathbf{E}'\|_2 \\ &\leq \frac{C_1 \sigma}{\|\boldsymbol{\lambda}\|_1}. \end{aligned}$$

Combining results above completes the proof.

G.4 Proof of Lemma 11

To prove Lemma 11, the first step is to separate the largest eigenvalue from others. Specifically, by Woodbury identity, \mathbf{U}_τ^{-1} can be expressed as

$$\mathbf{U}_\tau^{-1} = (\tau \mathbf{I} + \sum_{i=2}^p \lambda_i \mathbf{z}_i \mathbf{z}_i^T + \lambda_1 \mathbf{z}_1 \mathbf{z}_1^T)^{-1} \quad (83)$$

$$= \mathbf{U}_{-1,\tau}^{-1} - \frac{\lambda_1 \mathbf{U}_{-1,\tau}^{-1} \mathbf{z}_1 \mathbf{z}_1^T \mathbf{U}_{-1,\tau}^{-1}}{1 + \lambda_1 \mathbf{z}_1^T \mathbf{U}_{-1,\tau}^{-1} \mathbf{z}_1}, \quad (84)$$

where $\mathbf{U}_{-1,\tau} = \tau \mathbf{I} + \sum_{i=2}^p \lambda_i \mathbf{z}_i \mathbf{z}_i^T$. By Lemma 13 above, with probability at least $1 - \delta$,

$$\frac{1}{C}(\tau + \sum_{i=2}^p \lambda_i) \leq \lambda_n(\mathbf{U}_{-1,\tau}) \leq \lambda_1(\mathbf{U}_{-1,\tau}) \leq C(\tau + \sum_{i=2}^p \lambda_i). \quad (85)$$

Then we need to bound $\|\mathbf{z}_1\|_2$ and $\|\mathbf{z}_k\|_2$. In Lemma 8.1, let $x < \frac{n}{c_0}$ with sufficiently large c_0 , if $n > C_0 \log(1/\delta)$ for some $C_0 > 1$, then there exist $C_1, C_2 > 1$ such that with probability at least $1 - \delta$,

$$\frac{1}{C_1} n \leq \|\mathbf{z}_i\|_2^2 \leq C_2 n, \quad i \in [p].$$

Now we are ready to derive the bounds in Lemma 11.

For $s = \mathbf{y}^T \mathbf{U}_\tau^{-1} \mathbf{y}$, by (84) and (85) and using the variational characterization of eigenvalues and $\mathbf{v}^T \mathbf{M} \mathbf{u} \leq \|\mathbf{v}\|_2 \|\mathbf{u}\|_2 \|\mathbf{M}\|_2$, with probability at least $1 - \delta$,

$$\begin{aligned} s &= \frac{\mathbf{y}^T \mathbf{U}_{-1,\tau}^{-1} \mathbf{y} + \lambda_1 \mathbf{z}_1^T \mathbf{U}_{-1,\tau}^{-1} \mathbf{z}_1 \mathbf{y}^T \mathbf{U}_{-1,\tau}^{-1} \mathbf{y} - \lambda_1 \mathbf{y}^T \mathbf{U}_{-1,\tau}^{-1} \mathbf{z}_1 \mathbf{z}_1^T \mathbf{U}_{-1,\tau}^{-1} \mathbf{y}}{1 + \lambda_1 \mathbf{z}_1^T \mathbf{U}_{-1,\tau}^{-1} \mathbf{z}_1} \\ &\leq \frac{\frac{C_1 n}{(\tau + \|\boldsymbol{\lambda}\|_{-1})} \left(1 + \frac{C_2 n \lambda_1}{\tau + \|\boldsymbol{\lambda}\|_{-1}}\right)}{1 + \frac{n \lambda_1}{C_3(\tau + \|\boldsymbol{\lambda}\|_{-1})}} \\ &\leq \frac{C_1 n}{(\tau + \|\boldsymbol{\lambda}\|_{-1})} \cdot \left(\frac{\tau + \|\boldsymbol{\lambda}\|_{-1} + C_2 n \lambda_1}{\tau + \|\boldsymbol{\lambda}\|_{-1}}\right) \cdot \left(\frac{C_3(\tau + \|\boldsymbol{\lambda}\|_{-1})}{C_3(\tau + \|\boldsymbol{\lambda}\|_{-1}) + n \lambda_1}\right) \\ &\leq \frac{C_1 n}{(\tau + \|\boldsymbol{\lambda}\|_{-1})} \cdot \left(\frac{C_2 C_3(\tau + \|\boldsymbol{\lambda}\|_{-1}) + C_2 n \lambda_1}{\tau + \|\boldsymbol{\lambda}\|_{-1}}\right) \cdot \left(\frac{C_3(\tau + \|\boldsymbol{\lambda}\|_{-1})}{C_3(\tau + \|\boldsymbol{\lambda}\|_{-1}) + n \lambda_1}\right) \\ &\leq \frac{C_4 n}{\tau + \|\boldsymbol{\lambda}\|_{-1}}. \end{aligned}$$

For the lower bound of s , we need to show $\mathbf{z}_1^T \mathbf{U}_{-1,\tau}^{-1} \mathbf{y}$ is sufficiently small compared with $\mathbf{z}_1^T \mathbf{U}_{-1,\tau}^{-1} \mathbf{z}_1$ and $\mathbf{y}^T \mathbf{U}_{-1,\tau}^{-1} \mathbf{y}$. We thus need the following Hanson-Wright inequality [Rudelson et al., 2013].

Lemma 16. *Let \mathbf{z} be a random vector whose elements are IID zero-mean sub-Gaussian random variable with parameter at most 1. Then, there exists universal constant $c > 0$ such that for any positive semi-definite matrix \mathbf{M} and for every $t > 0$, we have*

$$P\left(|\mathbf{z}^T \mathbf{M} \mathbf{z} - \mathbb{E}[\mathbf{z}^T \mathbf{M} \mathbf{z}]| > t\right) \leq \exp\left\{-c \min\left\{\frac{t^2}{\|\mathbf{M}\|_F^2}, \frac{t}{\|\mathbf{M}\|_2}\right\}\right\}.$$

Note $\|\mathbf{M}\|_F^2 \leq n\|\mathbf{M}\|_2^2$ and let $t = \frac{1}{C_0}n\|\mathbf{M}\|_2$ for sufficiently large constant C_0 to get with probability at least $1 - 2e^{-\frac{n}{c_1}}$,

$$|\mathbf{z}^T \mathbf{M} \mathbf{z} - \mathbb{E}[\mathbf{z}^T \mathbf{M} \mathbf{z}]| \leq \frac{1}{C_0}n\|\mathbf{M}\|_2. \quad (86)$$

Then we use the similar trick as [Muthukumar et al. \[2020a, D.3.1\]](#) and apply the parallelogram law to $\mathbf{z}_1^T \mathbf{U}_{-1,\tau}^{-1} \mathbf{y}$,

$$\mathbf{z}_1^T \mathbf{U}_{-1,\tau}^{-1} \mathbf{y} = \frac{1}{4}((\mathbf{z}_1 + \mathbf{y})^T \mathbf{U}_{-1,\tau}^{-1} (\mathbf{z}_1 + \mathbf{y}) - (\mathbf{z}_1 - \mathbf{y})^T \mathbf{U}_{-1,\tau}^{-1} (\mathbf{z}_1 - \mathbf{y})).$$

To use the Hanson-Wright inequality, we need to calculate the conditional expectation

$$\mathbb{E}[\mathbf{z}_1^T \mathbf{U}_{-1,\tau}^{-1} \mathbf{y} | \mathbf{U}_{-1,\tau}^{-1}] = \mathbb{E}[\text{Tr}(\mathbf{U}_{-1,\tau}^{-1} \mathbf{y} \mathbf{z}_1^T) | \mathbf{U}_{-1,\tau}^{-1}] = \text{Tr}(\mathbf{U}_{-1,\tau}^{-1} \mathbb{E}[\mathbf{y} \mathbf{z}_1^T]),$$

where we use the fact that \mathbf{y} and \mathbf{z}_1 are independent of $\mathbf{U}_{-1,\tau}^{-1}$. It is not hard to check that $\mathbb{E}[\mathbf{y} \mathbf{z}_1^T] = \mathbf{0}$, where $\mathbf{0}$ is the matrix with all elements 0. Now applying Lemma 16 to both $(\mathbf{z}_1 + \mathbf{y})^T \mathbf{U}_{-1,\tau}^{-1} (\mathbf{z}_1 + \mathbf{y})$ and $(\mathbf{z}_1 - \mathbf{y})^T \mathbf{U}_{-1,\tau}^{-1} (\mathbf{z}_1 - \mathbf{y})$ gives with probability at least $1 - 2e^{-\frac{n}{c_1}}$,

$$|\mathbf{z}_1^T \mathbf{U}_{-1,\tau}^{-1} \mathbf{y}| \leq \frac{2}{C_0}n\|\mathbf{U}_{-1,\tau}^{-1}\|_2.$$

Now for the numerator of s , using the bound of eigenvalues of $\mathbf{U}_{-1,\tau}$ in (85) and the fact that C_0 is sufficiently large gives with probability at least $1 - \delta$,

$$\lambda_1 \mathbf{z}_1^T \mathbf{U}_{-1,\tau}^{-1} \mathbf{z}_1 \mathbf{y}^T \mathbf{U}_{-1,\tau}^{-1} \mathbf{y} - \lambda_1 \mathbf{y}^T \mathbf{U}_{-1,\tau}^{-1} \mathbf{z}_1 \mathbf{z}_1^T \mathbf{U}_{-1,\tau}^{-1} \mathbf{y} \geq \frac{n^2 \lambda_1}{C_2(\tau + \|\boldsymbol{\lambda}\|_{-1})^2},$$

for some large C_2 . Therefore,

$$\begin{aligned} s &\geq \frac{\frac{n}{C_1(\tau + \|\boldsymbol{\lambda}\|_{-1})} \left(1 + \frac{n\lambda_1}{C_2(\tau + \|\boldsymbol{\lambda}\|_{-1})}\right)}{1 + \frac{C_3 n \lambda_1}{(\tau + \|\boldsymbol{\lambda}\|_{-1})}} \\ &\geq \frac{n}{C_1(\tau + \|\boldsymbol{\lambda}\|_{-1})} \cdot \left(\frac{C_2(\tau + \|\boldsymbol{\lambda}\|_{-1}) + n\lambda_1}{C_2(\tau + \|\boldsymbol{\lambda}\|_{-1})}\right) \cdot \left(\frac{(\tau + \|\boldsymbol{\lambda}\|_{-1})}{(\tau + \|\boldsymbol{\lambda}\|_{-1}) + C_3 n \lambda_1}\right) \\ &\geq \frac{n}{C_1(\tau + \|\boldsymbol{\lambda}\|_{-1})} \cdot \left(\frac{C_2(\tau + \|\boldsymbol{\lambda}\|_{-1}) + n\lambda_1}{C_2(\tau + \|\boldsymbol{\lambda}\|_{-1})}\right) \cdot \left(\frac{(\tau + \|\boldsymbol{\lambda}\|_{-1})}{(C_2 C_3(\tau + \|\boldsymbol{\lambda}\|_{-1}) + C_3 n \lambda_1)}\right) \\ &\geq \frac{n}{C_4(\tau + \|\boldsymbol{\lambda}\|_{-1})}. \end{aligned}$$

The derivation of bounds for t_k is the same as the procedure above.

For f_k , with probability at least $1 - \delta$,

$$\begin{aligned} |f_k| &= \left| \frac{\mathbf{y}^T \mathbf{U}_{-1,\tau}^{-1} \mathbf{z}_k + \lambda_1 \mathbf{y}^T \mathbf{U}_{-1,\tau}^{-1} \mathbf{z}_k \mathbf{z}_1^T \mathbf{U}_{-1,\tau}^{-1} \mathbf{z}_1 - \lambda_1 \mathbf{y}^T \mathbf{U}_{-1,\tau}^{-1} \mathbf{z}_1 \mathbf{z}_1^T \mathbf{U}_{-1,\tau}^{-1} \mathbf{z}_k}{1 + \lambda_1 \mathbf{z}_1^T \mathbf{U}_{-1,\tau}^{-1} \mathbf{z}_1} \right| \\ &\leq \frac{\frac{C_1 n}{(\tau + \|\boldsymbol{\lambda}\|_{-1})} \left(1 + \frac{C_2 n \lambda_1}{\tau + \|\boldsymbol{\lambda}\|_{-1}}\right)}{1 + \frac{n\lambda_1}{C_3(\tau + \|\boldsymbol{\lambda}\|_{-1})}} \\ &\leq \frac{C_4 n}{\tau + \|\boldsymbol{\lambda}\|_{-1}}. \end{aligned}$$

Similarly we can obtain upper bounds for $\|\mathbf{y}^T \mathbf{U}_\tau^{-1}\|_2$ and $\|\mathbf{z}_k^T \mathbf{U}_\tau^{-1}\|_2$.

For f_1 ,

$$\begin{aligned}
|f_1| &= \left| \frac{\mathbf{y}^T \mathbf{U}_{-1,\tau}^{-1} \mathbf{z}_1 + \lambda_1 \mathbf{z}_1^T \mathbf{U}_{-1,\tau}^{-1} \mathbf{z}_1 \mathbf{y}^T \mathbf{U}_{-1,\tau}^{-1} \mathbf{z}_1 - \lambda_1 \mathbf{y}^T \mathbf{U}_{-1,\tau}^{-1} \mathbf{z}_1 \mathbf{z}_1^T \mathbf{U}_{-1,\tau}^{-1} \mathbf{z}_1}{1 + \lambda_1 \mathbf{z}_1^T \mathbf{U}_{-1,\tau}^{-1} \mathbf{z}_1} \right| \\
&= \left| \frac{\mathbf{y}^T \mathbf{U}_{-1,\tau}^{-1} \mathbf{z}_1}{1 + \lambda_1 \mathbf{z}_1^T \mathbf{U}_{-1,\tau}^{-1} \mathbf{z}_1} \right| \\
&\leq \frac{\frac{C_1 n}{(\tau + \|\boldsymbol{\lambda}\|_{-1})}}{1 + \frac{n \lambda_1}{C_2(\tau + \|\boldsymbol{\lambda}\|_{-1})}} \\
&\leq \frac{C_1 n}{(\tau + \|\boldsymbol{\lambda}\|_{-1})} \cdot \left(\frac{C_2(\tau + \|\boldsymbol{\lambda}\|_{-1})}{C_2(\tau + \|\boldsymbol{\lambda}\|_{-1}) + n \lambda_1} \right) \\
&\leq \frac{C_3 n}{\tau + \|\boldsymbol{\lambda}\|_{-1} + n \lambda_1}.
\end{aligned}$$

For g_1 , we have

$$\begin{aligned}
|g_1| &= \left| \frac{\mathbf{z}_k^T \mathbf{U}_{-1,\tau}^{-1} \mathbf{z}_1 + \lambda_1 \mathbf{z}_1^T \mathbf{U}_{-1,\tau}^{-1} \mathbf{z}_1 \mathbf{z}_k^T \mathbf{U}_{-1,\tau}^{-1} \mathbf{z}_1 - \lambda_1 \mathbf{z}_k^T \mathbf{U}_{-1,\tau}^{-1} \mathbf{z}_1 \mathbf{z}_1^T \mathbf{U}_{-1,\tau}^{-1} \mathbf{z}_1}{1 + \lambda_1 \mathbf{z}_1^T \mathbf{U}_{-1,\tau}^{-1} \mathbf{z}_1} \right| \\
&= \left| \frac{\mathbf{z}_k^T \mathbf{U}_{-1,\tau}^{-1} \mathbf{z}_1}{1 + \lambda_1 \mathbf{z}_1^T \mathbf{U}_{-1,\tau}^{-1} \mathbf{z}_1} \right| \\
&\leq \frac{\frac{C_1 n}{(\tau + \|\boldsymbol{\lambda}\|_{-1})}}{1 + \frac{n \lambda_1}{C_2(\tau + \|\boldsymbol{\lambda}\|_{-1})}} \\
&\leq \frac{C_1 n}{(\tau + \|\boldsymbol{\lambda}\|_{-1})} \cdot \left(\frac{C_2(\tau + \|\boldsymbol{\lambda}\|_{-1})}{C_2(\tau + \|\boldsymbol{\lambda}\|_{-1}) + n \lambda_1} \right) \\
&\leq \frac{C_3 n}{\tau + \|\boldsymbol{\lambda}\|_{-1} + n \lambda_1}.
\end{aligned}$$

This completes the proof.

H Proofs for Section 7

The proofs follow similar conceptual steps to the noiseless case, but several technical adjustments are needed. This is because: on the one hand, the clean label vector \mathbf{y} enters the features equation $\mathbf{X} = \mathbf{y} \boldsymbol{\eta}^T + \mathbf{Q}$; on the other hand, the estimator $\hat{\boldsymbol{\eta}}$ is generated according to the noisy label vector \mathbf{y}_c . We start from defining some additional primitive quadratic forms on $\mathbf{U}_0 = \mathbf{Q} \mathbf{Q}^T$:

$$\begin{aligned}
s_c &= \mathbf{y}_c^T \mathbf{U}_0^{-1} \mathbf{y}, \\
h_c &= \mathbf{y}_c^T \mathbf{U}_0^{-1} \mathbf{d}, \\
g_{c,i} &= \mathbf{y}_c^T \mathbf{U}_0^{-1} \mathbf{e}_i, \quad i \in [n], \\
s_{cc} &= \mathbf{y}_c^T \mathbf{U}_0^{-1} \mathbf{y}_c,
\end{aligned} \tag{87}$$

The subscript c here emphasizes that the corrupted noise vector enters these quantities (unlike the corresponding ones in Appendix A). The lemma below is our analogue to Lemma 6.

Lemma 17. Recall $D := s(\|\boldsymbol{\eta}\|_2^2 - t) + (h + 1)^2$, then

$$\mathbf{y}_c^T (\mathbf{X} \mathbf{X}^T)^{-1} = \mathbf{y}_c^T \mathbf{U}_0^{-1} - \frac{1}{D} \mathbf{v} \begin{bmatrix} \|\boldsymbol{\eta}\|_2 \mathbf{y}^T \\ \mathbf{y}^T \\ \mathbf{d}^T \end{bmatrix} \mathbf{U}_0^{-1},$$

where

$$\mathbf{v} = \left[\|\boldsymbol{\eta}\|_2 s_c + \|\boldsymbol{\eta}\|_2 (s_c h - s h_c), h_c h + h_c - s_c t - \|\boldsymbol{\eta}\|_2^2 (s_c h - s h_c), s_c + s_c h - s h_c \right].$$

Next, the lemma below gives upper/lower bounds for the newly defined quadratic forms in (87).

Lemma 18. *Assume $\Sigma = \mathbf{I}$ and $p > Cn \log n + n + 1$ for a sufficiently large constant C . Fix $\delta \in (0, 1)$ and suppose n is large enough such that $n > c/\delta$ for some $c > 1$. Then, there exist constants C_i 's > 1 such that with probability at least $1 - \delta$, the following results hold:*

$$\begin{aligned} \frac{n}{C_1 p} \leq s_c &\leq \frac{C_1 n}{p}, \\ -\frac{C_2 n \|\boldsymbol{\eta}\|_2}{p} \leq h_c &\leq \frac{C_2 n \|\boldsymbol{\eta}\|_2}{p}, \\ \frac{n}{C_3 p} \leq s_{cc} &\leq \frac{C_3 n}{p}. \end{aligned}$$

Note that the bounds for the quadratic forms above are of the same order as those for the corresponding quadratic forms defined with \mathbf{y} , e.g., both s and s_c are at the order of $\Theta(n/p)$. Now we are ready to prove the theorems.

H.1 Proof of Theorem 6

Similar to the proofs in Appendix B, we again start from the duality argument of Muthukumar et al. [2020a] and so we need to find the conditions ensuring

$$y_{c,i} \mathbf{y}_c^T (\mathbf{X} \mathbf{X}^T)^{-1} \mathbf{e}_i > 0, \text{ for all } i \in [n], \quad (88)$$

where $y_{c,i}$ is the i -th element of \mathbf{y}_c . Lemma 17 and some algebra steps give:

$$\begin{aligned} \mathbf{y}_c^T (\mathbf{X} \mathbf{X}^T)^{-1} \mathbf{e}_i &= g_{c,i} \\ &- \frac{1}{D} \left[\|\boldsymbol{\eta}\|_2 s_c + \|\boldsymbol{\eta}\|_2 (s_c h - s h_c), h_c h + h_c - s_c t - \|\boldsymbol{\eta}\|_2^2 (s_c h - s h_c), s_c + s_c h - s h_c \right] \begin{bmatrix} \|\boldsymbol{\eta}\|_2 g_i \\ g_i \\ f_i \end{bmatrix} \\ &= \frac{A + B}{s(\|\boldsymbol{\eta}\|_2^2 - t) + (h + 1)^2}, \end{aligned}$$

where

$$\begin{aligned} A &= g_{c,i} + 2g_{c,i}h - s_c f_i \\ B &= \|\boldsymbol{\eta}\|_2^2 (g_{c,i}s - g_i s_c) + g_i s_c t - g_{c,i} s t + g_{c,i} h^2 - g_i h_c h - g_i h_c + s f_i h_c - s_c h f_i. \end{aligned}$$

Let us start with an observation regarding the numerator $A + B$. We have already derived conditions making $y_{c,i} A > 0$ in Appendix B.2 (to be precise, Appendix B.2 considers $y_i(g_i + g_i h - s f_i)$, but the quadratic forms are of the same order, so the same results apply). Specifically, when showing $y_{c,i} A > 0$, we first have

$$y_{c,i} g_{c,i} > 1/(Cp) > 0$$

with high probability (obtained by Lemma 10). Then, in Appendix B.2, we show that the rest of the terms in A , i.e., $|g_{c,i}h|, |s_c f_i|$, are sufficiently small compared to $1/(Cp)$. Note that when there is no label noise, i.e., $\gamma = 0$, then $g_{c,i} = g_i, s_c = s, h_c = h$ and $A + B = g_i + g_i h - s f_i$, which becomes the same as what we have in Appendix B.2.

Now, in order to derive conditions under which $y_{c,i}(A + B) > 0$, we first decompose

$$A + B = g_{c,i} + A_h - A_f + A_s,$$

where

$$\begin{aligned} A_h &= 2g_{c,i}h + g_{c,i}h^2 - g_i h_c h - g_i h_c \\ A_f &= s_c f_i - s f_i h_c + s_c h f_i \\ A_s &= g_{c,i} \|\boldsymbol{\eta}\|_2^2 s - g_i \|\boldsymbol{\eta}\|_2^2 s_c + g_i s_c t - g_{c,i} s t. \end{aligned}$$

The idea is to show that: (a) in A_h , the term $g_{c,i}h$ is dominant; (b) in A_f , $s_c f_i$ is the dominant term; (c) $|A_s|$ is sufficiently smaller than $1/(Cp)$. To achieve this, we need

$$p > C_0 \max\{n\sqrt{\log(2n)}\|\boldsymbol{\eta}\|_2, n\|\boldsymbol{\eta}\|_2^2\} \quad (89)$$

for a sufficiently large constant C_0 . The reason is that in A_h and A_f , $|h|$ (and $|h_c|$) is upper bounded by $O(n\|\boldsymbol{\eta}\|_2/p)$ with high probability. In A_s , $s_c\|\boldsymbol{\eta}\|_2^2 \leq O(n\|\boldsymbol{\eta}\|_2^2/p)$ and $st \leq O(n^2\|\boldsymbol{\eta}\|_2^2/p^2)$ with high probability. Therefore, (89) ensures the terms mentioned above are sufficiently smaller than 1 as desired.

H.2 Proofs of Theorem 7 and Corollary 7.1

Again, similar to the proofs in Appendix C.2, we need to lower bound the ratio

$$\frac{(\mathbf{y}_c^T(\mathbf{X}\mathbf{X}^T)^{-1}\mathbf{X}\boldsymbol{\eta})^2}{\mathbf{y}_c^T(\mathbf{X}\mathbf{X}^T)^{-1}\mathbf{y}_c}. \quad (90)$$

Here we will lower bound $\mathbf{y}_c^T(\mathbf{X}\mathbf{X}^T)^{-1}\mathbf{X}\boldsymbol{\eta}$ and upper bound $\mathbf{y}_c^T(\mathbf{X}\mathbf{X}^T)^{-1}\mathbf{y}_c$. Lemma 17 and some algebra steps give:

$$\mathbf{y}_c^T(\mathbf{X}\mathbf{X}^T)^{-1}\mathbf{X}\boldsymbol{\eta} = \|\boldsymbol{\eta}\|_2^2 \mathbf{y}_c^T(\mathbf{X}\mathbf{X}^T)^{-1}\mathbf{y} + \mathbf{y}_c^T(\mathbf{X}\mathbf{X}^T)^{-1}\mathbf{Q}\boldsymbol{\eta} = \frac{s_c\|\boldsymbol{\eta}\|_2^2 - s_ct + h_ch + h_c}{s(\|\boldsymbol{\eta}\|_2^2 - t) + (h+1)^2}.$$

Similarly, the denominator $\mathbf{y}_c^T(\mathbf{X}\mathbf{X}^T)^{-1}\mathbf{y}_c$ is

$$\frac{s_{cc} + \|\boldsymbol{\eta}\|_2^2(s_{cc}s - s_c^2) + s_c^2t - s_{cc}st + 2s_{cc}h + s_{cc}h^2 + sh_ch - 2s_{cc}h_ch - 2s_ch_c}{s(\|\boldsymbol{\eta}\|_2^2 - t) + (h+1)^2}.$$

Combining the two expressions above gives that we need to lower bound:

$$\frac{(s_c\|\boldsymbol{\eta}\|_2^2 - s_ct + h_ch + h_c)^2}{D_s(s(\|\boldsymbol{\eta}\|_2^2 - t) + (h+1)^2)}, \quad (91)$$

where

$$D_s = s_{cc} + \|\boldsymbol{\eta}\|_2^2(s_{cc}s - s_c^2) + s_c^2t - s_{cc}st + 2s_{cc}h + s_{cc}h^2 + sh_ch - 2s_{cc}h_ch - 2s_ch_c.$$

Recall that in Appendix C.2, we have lower bounded $\frac{(s(\|\boldsymbol{\eta}\|_2^2 - t) + h^2 + h)^2}{s(s(\|\boldsymbol{\eta}\|_2^2 - t) + (h+1)^2)}$ and since s_{cc}, s_c, s are of the

same order and h_c, h are also of the same order, we actually have the same bound for $\frac{(s_c\|\boldsymbol{\eta}\|_2^2 - s_ct + h_ch + h_c)^2}{s(\|\boldsymbol{\eta}\|_2^2 - t) + (h+1)^2}$ in (91). The next step is to show that D_s is close to s_{cc} . This is true since due to the assumption $p > C \max\{n\sqrt{\log(2n)}\|\boldsymbol{\eta}\|_2, n\|\boldsymbol{\eta}\|_2^2\}$ for a large constant C , the bounds for terms such as $\|\boldsymbol{\eta}\|_2^2s, st, h^2, h_c$ are sufficiently small compared to 1 (we also illustrate this under (89)). Therefore, in D_s , s_{cc} is the dominant term and we finally need to lower bound the term

$$\frac{(s_c\|\boldsymbol{\eta}\|_2^2 - s_ct + h_ch + h_c)^2}{s_{cc}(s(\|\boldsymbol{\eta}\|_2^2 - t) + (h+1)^2)}.$$

This satisfies the same bound as $\frac{(s(\|\boldsymbol{\eta}\|_2^2 - t) + h^2 + h)^2}{s(s(\|\boldsymbol{\eta}\|_2^2 - t) + (h+1)^2)}$ in Appendix C.2. Since $p > Cn\|\boldsymbol{\eta}\|_2^2$ falls into the low-SNR regime in Corollary 4.1, we can directly apply the results of low-SNR regime in Corollaries 4.1 and 5.2, which gives the desired.

H.3 Proofs of auxiliary lemmas

We first prove Lemma 17.

Proof of Lemma 17. The proof follows Appendix G.2 except for in the last steps, we have

$$\mathbf{y}_c^T (\mathbf{X}\mathbf{X}^T)^{-1} = \mathbf{y}_c^T \mathbf{U}_0^{-1} - [\|\boldsymbol{\eta}\|_{2s_c} \quad h_c \quad s_c] \mathbf{A}^{-1} \begin{bmatrix} \|\boldsymbol{\eta}\|_{2s} \mathbf{y}^T \\ \mathbf{y}^T \\ \mathbf{d}^T \end{bmatrix} \mathbf{U}_\tau^{-1}, \quad (92)$$

where \mathbf{A}^{-1} is

$$\frac{1}{D} \begin{bmatrix} (h+1)^2 - st & \|\boldsymbol{\eta}\|_2(st - h - h^2) & -\|\boldsymbol{\eta}\|_{2s} \\ -\|\boldsymbol{\eta}\|_{2s} & h+1 + \|\boldsymbol{\eta}\|_{2s}^2 & -s \\ \|\boldsymbol{\eta}\|_2(st - h - h^2) & \|\boldsymbol{\eta}\|_2^2 h^2 - t(1 + \|\boldsymbol{\eta}\|_{2s}^2) & h+1 + \|\boldsymbol{\eta}\|_{2s}^2 \end{bmatrix},$$

with $D = s(\|\boldsymbol{\eta}\|_2^2 - t) + (h+1)^2$. Then plugging the expression above in (92) completes the proof. \square

We now prove Lemma 18. We first start from a lemma bounding $\|\mathbf{y}_c + \mathbf{y}\|_2^2$ and $\|\mathbf{y}_c - \mathbf{y}\|_2^2$.

Lemma 19. *Assuming the probability γ of a label flipping is small enough such that $1 - \gamma \geq 1 - (1/C_0)$ for some large constant C_0 , there exist large constants $C_1, C_2 > 1$ such that the event*

$$\mathcal{E}_y := \left\{ \|\mathbf{y}_c + \mathbf{y}\|_2^2 \geq 4\left(1 - \frac{1}{C_1}\right)n \quad \text{and} \quad \|\mathbf{y}_c - \mathbf{y}\|_2^2 \leq \frac{4}{C_1}n \right\}, \quad (93)$$

holds with probability at least $1 - 4e^{-\frac{n}{C_2}}$.

Proof. We first look at $(\tilde{y}_i + y_i)^2$, which evaluates to either 4 or 0. Since bounded, these variables are independent sub-Gaussians. The mean of $\|\mathbf{y}_c + \mathbf{y}\|_2^2$ is $4(1 - \gamma)n$. Therefore, Hoeffding's bound [Wainwright \[2019, Ch. 2\]](#) gives

$$\mathbb{P}\left(\left|\|\mathbf{y}_c + \mathbf{y}\|_2^2 - 4(1 - \gamma)n\right| \geq t\right) \leq 2 \exp\left(-\frac{t^2}{Cn}\right).$$

We complete the proof by setting $t = \frac{n}{C_3}$ for a large enough constant C_3 . $(\tilde{y}_i - y_i)^2$ also evaluates to either 4 or 0 and the mean of $\|\mathbf{y}_c - \mathbf{y}\|_2^2$ is $4\gamma n$. Thus, we can repeat the previous derivation to obtain the advertised results. \square

Now we are ready to prove Lemma 18.

Proof of Lemma 18. The bounds for h_c, s_{cc} and the upper bound for s_c follow exactly as in Lemma 7 since $\|\mathbf{y}_c\|_2^2 = n$ same as $\|\mathbf{y}\|_2^2 = n$. We now derive the lower bound for s_c . We will need the following standard lemma (here adapted from [Muthukumar et al. \[2020a, Lemma 2\]](#)) to bound quadratic forms of a Wishart matrix.

Lemma 20. *Define $d'(n) := (p - n + 1)$. Let matrix $\mathbf{M} \sim \text{Wishart}(p, \mathbf{I}_n)$. For any unit-frobenius norm vector \mathbf{v} and any $t > 0$, we have*

$$\begin{aligned} \mathbb{P}\left(\frac{1}{\mathbf{v}^T \mathbf{M}^{-1} \mathbf{v}} > d'(n) + \sqrt{2td'(n)} + 2t\right) &\leq e^{-t} \\ \mathbb{P}\left(\frac{1}{\mathbf{v}^T \mathbf{M}^{-1} \mathbf{v}} < d'(n) - \sqrt{2td'(n)}\right) &\leq e^{-t}, \end{aligned}$$

provided that $d'(n) > 2 \max\{t, 1\}$.

We use the parallelogram law to write

$$\mathbf{y}_c^T \mathbf{U}_0^{-1} \mathbf{y} = \frac{1}{4} \left((\mathbf{y}_c + \mathbf{y})^T \mathbf{U}_0^{-1} (\mathbf{y}_c + \mathbf{y}) - (\mathbf{y}_c - \mathbf{y})^T \mathbf{U}_0^{-1} (\mathbf{y}_c - \mathbf{y}) \right).$$

Let $t = \log n$ and recall that $d'(n) > Cn \log n$ for a sufficiently large constant C . To lower bound s_c , conditioned on event \mathcal{E}_y , we have with probability at least $1 - \frac{1}{n}$,

$$\begin{aligned} \mathbf{y}_c^T \mathbf{U}_0^{-1} \mathbf{y} &\geq \frac{1}{4} \left(\frac{4(1 - 1/C_1)n}{(d'(n) + \sqrt{2 \log(n) d'(n)} + 2 \log(n))} - \frac{(4/C_1)n}{(d'(n) - \sqrt{2 \log(n) d'(n)})} \right) \\ &\geq \frac{(1 - 1/C_1)n(d'(n) - \sqrt{2 \log(n) d'(n)}) - (1/C_1)n(d'(n) + \sqrt{2 \log(n) d'(n)} + 2 \log(n))}{(d'(n) - \sqrt{2 \log(n) d'(n)})(d'(n) + \sqrt{2 \log(n) d'(n)})} \\ &\geq \frac{(1 - 1/C_3)nd'(n)}{C_4 d'(n)^2} \\ &\geq \frac{n}{C_5 p}, \end{aligned}$$

where we replaced $\log(n)$ with $d'(n)/C$ using the fact that $d'(n) > Cn \log n$ for a sufficiently large constant C above. Let \mathcal{E} be the desired event that $\mathbf{y}_c^T \mathbf{U}_0^{-1} \mathbf{y} \geq n/(Cp)$. We then complete the proof by adjusting the probability using $\mathbb{P}(\mathcal{E}^c) \leq \mathbb{P}(\mathcal{E}^c | \mathcal{E}_y) + \mathbb{P}(\mathcal{E}_y^c) \leq (1/n) + 4 \exp(-n/c_1) \leq c_2/n$. \square

I On linear separability of GMM

The main result of this section Lemma 22 proves that GMM data are linearly separable with high-probability as long as $p > n + 2$. The arguments presented are pretty standard in the literature, but included here for completeness. Sharp separability thresholds for the GMM have been recently derived in Deng et al. [2019].

We will first need the following technical lemma that lower bounds the minimum singular value of a non-zero mean isotropic Gaussian matrix. The result is a minor extension of the standard proof using Gordon's Gaussian min-max inequality for the case of a centered isotropic Gaussian matrix (e.g. see Vershynin [2018, Exercise 7.3.4]).

Lemma 21. *Let $Q \in \mathbb{R}^{p \times n}$ a matrix with IID standard normal entries and $\mathbf{y} \in \mathbb{R}^n$, $\boldsymbol{\eta} \in \mathbb{R}^p$ fixed vectors. Consider the matrix $\mathbf{A} = \boldsymbol{\eta} \mathbf{y}^T + Q$. For every $t > 0$ it holds that*

$$\min_{\|\mathbf{u}\|_2=1} \|\mathbf{A} \mathbf{u}\|_2 \geq \sqrt{p-2} - \sqrt{n} - t \quad (94)$$

with probability at least $1 - 4e^{-t^2/8}$.

Proof. We now prove the lemma using Gordon's Gaussian comparison inequality [Gordon, 1985]. Specifically, we apply a version that appears in Thrampoulidis et al. [2015]. We start by writing

$$\Phi(\mathbf{A}) := \min_{\|\mathbf{u}\|_2=1} \|\mathbf{A} \mathbf{u}\|_2 = \min_{\|\mathbf{u}\|_2=1} \max_{\|\mathbf{w}\|_2=1} \mathbf{w}^T Q \mathbf{u} + (\mathbf{w}^T \boldsymbol{\eta})(\mathbf{y}^T \mathbf{u})$$

Now, following Thrampoulidis et al. [2015, Thm. 3(i)] we focus on the following auxiliary problem where $\mathbf{g} \in \mathbb{R}^n$ and $\mathbf{h} \in \mathbb{R}^d$ have iid standard normal entries:

$$\phi(\mathbf{g}, \mathbf{h}) := \min_{\|\mathbf{u}\|_2=1} \max_{\|\mathbf{w}\|_2=1} \mathbf{h}^T \mathbf{w} + \mathbf{g}^T \mathbf{u} + (\mathbf{w}^T \boldsymbol{\eta})(\mathbf{y}^T \mathbf{u}).$$

By decomposing $\mathbf{w} = \alpha \frac{\boldsymbol{\eta}}{\|\boldsymbol{\eta}\|_2} + \mathbf{P}_\boldsymbol{\eta}^\perp \mathbf{w}$ for $\alpha := \frac{\boldsymbol{\eta}^T \mathbf{w}}{\|\boldsymbol{\eta}\|_2} \in [0, 1]$ and $\mathbf{P}_\boldsymbol{\eta}^\perp = \mathbf{I}_d - \frac{\boldsymbol{\eta} \boldsymbol{\eta}^T}{\|\boldsymbol{\eta}\|_2^2}$, we can see that

$$\phi(\mathbf{g}, \mathbf{h}) = \min_{\|\mathbf{u}\|_2=1} \max_{\alpha \in [0, 1]} \|\mathbf{P}_\boldsymbol{\eta}^\perp \mathbf{h}\|_2 \sqrt{1 - \alpha^2} + \alpha \frac{\boldsymbol{\eta}^T \mathbf{h}}{\|\boldsymbol{\eta}\|_2} + \mathbf{g}^T \mathbf{u} + (\mathbf{y}^T \mathbf{u}) \alpha \|\boldsymbol{\eta}\|_2 \quad (95)$$

$$\geq \min_{\|\mathbf{u}\|_2=1} \|\mathbf{P}_\boldsymbol{\eta}^\perp \mathbf{h}^T\|_2 + \mathbf{g}^T \mathbf{u} \quad (96)$$

$$= \|\mathbf{P}_\boldsymbol{\eta}^\perp \mathbf{h}\|_2 - \|\mathbf{g}\|_2 \quad (97)$$

But now from standard concentration arguments (e.g. see [Oymak et al. \[2013, Lemma B.2\]](#), for all $t > 0$ with probability at least $1 - 2e^{-t^2/2}$ it holds that $\|\mathbf{P}_{\eta}^{\perp} \mathbf{h}\|_2 - \|\mathbf{g}\|_2 \geq \sqrt{p-2} - \sqrt{n} - 2t$. We now invoke Gordon's inequality to complete the proof:

$$\Pr\left(\Phi(\mathbf{A}) \leq \sqrt{p-2} - \sqrt{n} - t\right) \leq 2\Pr\left(\phi(\mathbf{g}, \mathbf{h}) \leq \sqrt{p-2} - \sqrt{n} - t\right) \leq 4e^{-t^2/8}. \quad (98)$$

□

We are now ready to state and prove the main result of this section.

Lemma 22. *Let training data $\{(\mathbf{x}_i, y_i)\}_{i \in [n]}$ be generated from the GMM in Equation (1). Assume $p > n + 2 + t$ for some $t > 0$. Then with probability at least $1 - 4e^{-t^2/8}$ the following statements hold:*

- (i) *The min-norm interpolator is feasible, i.e. there exists $\boldsymbol{\beta} \in \mathbb{R}^d$ such that for all $i \in [n]$: $y_i = \mathbf{x}_i^T \boldsymbol{\beta}$.*
- (ii) *The training data are linearly separable, i.e. there exists $\boldsymbol{\beta} \in \mathbb{R}^d$ such that for all $i \in [n]$: $y_i(\mathbf{x}_i^T \boldsymbol{\beta}) \geq 1$.*

Proof. To prove the first statement we need to show that the feature matrix $\mathbf{X} \in \mathbb{R}^{n \times d}$ has full row-rank with high probability. Equivalently, we show that $\min_{\|\mathbf{u}\|_2=1} \|\mathbf{X}^T \mathbf{u}\|_2 > 0$ with high-probability. This is a direct application of Lemma 21 above for $\mathbf{A} = \mathbf{X}^T$.

Now we prove the second statement. From part (i), there exists $\boldsymbol{\beta}$ such that $y_i = \mathbf{x}_i^T \boldsymbol{\beta}, i \in [n]$. Since $y_i \in \{\pm 1\}, i \in [n]$ it then holds that $y_i(\mathbf{x}_i^T \boldsymbol{\beta}) = 1, i \in [n]$. Thus, the same vector $\boldsymbol{\beta}$ from part (i) that interpolates the data is also a linear separator. □